INVESTIGATION OF SOME BIOCHEMICAL PARAMETERS RELATING TO ENERGY METABOLISM IN EXPERIMENTAL RODENT TUMOURS AFTER EXPOSURE TO IONIZING RADIATION AND MAGNETIC FIELDS

By

David Szeinfeld Loef

A T H E S I S

Submitted to the University of Cape Town for the Degree of

DOCTOR OF PHILOSOPHY

1987

The University of Cape Town has been given the right to reproduce this thesis in whole or in part. Copyright is held by the author.

The copyright of this thesis vests in the author. No quotation from it or information derived from it is to be published without full acknowledgement of the source. The thesis is to be used for private study or non-commercial research purposes only.

Published by the University of Cape Town (UCT) in terms of the non-exclusive license granted to UCT by the author.

University of Cape Town

To the memory of my father and to Edy, my wife.

CONTENTS

ABSTRACT

The work described in this thesis deals with the effects of ionizing and non ionizing radiation, upon rodent tumour metabolism and growth and comparable properties of B16 melanoma cell cultures. Metabolic processes investigated were related to energy production and possible repair mechanisms after radiation induced damage. Further, some effects of the drug mitoxantrone on energy yield were also studied "in vivo" and "in vitro".

Three strains of mouse (CBA, BALB c and WHT) were used and one strain of rat (WAG/Rij). Their tumours investigated in vivo were CaNT, rhabdomyosarcoma, Fib/t and R1 respectively. The following sources of radiation were used: 100, 250 kVp of x-rays, ^{60}Co gammas, 8 MV x-rays (from a linear accelerator), and magnetic fields of 0.5 Tesla (constant) and 5×10^{-3} Tesla/m (varying). The biochemical parameters measured were levels of adenosine-5'-triphosphate (ATP) isocitrate dehydrogenase (ICDH), glucose-6-phosphate dehydrogenase, (G6P-DH), phosphomannose isomerase (PMI) and tissue sulphydryl. This was done with tumours under normoxic and hypoxic conditions. Growth rate and nuclear magnetic resonance relaxation time constants T_1 and T_2 were measured in CaNT tumours. Their ultrastructural changes using electron micrographs were investigated after x-irradiation. Further, the effects of mitoxantrone upon ATP production were measured in CaNT tumours. In addition the radiation response of B16 melanoma cells after exposure to ^{60}Co gammas was studied, with and without treatment using mitoxantrone.

Changes in levels of ATP and activities of G6P-DH and ICDH were observed at different times after irradiation in the varying conditions studied, but no significant change in tissue sulphydryl levels was detected. Further it was shown in B16 cells that radiosensitivity could be modified using mitoxantrone (which reduces ATP production) such that a greater cell kill could be achieved. Tumour growth rate slowed with exposure to the magnetic fields.

The results which can be considered to be interesting from a basic science point of view, may also be indicative of a complex metabolic response to irradiation. This work has described relations between different qualities of radiation and aspects of energy producing metabolic reactions in the tumours investigated.

ACKNOWLEDGEMENTS

I wish to acknowledge my gratitude to Dr G Blekkenhorst who has acted as thesis advisor for this work. He has always made himself readily available to discuss both detail and broad aspects of the research described in this thesis and has greatly facilitated my progress with his insight and guidance.

My profound thanks to Professor G R H Sealy, Head of the Department of Radiotherapy at Groote Schuur Hospital and the University of Cape Town, are due for many reasons. He allowed me to work in his laboratory and freely made available his extensive knowledge and experience. His encouragement, constructive comments and criticism contributed significantly to the research work presented here.

Among the members of the Department of Radiotherapy whose help I wish to acknowledge especially are, Mark Davoren, for his aid in the in vitro studies, Andrê Hendrikse for his assistance and kindness, especially when I first joined the Department, and changed my pattern of life in a new environment, Patricia Dowman for her sympathetic attitude and support in the Radiobiology Laboratory, Gladstone Nongalaza for his cheerful assistance, Dr W Levin for his advice and exchanges of ideas. All the staff of the Laboratory of Radiobiology encouraged and helped me whenever possible and for this I thank them. The Departmental Radiographers always assisted willingly with the irradiations for which I am very grateful. All the doctors other members of the Department of Radiotherapy in one way or another way helped to make me feel at home, which I acknowledge thankfully. Dr R S Sparks of the Department of Mathematical Statistics, University of Cape Town provided considerable assistance with the programming of the statistical analyses using the linear quadratic model, which is much appreciated.

At the South African Medical Research Council I am pleased to recognise the great help and assistance of Dr S Wynchank, Director of the Research Institute for Medical Biophysics, Dr C J Lombard of the Institute of Biostatistics for his

deeply appreciated statistical interpretation of my experimental results, Paul Selby for his assistance and support, Leon du Toit and Mrs Barbara van Dyk for their help in the use of the nuclear magnetic resonance imager, Mike Kayser for his expert assistance concerning electron microscopy, Miss Janet Butler for her skilful preparation of graphs and figures in this thesis, all the members of the Institute staff for their valued discussions and encouragement and the Medical Research Council Headquarters personnel for their helpfulness.

Professor W Becker and Dr C Albrecht of the Medical Faculty of the University of Stellenbosch are thanked for their valuable discussions concerning interpretation of electron micrographs.

The financial assistance provided by the South African Medical Research Council for the work presented in this thesis is gratefully acknowledged.

Further support was granted by the award of two scholarships from the University of Cape Town. I wish to express my considerable gratitude for this support.

To Mrs Elize Mostert I offer my sincerest thanks for her efficient typing of the manuscript and for her good natured patience at all times up to the final version.

Finally for my wife Edy, who sacrificed so much, shared all the difficulties, always encouraged and cared for me to allow this thesis to be completed, I want to express my incommensurable thankfulness for so much support and love.

CHAPTER 1

INTRODUCTION

Cancer has caused much pain and suffering through the ages, and a great deal of effort has been and is presently being expended to research more effective means of treatment of this scourge (1). The importance of this continued effort can be gauged from the estimate of several scientists that the spectrum of this kind of disease now affects over 30% of the Westernized world (2, 3). One of the treatment modalities now used is irradiation with ionizing radiation, and it is estimated that about one fifth of cancer sufferers receive radiotherapy at some stage of their disease (4).

Radiotherapy has its origins in the realization very soon after the discovery of x-rays by Wilhelm Roentgen that ionizing radiation could damage cells. Radiation oncology has made great strides especially in the last 45 years, and radiation is very much established as one of the three major methods of cancer treatment, the others being surgery and chemotherapy (5).

Recent evidence suggests that cellular oncogenes are associated with cellular malignant transformation, presumably through effects on normal differentation genes. Perhaps regulatory genes turn off oncogenes, at the appropriate time in development. Such regulatory loci could be the anti-oncogenes. A deletion or mutation stopping the normal function of an anti-oncogene would allow inappropriate transcription of the corresponding oncogene. This sequence of events could cause a tumour if if took place in a cell type that is responsive to that oncogene. Malignant transformation may also be related to proto-oncogenes which are precursors of oncogenes (6) and can be conserved during evolution. Relatives of human proto-oncogenes have been found in DNA of a number of mammals, birds and even in the fruit fly. The proto-oncogenes would presumably not have been conserved, almost without change, in the genome unless they had some important normal cellular metabolic function. It is not exactly known what the role is of such genes in normal metabolism, but there are some indications that it is associated with control of cellular proliferation. With

the present state of knowledge concerning oncogenes and proto-oncogenes it seems that in normal cells there are genes present, which can suffer either mutation or misregulation. These changes can transform a normal cell's phenotype to a premalignant or malignant phenotype (7, 8) with possible loss of control of cell division, invasiveness and metastasis (9). It is important to realise that cancer cells contain all the biochemical mechanisms responsible for implementing all cell functions, many of which operate as in normal cells.

Nevertheless, an important difference between normal and malignant tissue lies in intercellular organisation. There appears to be decreased cohesion between cancer cells. The tumour cell membrane has many defective junctions (membrane passageways) and often modified numbers of beta-adrenergic and other hormone receptors in the membrane (10, 11). Owing to the haphazard manner in which the vascular pattern develops in malignant tumours, abnormal cellular spatial relationships exist within the tumour. This results in the malignant tumour having in addition to oxygenated cells, which may be dividing or non-dividing, poorly oxygenated cells (hypoxic cells) which would be located some distance from the blood vessel. There will also be areas within tumours, which have been starved of all nutrients including oxygen, where the cells are necrotic (12).

As a result of irradiation of tumours with ionizing radiation, three gross effects are to be expected. Firstly, some cells will suffer reproductive death, that is, they are effectively sterilized. Secondly, some cells will suffer some damage which is potentially repairable, and thirdly, there may be no observable effect. There is ongoing debate as to what part of the cell must be "hit" so as to cause reproduction death (13). It has been suggested that the critical intracellular target may be deoxyribonucleic acid (DNA) for most cell types (lymphoid cells are an exception), although the possibility exists that damage to a membrane protein complex located near DNA, or to the nuclear membrane itself, cannot be excluded (14, 15, 16). It may be that radiation causes widespread lesions at a number of intracellular sites, with resultant cell death or with resultant damage in the cells which is potentially repairable (17, 18). It can be deduced that the type and magnitude of radiation damage and its effect

on tumour cell metabolism will depend to a large degree on whether or not the potentially repairable damage is indeed repaired (19, 20, 21). If the damaged cells had no repair capability, the cells might tend to amplify the damage, which would in turn lead to metabolic disturbances and finally cell death, i e an increased cell kill might be expected. Consequently if the potentially repairable damage is repaired, a decreased cell kill would be expected (22, 23). One of the objectives of this thesis was to enquire into some of the biochemical factors in terms that might change following ionizing radiation, with particular emphasis on those which may be related to cellular repair processes (24, 25, 26). However the full implications of biochemical perturbations induced by radiation are not yet fully understood. The present work attempts to improve understanding of their significance.

The biochemical parameters selected for investigation were adenosine triphosphate, isocitrate dehydrogenase, glucose-6-phosphate dehydrogenase, phosphomannose isomerase and thiols. Tumour cell ultrastructure was investigated by electron microscopy following ionizing irradiation.

The second major aim of this thesis is to examine some effects of magnetic fields in experimental tumours. The tumours are basically diamagnetic and magnetic fields can deform atomic and molecular structures and exert forces and torques on particles in the tumour cell (28, 29, 30). Molecular or subcellular structures with anisotropy in magnetic susceptibility can be influenced by a twisting force, depending on the orientation of the structure to the applied magnetic field (31, 32, 33). The field also can induce certain spatial and directional asymmetries in electron currents (11, 34). These physical effects in turn modify various chemical processes as well as some electrochemical processes which may result in a variety of biological effects. The parameters selected for study in magnetic fields were tumour growth rate and the specific activities of:

(a) Glucose-6-phosphate dehydrogenase (G6P-DH)

(b) Phosphomannose isomerase (PMI)

The opportunity also arose whereby it was possible to determine T_1 (spin-lattice relaxation time) and T_2 (spin-spin relaxation time) in murine tumours using a magnetic resonance imager (35, 36).

CHAPTER 2

RADIATION BIOLOGY AND METABOLIC RESPONSE TO INJURY IN EXPERIMENTAL RODENT TUMOURS

2.1 Historical considerations:

(a) Ionizing radiation.

It is interesting to consider some of the historical aspects of the development of basic research in radiation biology (37). Some new lines of research were initiated by some quite accidental observations once the scene had been set by the discovery of ionizing radiation. Becquerel, who absent-mindedly carried a radium preparation around in his coat pocket, found this caused an inflammation of the skin and subsequently cancer due to this radioisotope was described. Soon after Wilhelm Roentgen's discovery of x-rays in November 1895 considerable information was obtained about the physical properties, interactions with matter and biological effects of x-radiations (38). After the discovery of x-rays, there were many scientists who, marvelling at their penetrating power, never tired of looking at images of the skeleton of their own hands. However, their enjoyment was soon dampened by the observation of peculiar changes in the exposed skin. The beginning of the development of this multi-disciplinary area of research was characterized by qualitative radiation biology which followed these initial observations and was related to morphological and descriptive investigations. Later on, in the late 1940s the advance of further basic knowledge in chemistry, physics and biology led to the development of radiation biology as a quantitative science (39). This period is characterized by the use of mathematical and statistical methods. A high point of interest was realised when the books of D.E. Lea (1946), N.W. Timofeeff-Ressovsky, and K.G. Zimmer (1947) finally established radiation biology as an independent branch of science.

During the past four decades more insight developed into biological phenomena induced by radiation. This understanding was related to study of modifying external conditions, for example altering temperature, tension of O_2, or adding substances that changed radiation sensitivity (40). Also results using radiations of different qualities were obtained and a number of explanations attempting to interpret the phenomena of radiation damage and repair mechanisms in cells were made. (41, 42, 43, 44).

(b) Magnetic Fields.

There is experimental evidence concerning the possible influence of magnetic forces on living organisms (45, 46). Several investigations have reported a delay in growth as an effect of magnetic fields both at the cellular level "in vivo" and "in vitro" as, for example in tumour tissue as well as in whole organisms such as mice (28, 47, 48). Some representative historical data of biomagnetic effects on growth (11) are given as Tables (2.1) and (2.2).

The existing experimental results of the effects of magnetic fields on metabolic rates are difficult to interpret. Some reactions are accelerated, some are decelerated and some are not affected at all by magnetic fields. Mechanisms whereby magnetic fields might influence metabolic changes include macromolecule orientation changes leading to modification of both biochemical kinetics and membrane permeability (49, 50, 51, 52). Also the magnetic dependence of the triplet yield in the formation of paramagnetic metabolic transients in the cells is affected by magnetic fields (53, 54).

TABLE 2.1: BIOMAGNETIC EFFECTS ON GROWTH RATES IN LIVING ORGANISMS

Organism	Fields (T)	Exposure	Effects Observed
Young mice	0.59	30-60 days	Retarded weight gain
Guinea pigs	0.7	500 hours	Necrosis, edemas, hemorrhage
Rabbits, cats, rats	0.2-0.3		Dystrophy in neuroglia
Frog embryo	1		Development retarded
Frog embryo	0.7		Development retarded
Pigeon embryo	4.7		Development retarded
Chicken embryo	0.003	2 days	Anomalous growth
Pigeon embryo	0.0005		Development retarded
Drosophila (fruit flies)	1.2	1 hour	100% mortality
Bacteria, yeast	1.1		No effects
Bacteria, yeasts, molds	0.3	48 hours	No effects
Plants	0.02-0.21		Growth inhibition
Plant	0.7		Faster growth
Algae, paramecium	0.1	7-21 days	Reproduction rate decreased

TABLE 2.2: BIOMAGNETIC EFFECTS ON GROWTH RATES IN TUMOURS

Tumours	Fields (T)	Exposure	Effects Observed
Epidermoid carcinoma KB	0.4	3 days	9 ± 7% decrease in cells 31 ± 11% increase (normal)
HeLa	0.5-0.77		No effects
HeLa	0.12		No effects
HeLa, KB, W138	0-0.12		No effects
Ehrlich adenocarcinoma	0.15-0.17		Reduced growth rates
Ehrlich	0.3-0.4		0-40% reduction in growth
Ehrlich	0.73	1-3 hours	Cell degeneration
Ehrlich, S-37 ascites	0.73	Few hours	Cell degeneration
Ehrlich, S-37 ascites	0.44-0.8	18 hours	30-100% degeneration
Mice tumors (H2712, C3HBA, T2146)	0.3-0.45		Tumor rejection in some animals
Crown gall tumor	0.01-0.22	3 months	Tumor regression
Heteroploid L-29 mammalian cells	0.5	7 days	Growth inhibition
Diploid WI-38 mammalian cells	0.5	7 days	Growth inhibition
Adenocarcinoma	3.8	18 days	45% reduction in growth

2.2 Processes of ionizing radiation absorption.

When trying to understand the development of radiation damage, it is convenient to divide the complex chain of events that follow absorption of high-energy radiation in living organisms into four temporal stages.

I. During the first or physical stage after absorption of radiation energy is transferred. This process leads mainly to molecular excitations and ionizations. The absorption of electromagnetic radiation proceeds by three specific mechanisms: (a) the photoelectric effect, (b) Compton effect and (c) pair production. The relative likelihood of each mechanism occurring depends on the energy of the quantum of radiation.

(a) Photoelectric effect.

In this process the incident photon transfers all of its energy to an atomic electron. The initial kinetic energy of the electron (E_{Kin}) is equal to the quantum energy (hf) minus the electron's binding energy A:

$$E_{Kin} = hf - A$$

The probability that this process will occur is highest when the energy of the quantum coincides with the binding energy of the electron emitted.

(b) Compton effect.

In the Compton interaction, in contrast to the photoelectric effect, only a part of the energy of the incident quantum is transferred to the electron. This reduces the energy of the scattered quantum and therefore increases its wavelength. In addition the quantum changes its direction. The angle at which the electron is ejected compared to the incident direction of the photon, depends on the amount of energy

transferred to the electron. This energy is not necessarily large, for a 10 KeV photon always retains at least 95% of its initial energy.

(c) Pair production.

This interaction process becomes significant at quantum energies exceeding 1 MeV, and consists of the generation of an electron-positron pair, by an interaction with nuclear fields. The sum of the kinetic energies of the electron and the positron is equal to the energy of the quantum less twice the rest energy E_o of an electron of rest mass m_o.

($E_o = m_o C^2 = 0.51$ Mev,

$E_{e+} + E_{e-} = hf - 1.02$ MeV)

The energy ($hf - 2\, m_o\, C^2$) can be equally divided between the two particles with formation of an electron-positron pair. This process demonstrates the direct conversion of energy to mass, but it must occur in the presence of a third body, usually a nucleus. Conservation of momentum and energy are maintained by this reaction. This stage occurs very rapidly, in about 10^{-13}s.

II. The second or physico-chemical stage may consist of a single reaction or a complex succession of reactions. The molecular excitations and ionizations are extremely unstable and promptly undergo secondary reactions, either spontaneously or by collision with other molecules in their vicinity. About 10^{-10}s is required for the physico-chemical stage.

III. The third or chemical stage, which takes about 10^{-6}s, is associated with chemical changes due to the breakage of bonds. If the chain of events, initiated by the absorption of radiation, results from direct hits on target molecules within the cell, it is possible that the atoms of the components of biological molecules could be ionized or excited. This would initiate a

chain of events leading to changes in the nucleic acids, macromolecules within membranes, enzymes and other constituents, which may also be damaged by radiation (18, 55). This is the so-called direct action of radiation or the direct effect (Fig 2.1).

Alternatively, the radiation may interact with atoms or molecules in the cell to produce free radicals which are able to diffuse far enough to reach and damage critical targets. This indirect action theory proposes that radiant energy exerts its effect by producing free radicals within cells, according to the following sequence. Absorbed radiant energy leads to the radiolysis of cell water and the formation of the ionized water molecules H_2O^+ and H_2O^-. These dissociate to form the free radicals $H^\cdot$ and $OH^\cdot$. Free radicals can be defined as atoms or groups of atoms having an odd (unpaired) number of electrons that may enter into chemical-bond formation, which in turn initiate a chain of reactions with themselves, their own reaction products and tissue water to form other radicals such as $HO_2^\cdot$ and $O_2^{\cdot-}$

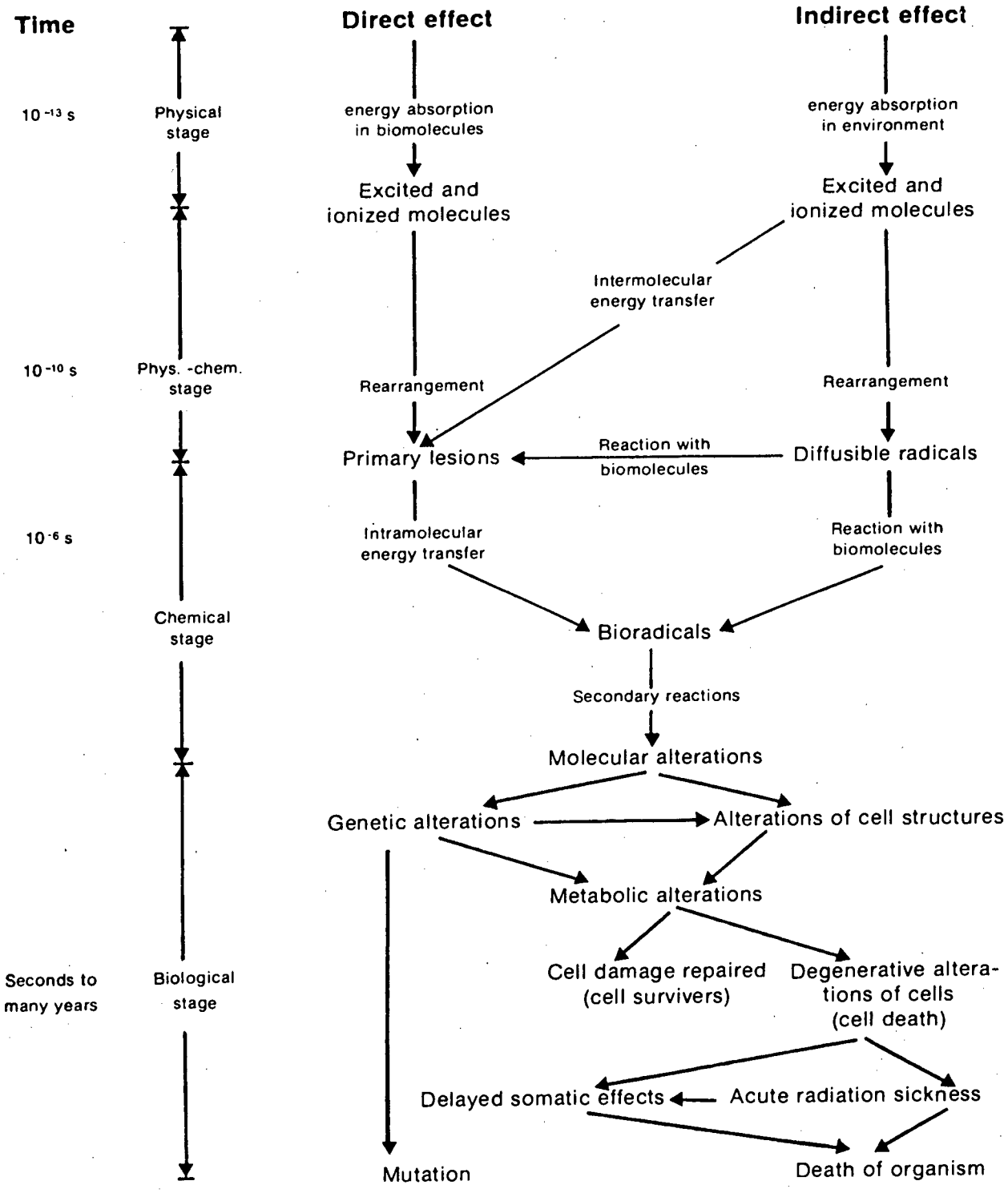

Fig 2.1 Direct and Indirect Effects of Radiation in living matter.

IV. Ultimately, in the biological state these free radicals can interact with critical components, such as membrane bound molecules, nucleic acids and enzymes. Following this sequence, a crucial biochemical change can take place, causing cell damage or death (56, 57). The transfer of energy to a target atom or molecule from the incident source of radiation energy occurs within very small fractions of a second, yet its biological effect may not become apparent for minutes or even decades. Radiation therefore can have latent sequelae. During this latent period, it must be assumed that sequential reactions are occurring that ultimately exert a detectable functional, biochemical or morphological effect (58).

Molecular changes occurring in an organism may cause alterations in the system which is passing through the "biological stage" (Fig 2.1), finally leading to the development of the observed biological effect (59).

The primary processes of radiation absorption can cause small but significant injuries in the organism as a whole. However, the type and magnitude of the damage can depend very much on whether the defect can be repaired (60, 61) or whether the metabolism in attempting to operate under these perturbed conditions, tends to amplify the damage (62, 63).

2.2.1. Target theory

The dose-response curve can be analyzed in terms of the target theory. It assumes that the events occurring as a result of the irradiation, named the "hits", happen independently. Therefore, the Poisson distribution (P(n)) may be used to calculate the probability that a particular member of the irradiated sample will receive n "hits".

$$\text{Probability of hits} = P(n) = \frac{(vD)^n \exp(-vD)}{n!}$$

where v is the volume of the target and D is the radiation dose. It is assumed that if a given member of the sample population is inactivated by n hits, then all the members of the sample that receive fewer than n hits will survive and are presumed to be unaffected by the radiation. Therefore, the probability of survival (N_{sur}/N_o) (where N_{sur} is the number which survive and N_o the initial number in the population) is:

$$\frac{N_{sur}}{N_o} = P(0)+\ldots P(n-1)$$

$$= \exp(-vD)\left(1 + vD + \frac{(vD)^2}{2!}+\cdots\frac{(vD)^{n-1}}{(n-1)!}\right)$$

$$= \exp(-vD)\sum_{0}^{n-1}\frac{(vD)^K}{K!}$$

If n = 1, then $\frac{N_{sur}}{N_o} = \exp(-vD)$

Therefore, if $(\ln \frac{N_{sur}}{N_o})$ is plotted versus D, the target volume is the slope of the line.

Since D = 1 when (N_{sur}/N_o) = 37% or 1/e,
the target volume is also the reciprocal of D_{37}, the dose at which about 37% of the targets survive, or are unaffected.

It is possible to derive expressions for systems with several targets. This is the case in which a given member of the sample must receive n hits on each of several different sensitive volumes within the given member in order to be inactivated. However, such situations are complicated and the inherent variations in the dose-response curves limit the accurate interpretation of the equations.

$$\frac{N_{sur}}{N_o} = 1 - W(D)$$

where W(D) is the probability that a dose D will produce an effect. The value of W(D) will range from 0 to 1 and clearly each hit will increase the value of W(D).

$$W(D) = \frac{dW(D)}{dD}$$

From this expression the variances are derived.

$$m_1 = \int_0^\infty DW(D)dD$$

$$m_2 = \int_0^\infty D^2W(D)dD$$

and $\sigma = m_2 - m_1^2$

The steepness of the dose-response curve may then be defined as:

$$S = m_1^2/\sigma^2$$

From this, it follows that $\bar{n}$, the average number of hits needed to produce an effect must be limited by the condition that

$$\bar{n} \geq S$$

Thus it is possible to determine the value of S from experiment, which gives the least number of hits required to describe the effect of the radiation. Most of the experimental evidence suggests that the dominant processes are single hit events. The dose-response curve is then obtained by plotting the survival fraction as a function of the amount of radiation incident upon the sample. An example is given in Fig (2.2).

The basic idea of the target theory can be expressed as an attempt to determine the number of "hits" per unit volume when ionizing radiation interacts with living matter. From this one derives the volume of the target and therefore the size of the radiation sensitive substructures of the biological system (39). These indicate that in the case of ionizing radiation a "hit" depends on a single transfer to the biological system of a certain amount of energy, the magnitude of which depends on the kind of damage and the system irradiated (64, 65).

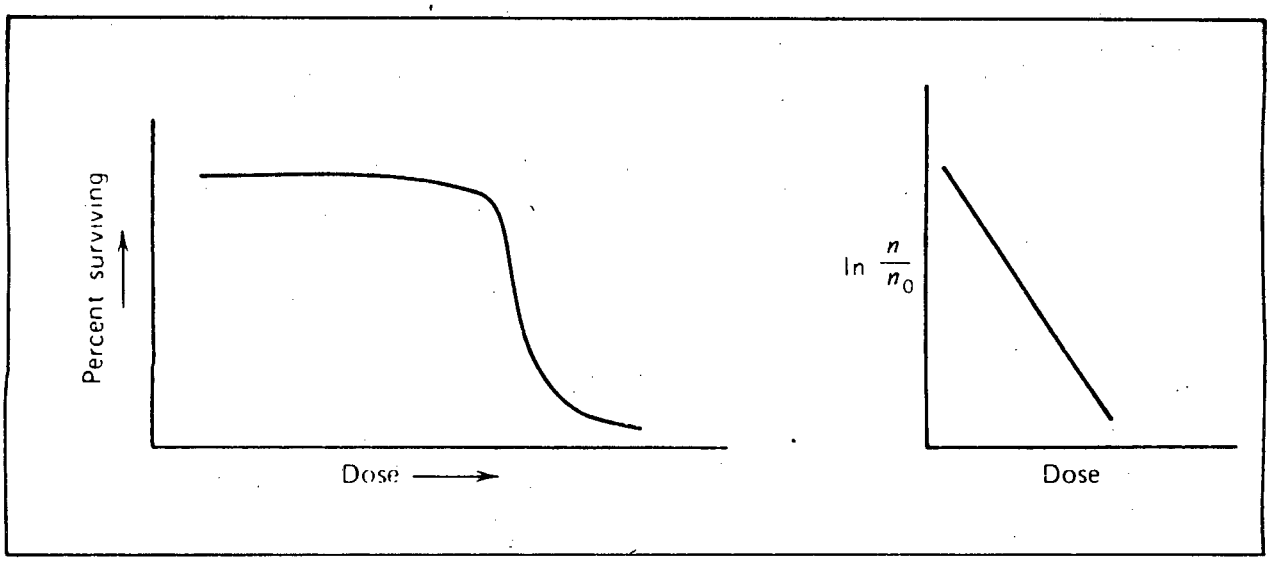

Fig 2.2 The dose response curve.

The notion of the target must not be overinterpreted. Damage to the "target" by "hits" from the radiation is certainly a reality, but action also occurs due to radiation effects elsewhere. This situation has led to the hypothesis of indirect effects in solutions by the radiation.

2.2.2. Radiolysis of water and the primary reactions of the products.

Exposure to ionizing radiation leads to the formation of highly reactive species in most solvents. In water absorption of radiation energy leads primarily to ionised water molecules (ionization potential 12.56 eV):

$$H_2O \rightarrow H_2O^+ + e^- \qquad (2.1)$$

The electron may become stabilized as a hydrated electron, e^-_{aq} and in this form it can produce effects far away from its point of origin because it can diffuse through the water for

considerable distances. The positive ion formed in this process can lead to the formation of OH$^{\cdot}$ radicals by:

$$H_2O^+ \rightarrow H^+ + OH^{\cdot} \qquad (2.2)$$

and the reaction of electrons with water molecules can lead to the production of H$^{\cdot}$ radicals

$$e^- + H_2O \rightarrow OH^- + H^{\cdot} \qquad (2.3)$$

The H$^{\cdot}$ and OH$^{\cdot}$ species as well are formed directly by excitation (about 7 eV) and dissociation of a water molecule

$$H_2O \rightarrow H_2O^* \rightarrow H^{\cdot} + OH^{\cdot} \qquad (2.4)$$

Although a pH dependence of the yields of water radicals might be expected on the basis of these reactions, it is only significant at very high or very low pH values. In the region where $3 < pH < 10$, the G-values (the number of products formed per 100 eV of absorbed radiation energy) for the above products are:

$G_{e^-_{aq}} = 2.3$; $G_{H^{\cdot}} = 0.6$; $G_{OH^{\cdot}} = 2.3$

Recombination processes lead to the formation of H_2, H_2O_2 and H_2O.

High linear energy transfer (LET) radiation, where the local concentration of water radicals is high, will favour recombination, and therefore the formation of H_2, H_2O and H_2O_2 at the expense of radical products. An increase in the yield of H_2 and H_2O_2 with increasing LET, and a consequent decrease in indirect action has been observed.

$$H^{\cdot} + OH^{\cdot} \rightarrow H_2O \qquad (2.5)$$

$$H^{\cdot} + H^{\cdot} \rightarrow H_2 \qquad (2.6)$$

$$HO^{\cdot} + HO^{\cdot} \rightarrow H_2O_2 \qquad (2.7)$$

The formation of free radicals during redox reactions is crucial because of the ubiquitous nature of these processes in living

cells. The two following equations represent the extension of the description of radiolysis of water, when oxygen is present:

$$O_2 + e^-_{aq} \rightarrow O_2^- \qquad (2.9)$$

$$O_2 + H^- \rightarrow HO_2^{\cdot} \qquad (2.10)$$

The free radicals may subsequently react with some critical component if the cell, which may include membranes DNA, RNA, proteins and induce crosslinks, scission and other rearrangements (18, 66, 67) (Fig 2.3).

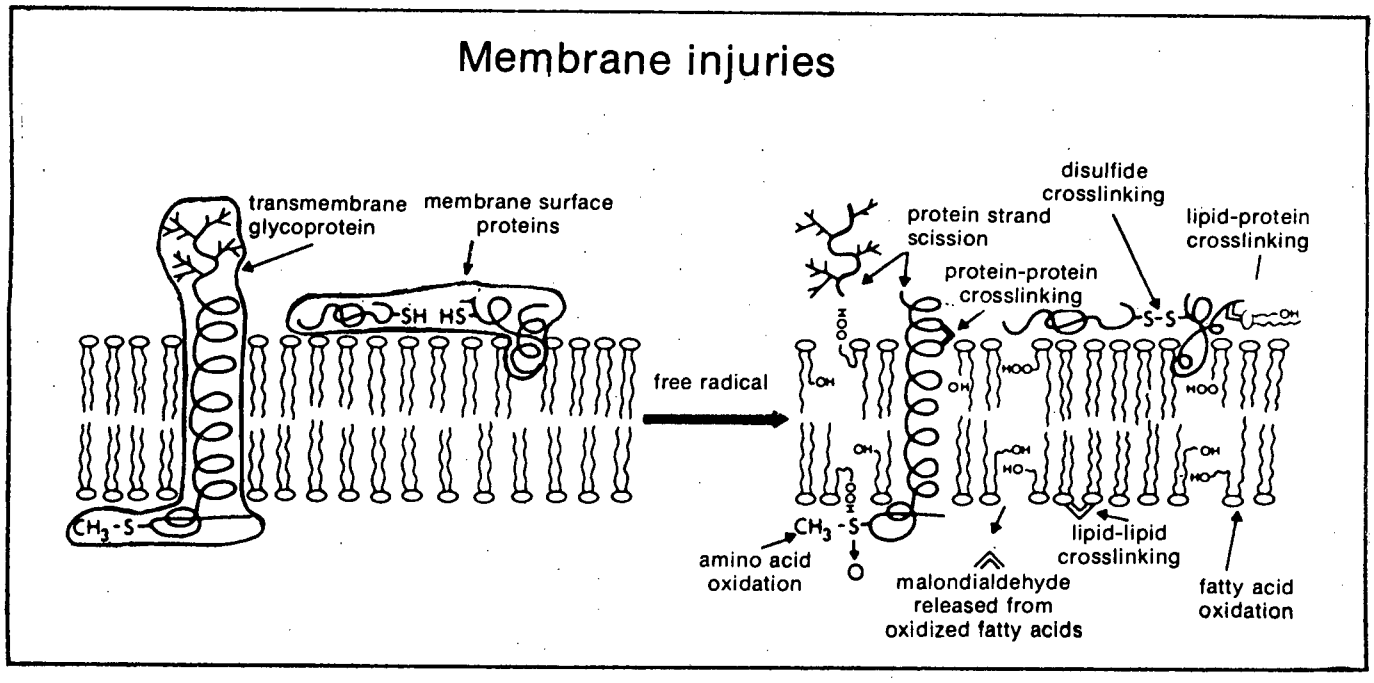

Fig 2.3 Free radical damage to membranes.

2.3 Nature of interactions of magnetic fields with biomolecular systems.

Magnetic fields disturb atomic and molecular energy distributions and wave functions and thus introduce certain spatial and directional asymmetries in electron currents. The extent of these distortions depends on quantum mechanical and thermodynamic considerations. The energy absorbed by the biomolecular system from the sources goes into excitation energy, kinetic energy and electromagnetic potential energy, part of which is dissipated in the form of heat.

The distortions caused by magnetic fields give rise in part to elastic forces (stress) associated with binding forces of the living organism, comprising the liquid and the biomolecules (31, 68). The magnetostriction does not affect the center of mass motion of the body, but it does affect the shape of the body and even in certain circumstances its stability. Destruction of cells may occur if the tensile strength of cell membranes is exceeded.

The magnetization energy or interaction energy (W) of a magnetic field (B') with biological molecules of diamagnetic susceptibility is given as:

$$W = -\tfrac{1}{2} \int_D M.B'dv \qquad (2.11)$$

where the volume integral is taken over the molecule and where M is the net magnetic dipole moment (both diamagnetic and paramagnetic) induced in the body per unit volume. For fields up to 2 Tesla (T) the magnetization energy for small structures is in the order of 10^{-19} to 10^{-21} Joule (J). Molecules and some organized cellular structures have magnetic susceptibilities that vary with direction, for example retinal rods (69), DNA liquid crystals and sickled red cells (70). If this magnetic anisotropy in susceptibility is sufficiently large, then a significant torque can be expected. Any resulting torque or force will depend on the orientation, difference of the susceptibilities between body and surroundings and the square of the magnitude of magnetic field.

The traction $\bar{t}$ on an arbitrary element of the body is given by the following expression:

$$\bar{t} = (\mu+\tfrac{1}{2}(b_2-b_1))\ \bar{H}\ (\bar{H}.\bar{n}) - \tfrac{1}{2}\ (\mu + b_2)H^2\ \bar{n}$$

where $\bar{n}$ is the unit normal (external) vector of the molecules or subcellular units and b_1 and b_2 are the rates of change in μ with respect to strains parallel and perpendicular to $\bar{H}$ respectively. It has been suggested that magnetic fields may affect cell division (71). Cell division is preceded by a DNA replication process which involves

many biochemical reactions requiring extremely complex arrangements of molecular and vital cellular components (72, 73). If these components have anisotropic magnetic susceptibilities, then not only the rotational diffusion rate, but also the relative orientation of these vital biomolecules would be altered. This may, for example, affect the transmembrane permeability, cellular replication and thermodynamic processes (See appendix A). Electron transfers are commonplace in chemical reactions. These reactions generally involve the formation of transient radical ion pairs.

Nonadiabatic electron transfers result in formation of a correlated radical ion pair. The magnetic external perturbations of the radical pairs' spin state may modify the course of some biochemical reactions, as well as various electrochemical processes resulting in a variety of biomagnetic effects (74, 75, 76).

2.4 Some aspects of the biology of neoplasms.

The word oncology is derived from two Greek words, oncos, meaning a mass or a tumour and logos, meaning a dissertation or a special study. Thus oncology is the study of tumours or neoplasia and neoplasm literally means new growth and the new growth is a neoplasm. In this thesis, the terms tumour, neoplasm and new growth will be used synonymously. Briefly, a tumour may be defined as an abnormal mass of tissue or an abnormal cell population with a capacity for progressive growth (77). The origins of a malignant cell population as well as the etiology of a particular type of cancer may very between different tissues within any given species. Nevertheless, two characteristic features which appear to be universally associated with all neoplastic cells are uncontrolled cell proliferation and possibly restricted or aberrant cell differentiation (78). These two phenotypes are not mutually exclusive and may arise by successive somatic cell mutations

and by epigenetic changes in the immediate environment surrounding a potential target stem cell. Abnormalities in the control of gene expression may be a contributing factor in the transformation process as a result of these mutational and/or epigenetic alterations. Many observations suggest that malignant transformation is the result either of abnormal expression of genes normally present in the genome of the host cell, or of some modification of an endogenous gene or genes (79). In either event, gene products such as transforming proteins are produced that alter cell differentiation, replicative activity and inter-cellular behaviour (80, 81). Tumour cells have a clonal origin and are converted to an "initiated" cell, which is a rather stable alteration in the genome (82). This may be true for those genes regulating cell growth and differentation of stem cells in tissues, which are undergoing regeneration or renewal. These processes are probably controlled by a complex interplay of various growth factors and morphogenic and differentiation - inducing factors. Morever, the growth and differentation of any particular population of cells does not proceed in an isolated environment in vivo, but is dependent upon appropriate heterotypic cell-cell interactions (83, 84).

2.4.1. Attributes of transformed tumour cells.

The intracellular, presumably molecular, event or events that bring about the conversion of normal cells to cancer cells is of course a critical issue that is still under investigation. But whatever is involved the phenotype of the tumour cells differs in many ways from the normal (85). These differences can be arbitrarily divided into:

(1) altered growth properties; (2) morphological changes; (3) karyotypic changes; (4) antigenic changes; (5) altered cell surface characteristics and (6) metabolic deviations.

(1) Altered growth properties.

Unregulated proliferation in a fundamental feature of all neoplastic cells. There is a loss of response to regulatory controls of disturbance in the homeostatic mechanism which controls the cell mass of a tissue (86). Failure to mature may play as important a role in the altered growth of cancer as unregulated proliferation. When cells fail to mature, they live much longer than normal cells because the former have not had a terminal differentiation.

(2) Morphological changes.

Lack of differentiation or anaplasia is marked by a number of morphological and functional changes. Both the cells and their nuclei characteristically display pleomorphism (variation in size and shape). Cells may be found that are many times larger than their neighbours and other cells may be extremely small and appear primitive. Characteristically, the nuclei contain an abundance of DNA and are extremely dark staining (hyperchromatic). The nuclei are disproportionately large for the cell and the nuclear-cytoplasmic size ratio may approach 1:1 instead of the normal 1:4 or 1:6. Electron microscopy shows

accentuation of the nuclear chromatin in clumps along the nuclear membrane, simplification of the rough endoplasmic reticulum, an increase of free ribosomes, and greater pleomorphism of the mitochondria.

Oxygen diffuses out from the capillaries and is avidly consumed by active metabolic activity of tumour cells. So it is depleted within a distance of 150-200 μm from the capillary (6, 87). Hence cells lying more than about 150 μm away from the capillary exist in hypoxic and anoxic states with progressive swelling of mitochondria, Golgi apparatus and lysosomes. This is concomitant with falling pH due to glycolysis, lactate accumulation and breakdown of phosphate esters (88). By histological examination of sections, it is possible to distinguish only two classes of cells namely, those which appear to be proliferating healthily and those which are dead or dying. In the anoxic stage necrosis of the cells refers to the sum of the morphological changes occurring within dead cells in tumour tissue. These changes are caused by depletion of oxygen supply and nutrients (89), with consequent mitochondrial dysfunction (lack of oxidative phosphorylation and ATP generation), development of profound disturbances in membrane function and rupture of lysosomes.

(3) Karyotypic changes.

The malignant cells of most types of tumours have chromosomal abnormalities. Most of the chromosomal alterations only became evident with the advent of the newer high resolution banding techniques that now reveal 1200 or more specific bands within the karyotype.

As mentioned in Chapter 1, in many forms of cancer the chromosomal abnormality is related to certain genes, called

oncogenes, through rearrangements of the DNA code, which permit these genes to be expressed and therefore the mechanism of neoplastic transformation assumes a stable alteration in gene expression (90, 91).

In 1911, Peyton Rous discovered the Rous sarcoma virus (RSV), a filterable agent that could produce sarcomas in inoculated chickens (92). However, it was not until many decades later that the gene responsible for tumour induction by the Rous virus was identified in the viral genome. In fact the product of a single gene appeared to be both necessary and sufficient for tumour formation. This was a considerable advance in understanding cancer. It came as a great surprise when it was discovered that the transforming gene, subsequently termed src, had a homologue in normal uninfected cells and that this cellular gene, termed C-src, was conserved not only in the chicken genome, but in the genome of all other vertebrates as well. This work provided the first evidence for the presence of potential transforming genes (oncogenes) in normal cells (93, 94). Several such oncogenes, caused by acute transforming retroviruses have been discovered (Table 2.3). The oncogene is that part of the virus genetically responsible for its ability to cause cancer. These genes are not essential for the growth of the viruses that carry them. However, this advance in the investigation of oncogenic retrovirus did not come from a study of the rapidly transforming viruses such as RSV, but rather from work on tumour viruses with long latent periods, such as the avian leukosis viruses (ALV) of chickens. These viruses were shown to cause tumours by activation of a cellular oncogene (95).

There are at least three different pathways for the initiation of neoplastic transformation: the insertion and expression of exogenous viral oncogenes, a change in the expression of a host gene induced by the insertion of viral DNA in, or adjacent to it, and non-virally mediated change in the expression of an endogenous cancer gene.

In addition to the specific karyotypic alterations in certain tumours, a wide range of non-specific numerical and structural chromosomal abnormalities are frequently present in solid neoplasms (96). These presumably represent secondary changes acquired in the course of tumour progression, related to some altered biological behaviour (97).

TABLE 2.3: RETROVIRAL ONCOGENES.

Retroviral oncogene	Name and origin of virus	Species of origin	Tumour
v-src	Rous sarcoma	Chicken	Sarcoma
v-fps	Fujinami sarcoma	Chicken	Sarcoma
v-fes	Snyder-Theilen feline sarcoma	Cat	Sarcoma
v-yes	Yamaguchi sarcoma	Chicken	Sarcoma
v-ros	Rochester 2 sarcoma	Chicken	Sarcoma
v-myc	Myelocytomatosis, strain MC29	Chicken	Carcinoma, Sarcoma, Myelocytoma
v-erb-A+B	Avian erythroblastosis	Chicken	Erythroleukemia
v-myb	Avian myeloblastosis	Chicken	Myeloblastic leukemia
v-rel	Reticuloendotheliosis, strain T.	Turkey	Lymphatic leukemia
v-mos	Moloney sarcoma	Mouse	Sarcoma
v-abl	Abelson leukemia	Mouse/cat	B-cell lymphoma
v-fos	FBJ murine osteosarcoma	Mouse	Sarcoma
v-raf	Recovered 3611	Mouse	Fibrosarcoma
v-Ha-ras	Harvey rat sarcoma	Rat/mouse	Sarcoma and erythroleukemia
v-Ki-ras	Kirsten rat sarcoma	Rat	Sarcoma and erythroleukemia
v-fms	SM feline sarcoma	Cat	Sarcoma
v-sis	Simian sarcoma	Woolly monkey/ cat	Sarcoma
v-fgr	Gardner-Rasheed sarcoma	Cat	Sarcoma
v-mil	MH2	Chicken	Sarcoma/carcinoma
v-ets	E26	Chicken	Erythroid Leukemia
v-ski	Sloan-Kettering	Chicken	Sarcoma

(4) Antigenic changes.

Cancer cells, when transformed in vitro or in vivo by carcinogenic agents express a range of antigens, most of which are found in normal cells. In addition they express a great many tumour associated antigens that may or may not be present in normal cells, but in any event are more abundant in tumour cells. These tumour-associated antigens, so-called "markers" of the tumour, can sometimes be used with appropriate immunocytochemical procedures to identify tumour cells histologically. Some tumour markers are produced in large quantities and released into the blood in sufficient amounts to be detectable by sensitive immunological assays, and thus provide clinical evidence of the presence of a neoplasm.

(5) Altered cell surface characteristics.

Extracellular regulators of many types probably interact with the cell membrane and then cytoplasmic mediators appear to transmit signals (98) from the membrane to the nucleus, where perhaps they control DNA-binding proteins. The cell membrane, therefore, is implicated in playing a critical role in cell proliferation (99). A number of alterations, have been shown in the plasma membranes of tumour cells and include the following: A loss, diminution, or in some cases acquisition, of such surface specialisations as microvilli and pseudopodia.

- Alterations in cell junctions
- Inconstant cytoskeletal alterations
- Alterations in surface electric charge
- Changes in surface-associated glycoproteins and proteins, particularly enzymes affecting membrane transport.

- Changes in glycolipids and lipids affecting permeability, surface receptors and surface antigens.
- Enhanced lectin agglutinability.
- Changes in responsiveness to inhibitory and stimulatory putative growth factors.
- Alterations of surface-associated and intracellular ions.

The above represents a very incomplete listing, but it indicates the scope of the changes.

Cell surface and membrane changes indicate that there are many deviations from normal that are usually found in tumour cells. Collectively these alterations give some explanation of the attributes of the malignant phenotype in the tumour cells (100).

(6) The metabolism of tumour cells

The stimulating and inhibiting influence of hormones on cell proliferation is known. Hormones may influence cell proliferation via the cyclic AMP/adenylate cyclase system (101, 102), (Fig 2.4).

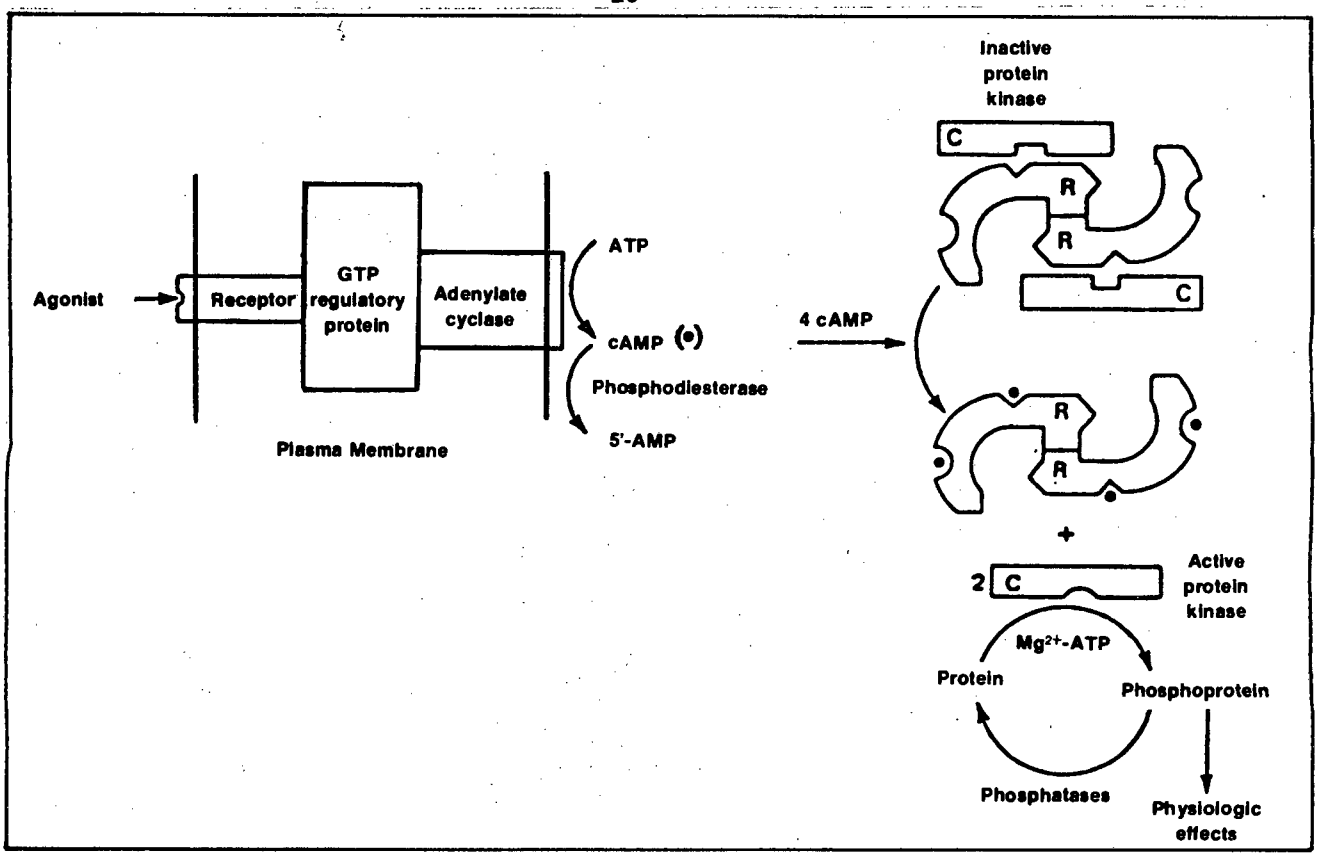

Fig 2.4 cAMP as a second messenger conveying the signal received from the agonist on the plasma membrane to the responsive enzymes within the cell.

Adenylate cyclase is located on the cell membrane and is involved in the formation of cAMP from ATP (Fig 2.5).

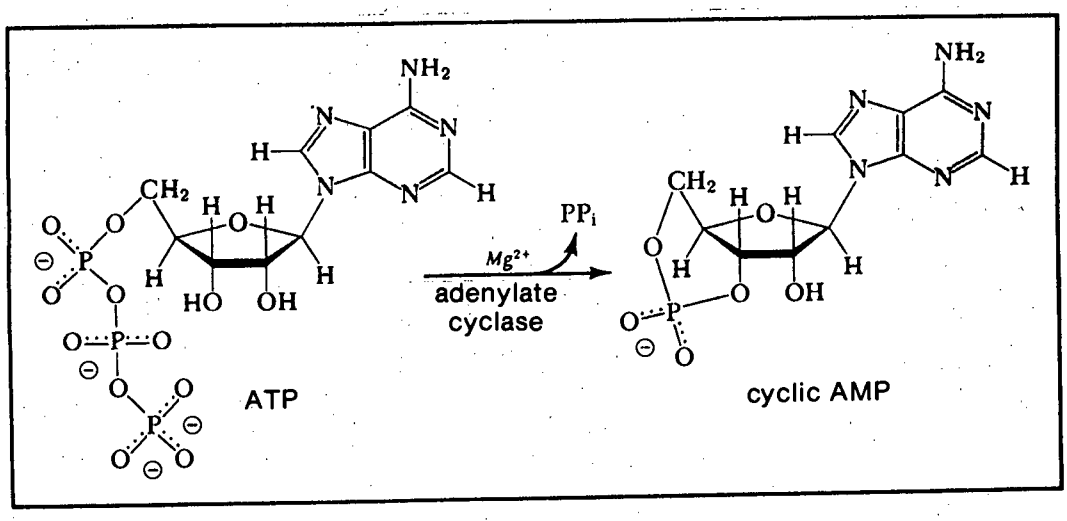

Fig 2.5 The formation of cAMP from ATP.

Cyclic AMP is an intracellular messenger (103). For example hormones that bind to membrane receptors assert their intracellular actions by modifying cAMP levels. It is therefore interesting that reduced cAMP is commonly found in transformed cells, suggesting lack of regulatory signals involved in control of cell growth and division. Underlying the lower levels of cAMP are reductions in membrane adenylate cyclase and increase in the cyclic nucleotide phosphodiesterase involved in its breakdown (104).

In the 1920s Warburg called attention to what he construed to be a fundamental metabolic alteration in cancer cells, namely an unusually high rate of anaerobic metabolism even in the presence of oxygen, so-called aerobic glycolysis (105). It is now recognized that this metabolic change reflects rapid growth of cells (106). There is increased synthesis of cellular constituents required for cell division. There is some conjecture as to the importance of glycolysis in rapidly dividing tissues, and includes the following points:

(1) The rapid proliferation of the cells may disorganize their blood supply to such an extent that sufficient oxygen cannot reach all the cells and anaerobic glycolysis is necessary to provide the energy for cell growth and division (107). Nonetheless, it should be borne in mind that some blood supply will be essential to provide glucose for the glycolytic process (108).

(2) In rapidly growing and dividing cells, several essential macromolecules need to be produced, for example DNA, RNA, protein, polysaccharides and lipids. It has been suggested that a high capacity of glycolysis is necessary to maintain

high concentrations of metabolic intermediates that can be used as precursors for macromolecular synthesis (109).

(3) The change towards a greater glycolytic potential is also accompanied by changes in isoenzyme patterns that are similar to those found in fetal tissue. It is possible that the genetic changes, that are ultimately responsible for the cause of the tumour, may coincidentally cause a change to a cell resulting in a greater glycolytic capacity.

One obvious feature of the tumour cells is that the normal regulation of cell growth and division is impaired or even lost (110).

2.5 Energy and Adenosine Triphosphate

The importance of energy to metabolic processes in heterotrophic organisms, where the nucleoside phosphate pool plays a central role in the transformation of energy from exergonic to endergonic processes, has been extensively reviewed by a number of authors (111, 112, 113). It is my intention, therefore, to discuss briefly the mechanism by which the cell derives its energy with special reference to adenosine triphosphate. Emphasis will however be placed on those areas which are of major importance to the present investigation.

2.5.1 Fuels and the source of cellular energy

The enzyme-catalysed biochemical reactions constituting metabolism include some in which large molecules are broken into smaller ones and others in which small molecules are used for the synthesis of larger and more complex molecules. The enzymatic breakdown or catabolism of cellular fuels involves two major phases in mammals. Firstly there is digestion in the alimentary canal which serves to break the large organic molecules present

in food into smaller molecules, which can be absorbed, distributed throughout the organism, and enter cells in the various tissues. Secondly the absorbed molecules are themselves further degraded in the individual cells of the body. Some of the chemical energy present in these compounds is transferred to other molecules, notably ATP which can be used directly to provide energy (114, 115, 116). In addition, the same products of digestion are used to synthesise new molecules in anabolic processes. These are required for a variety of purposes: to achieve growth and repair of the organism, to replace molecules of the organism which have broken down and to replenish the stores of fuel which subsequently undergo catabolism (117). The important energy-yielding (for example ATP producing) processes in the degradation of organic molecules are oxidative reactions with molecular oxygen acting as the final oxidizing agent. The oxidative processes leading most directly to ATP synthesis, namely the tricarboxylic acid cycle, electron transfer and oxidative phosphorylation Fig (2.6) have been extensively studied by many authors (118, 119, 120, 121).

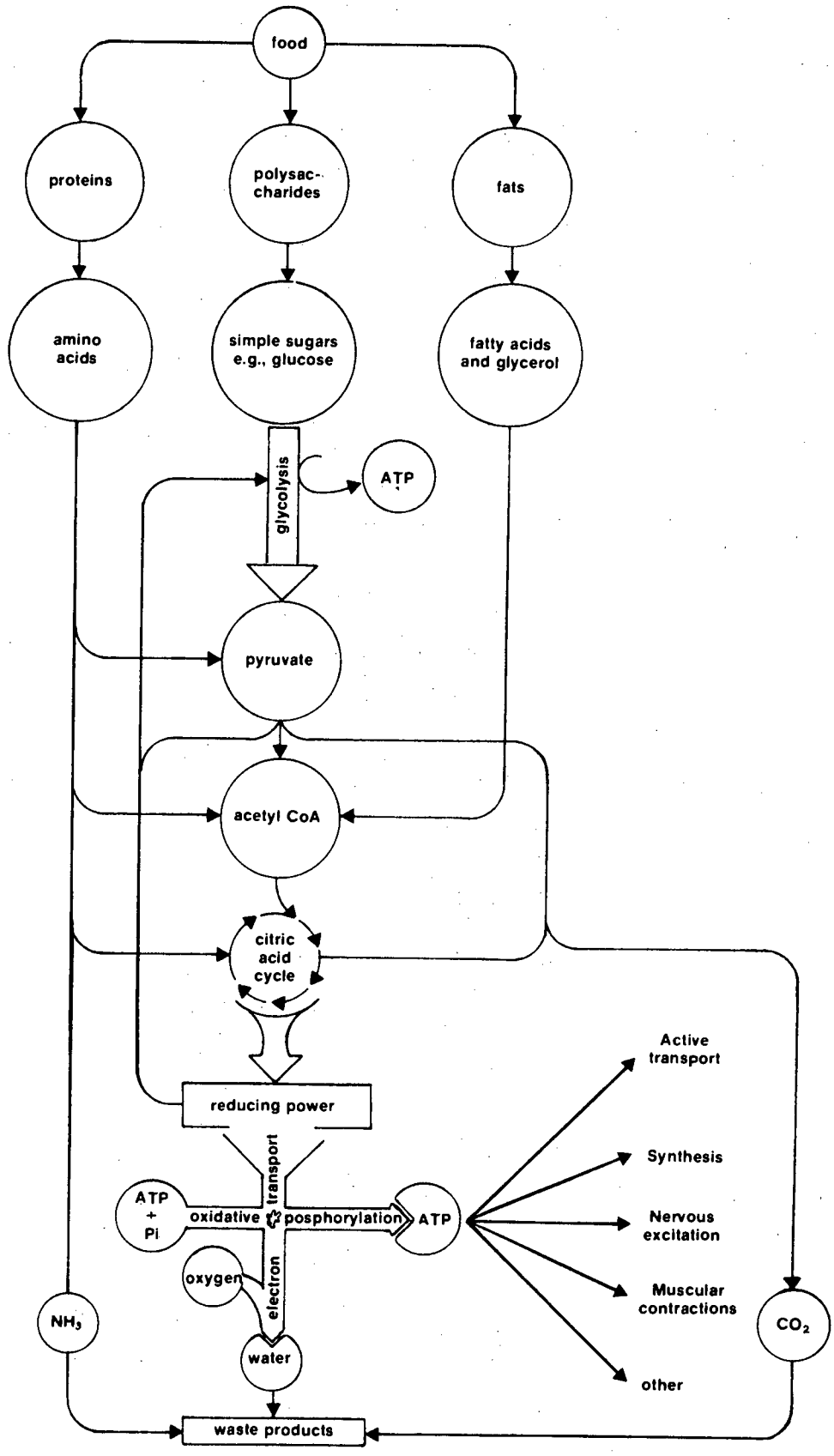

Fig 2.6 Major pathways for ATP synthesis

Through the generation of ATP, the energy originally derived from carbohydrates and fats is redistributed as a conveniently packaged form of free energy, that is easily released (122, 123). Roughly 10^9 molecules of ATP are in solution throughout the intracellular space of a typical cell. The energetically favourable hydrolysis back to ADP and phosphate provides the driving energy for a variety of energetically non-equilibrium reactions (See Appendix A). The yield of ATP from various fuels under aerobic and anaerobic conditions is shown in Table 2.4.

TABLE 2.4: THE YIELD OF ATP FROM VARIOUS FUELS.

Fuel	Conditions	ATP yield (mol) per mol of fuel utilized
Glucose	Aerobic, complete oxidation	38
Glucose	Anaerobic, conversion to lactate	2
Glycogen	Aerobic, complete oxidation	39
Glycogen	Anaerobic, conversion to lactate	3
Palmitate	Aerobic, complete oxidation	129
Acetate	Aerobic, complete oxidation	24

2.5.2 The thermodynamic role of ATP in metabolism.

Adenosine-5'-triphosphate (ATP) is synthesised from ADP and inorganic phosphate (Pi) during the catabolism of fuels such glucose, glycogen or fats. It is used in such processes as muscle contraction, active transport, repair mechanism after metabolic injuries, biosynthesis, etc (124, 125).

The hydrolysis of ATP at pH 7.4 and in the presence of Mg^{2+} can be represented as follows:

$0.88\ MgATP^{2-} + 0.014H\ ATP^{3-} + 0.106\ ATP^{4-} + H_2O \rightarrow 0.40\ MgADP^{-} + 0.06\ H\ ADP^{2-} + 0.54\ ADP^{3-} + 0.04\ MgHPO_4 + 0.10H_2PO_4^{-} + 0.86HPO_4^{2-} + 0.44\ Mg^{2+} + 0.85H^{+}$.

The standard free energy (ΔG) of hydrolysis of ATP, measured at 25°C and pH 7.4, is -8.8Kcal (-36.8 KJ) per mole.

The cells utilize the free energy available from phosphate transfers involving ATP to ensure that certain reactions are energetically favourable (126).

The reason for the relatively large change in free energy when ATP is hydrolyzed under standard conditions is that the products of the reaction (ADP and Pi) are much more stable than ATP at or around pH 7.4. At least three factors contribute to this increased stability (Fig 2.7).

(1) Resonance stability

Compounds are more stable when their bonding electrons are distributed over more than one covalent bond (delocalization). This can be indicated by consideration of a number of extreme structures (resonance or canonical forms) in which the electrons are delocalized with the actual structure in them considered to be intermediate between these forms.

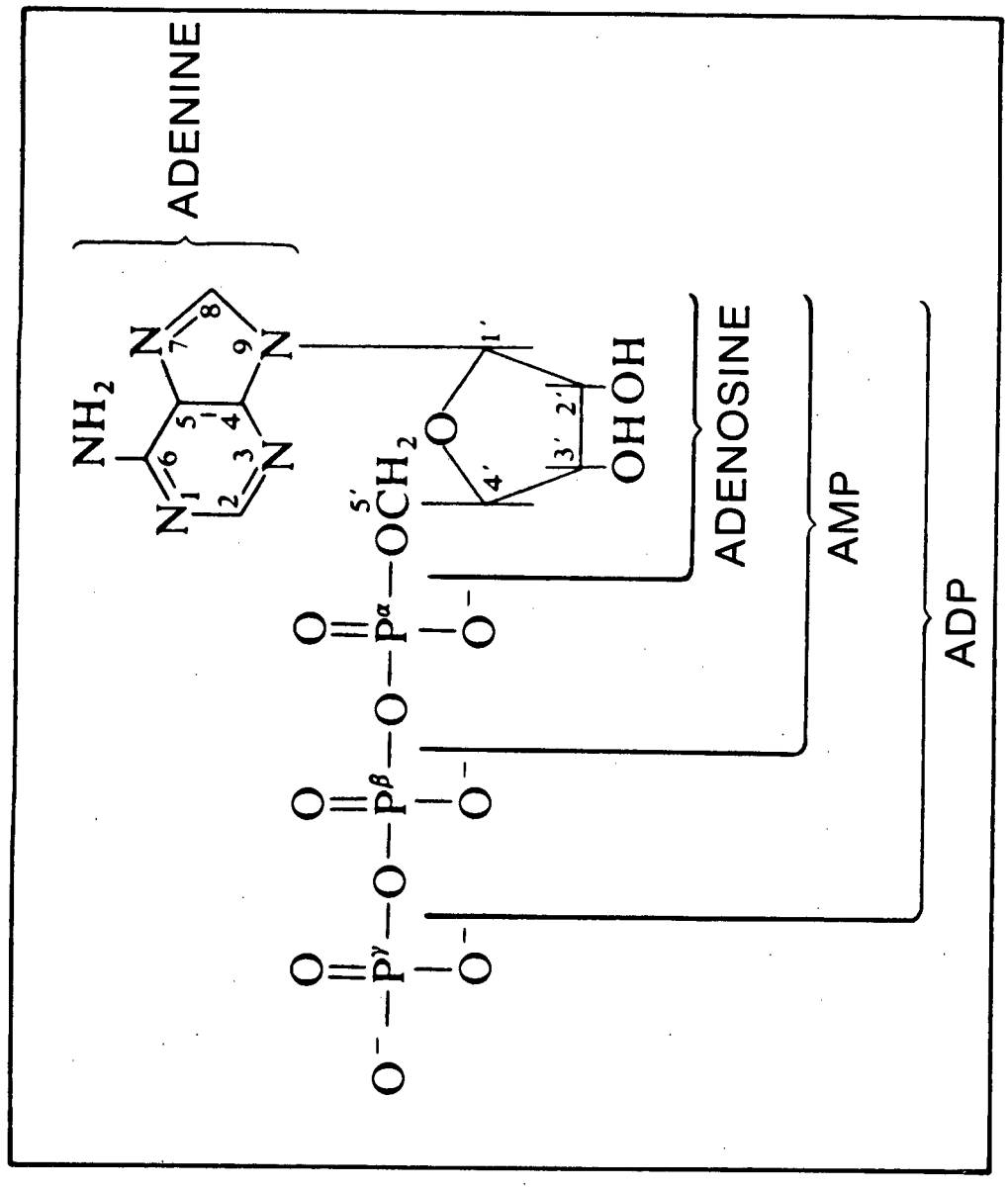

Fig 2.7 Structural formula of ATP

In the phosphate ion all the oxygen atoms are equivalent, so that the actual structure is intermediate between the following resonance forms:

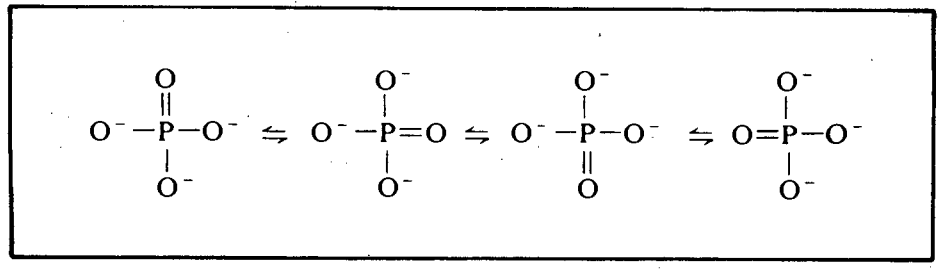

(2) Charge repulsion

At physiological hydrogen ion concentrations the phosphorus atoms of ATP are bound to negatively charged oxygen atoms.

Repulsion between these charges causes strain in the molecule which is relieved on hydrolysis when the charges can separate.

(3) Ionization

On hydrolysis of ATP two new acid groups occur:

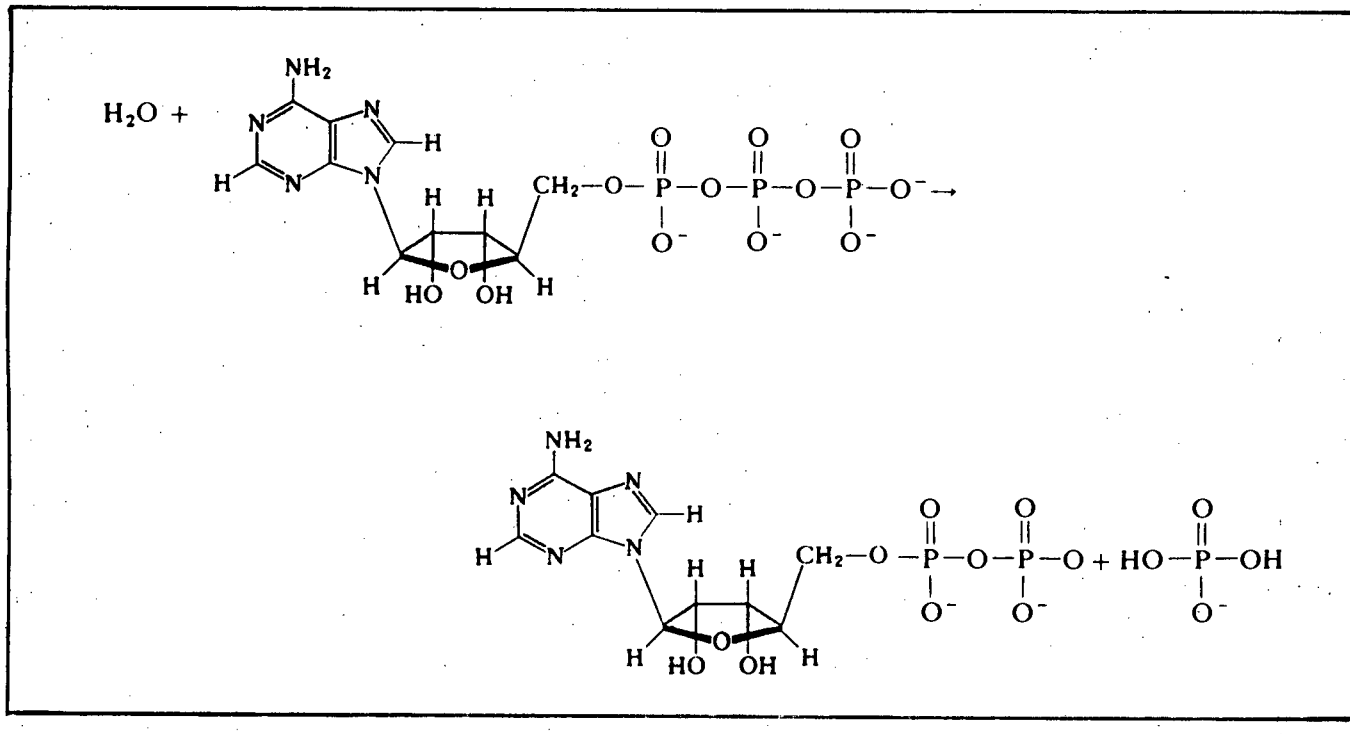

At pH 7.4 one of these groups is partly ionized according to the equation:

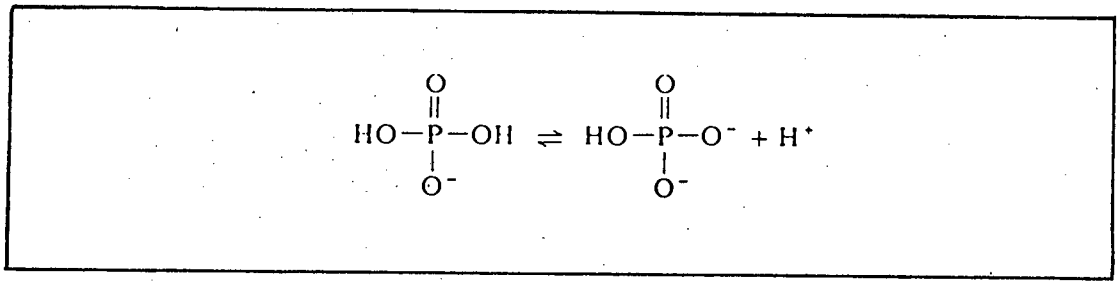

This ionization has a large negative ΔG which contributes to the overall ΔG for ATP hydrolysis.

Factors 2 (charge repulsion) and 3 (ionization) suggest that the ΔG of ATP hydrolysis will be highly pH dependent. That this is the case is seen by comparing the value of ΔG near pH = 0 (-1.25 KJ/mole) with that at pH = 7.4 (-36.8 KJ/mole).

The interplay between various high-energy phosphates is related to the nucleoside phosphate pool. Exergonic processes, such as the oxidation of fuels, drive the phosphorylation of ADP from ATP. Part of the ATP is used to phosphorylate nucleoside mono phosphates to form nucleoside diphosphates and to phosphorylate nucleoside diphosphates to form nucleoside triphosphates.

ATP is used in rephosphorylation of other kinds of nucleotides. Thus the expenditure of any other high-energy phosphate for endergonic purposes, such as the biosynthetic formation of tissue components, and anabolic processes in repairing damage after metabolic injuries (127, 128, 129) is equivalent to the conversion of ADP to ATP. This implies the ultimate result in each case is the replenishment of the high-energy phosphates (Fig 2.8) by highly exergonic processes coupled to the phosphorylation of ADP (130, 131).

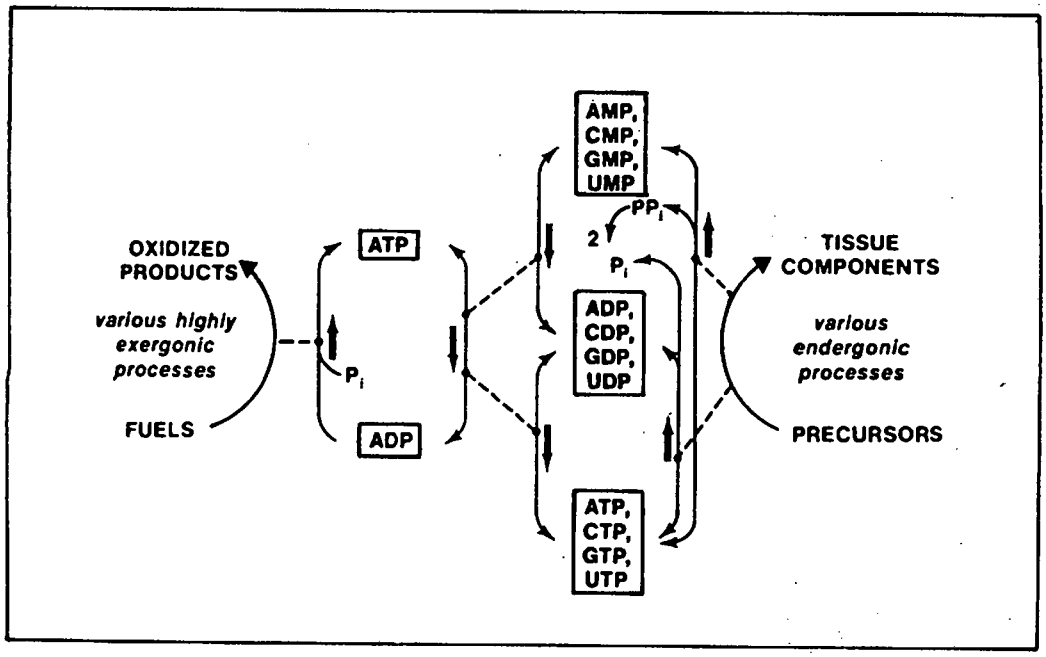

Fig 2.8 The nucleoside phosphate pool

Acknowledging that certain reactions involving ATP are localized in certain regions of the cell is not proof of a functional compartmentalisation. The effects of a biochemical change in one region of the cell are felt very rapidly throughout the cell, for these reactions behave like a functional syncitium.

2.5.3 Intermediary metabolism of carbohydrates.

The metabolism of carbohydrates may be subdivided as follows:

(1) Glycolysis: The oxidation of glucose or glycogen to pyruvate and lactate by the Embden-Meyerhof pathway.

(2) Glycogenesis: The synthesis of glycogen from glucose.

(3) Glycogenolysis: The breakdown of glycogen.

(4) The oxidation of pyruvate to acetyl CoA: This is the necessary step prior to the entrance of the products of glycolysis into the citric acid cycle, which is the final common pathway for the oxidation of carbohydrates, fat and protein.

(5) The hexose monophosphate shunt (pentose phosphate pathway): An alternative pathway to the Embden-Meyerhof pathway for the oxidation of glucose. Its primary function is the synthesis of important intermediates such as NADPH and ribose.

(6) Gluconeogenesis: The formation of glucose or glycogen from noncarbohydrate sources.

2.5.4 The hexose monophosphate shunt.

It is appropriate to consider this pathway in more detail, because it is related to some of the biochemical parameters that were investigated in this work under normoxic and hypoxic conditions in rodent tumours, in response to radiation. The major functions of the hexose monophosphate shunt are to provide NADPH for reductive syntheses outside the mitochondria and to provide ribose for nucleic acid synthesis (132, 133).

The sequence of reactions of the shunt pathway may be conveniently divided into two phases. In the first, glucose 6-phosphate undergoes dehydrogenation and decarboxylation to give ribulose-5-phosphate. Dehydrogenation of glucose 6-phosphate to 6-phosphogluconate occurs via the formation of 6-phosphogluconate catalyzed by action of glucose 6-phosphate dehydrogenase, an NADP-dependent enzyme (134). The hydrolysis of 6-phosphogluconolactone is accomplished by the enzyme gluconolactone hydrolase. A second oxidative step is catalyzed by 6-phosphogluconate dehydrogenase, which also requires $NADP^+$ as hydrogen acceptor (Fig 2.9).

In the second phase, ribulose 5-phosphate is converted back to glucose 6-phosphate through fructose 6-phosphate by a series of reactions involving mainly 2 enzymes: transketolase and transaldolase.

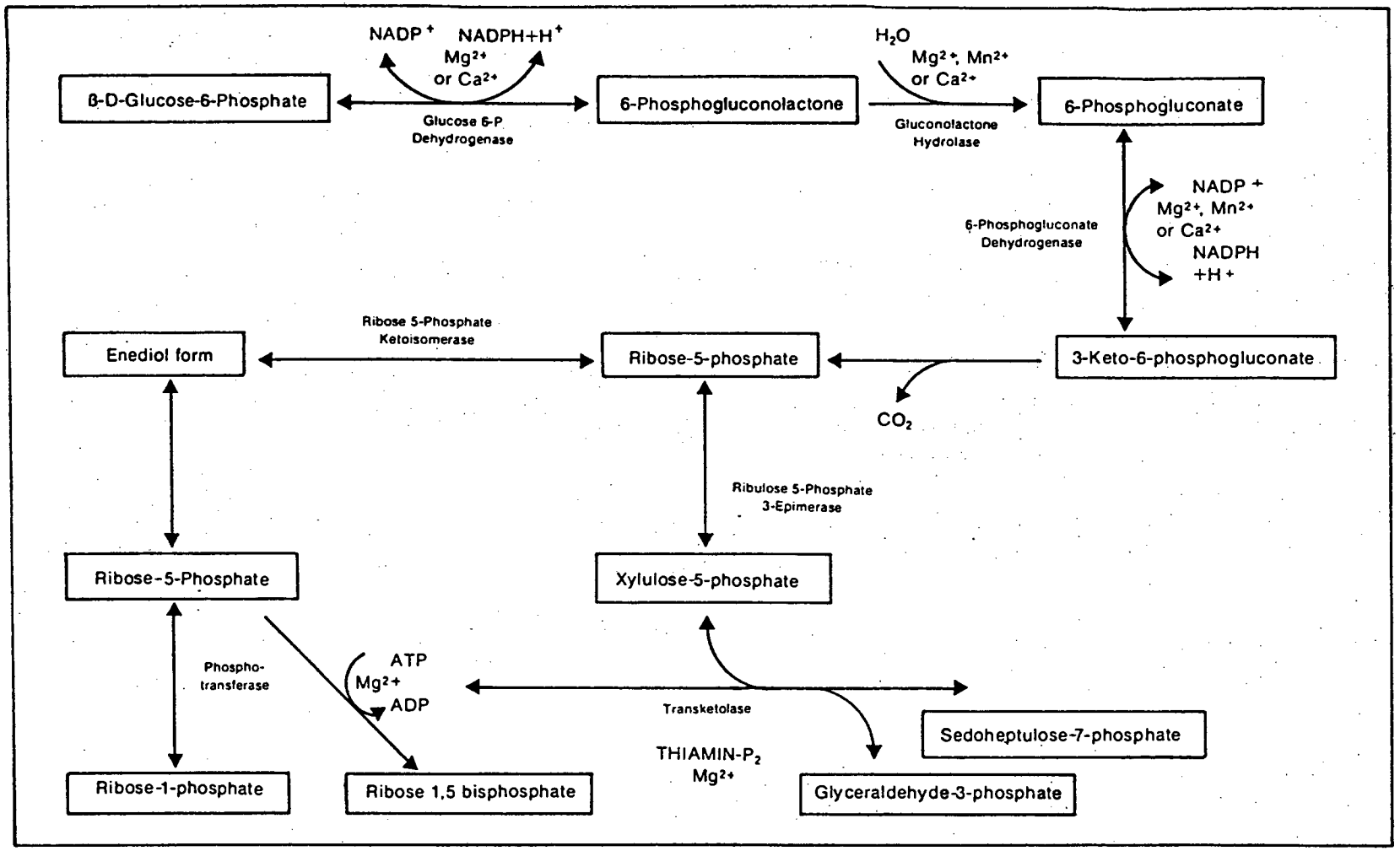

Fig 2.9 The hexose monophosphate shunt.

A summary of the total reaction of the hexose monophosphate pathway may be represented as:

$$3\ \text{Glucose 6-P} + 6\text{NADP}^+ \rightarrow 3CO_2 + 2\ \text{Glucose 6-P} + \text{Glyceraldehyde 3P} + 6\text{NADPH} + 6H^+$$

2.5.5 The metabolic significance of the hexose monophosphate shunt.

Most of the tissues in which the pathway is active use NADPH from the shunt in the synthesis of fatty acids or steroids and in the synthesis of amino acids via glutamate dehydrogenase. It is probable that the presence of active lipogenesis, or of a system which utilizes NADPH, stimulates an active degradation of glucose via the shunt pathway.

The hexose monophosphate shunt provides NADPH for the reduction of oxidized glutathione (G-S-S-G) to reduced glutathione (2GSH), catalysed by glutathione reductase (135).

$$\text{G-S-S-G} + \text{NADPH} + H^+ \xrightarrow[\text{reductase}]{\text{Glutathione}} 2\text{GSH} + \text{NADP}^+$$

Reduced glutathione is important in protecting the cell against free-radical damage initiated by oxygen radicals.

For example superoxide can inactivate the damaging superoxide radical with production of another toxic species, namely hydrogen peroxide

$$O_2^- + O_2^- + 2H^+ \xrightarrow[\text{dismutase}]{\text{Superoxide}} H_2O_2 + O_2$$

In turn reduced glutathione removes H_2O_2 from the cell in a reaction catalyzed by glutathione peroxidase.

$$2GSH + H_2O_2 \xrightarrow[\text{peroxidase}]{\text{Glutathione}} G\text{-}S\text{-}S\text{-}G + 2H_2O$$

Then, the oxidized glutathione is reduced with NADPH from the pentose phosphate pathway.

The hexose monophosphate shunt also provides pentoses for nucleotide and nucleic acid synthesis (136) (Fig 2.9).

2.5.6 Source of Reducing Equivalents (NADPH) by Isocitrate Dehydrogenase.

Both in the cytosol and in the mitochondria there is an NADP-coupled isocitrate dehydrogenase (Fig 2.10).

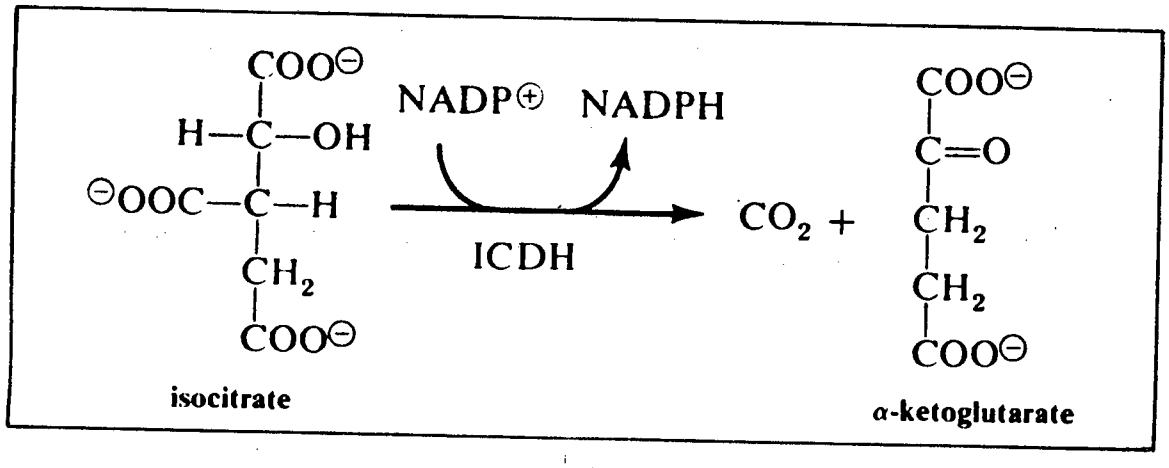

Fig 2.10 Generation of NADPH by isocitrate dehydrogenase.

This enzyme catalyzes the same oxidative decarboxylation of isocitrate that occurs in cytosol and mitochondria during the citric acid cycle. However, in the mitochondria there can be an alternative or additional reaction which uses NAD as the oxidizing agent (137).

The extra energy liberated (ΔG = 17.5 KJ/mole) by the decarboxylation drives the reaction toward completion, generating

a high (NADPH)/(NADP) ratio. It is of interest to note that although some oxidoreductases can utilize both NAD^+ and $NADP^+$ as electron acceptors, most use exclusively one or the other. As a broad generalization oxidoreductases functioning in biosynthetic or anabolic processes in mammalian systems (e g fatty acid or sterol synthesis) tend to use NADPH as reductant, while those functional in degradative or catabolic processes (e g glycolysis or fatty acid oxidation) tend to use NAD^+ as oxidant.

The oxidative reactions of the hexose monophosphate shunt, and the extramitochondrial isocitrate dehydrogenase reaction appear to be a very important route for generating NADPH (138), in addition to the malic enzyme (NADP malate dehydrogenase) in the biosynthesis of fatty acids (139) (Fig 2.11).

2.5.7 Glycolytic metabolic intermediates related to mannose residues.

D-Mannose in a major constituent of the asparagine linked oligoscacharides of eukaryotic glycoproteins (140). The group includes plasma proteins and membrane components such as acetylcholine receptors (141).

The mannose donor for oligosaccharide synthesis in GDP-α mannose, which is formed from α-D-mannose-1-P and GTP by action of a specific pyrophosphorylase.

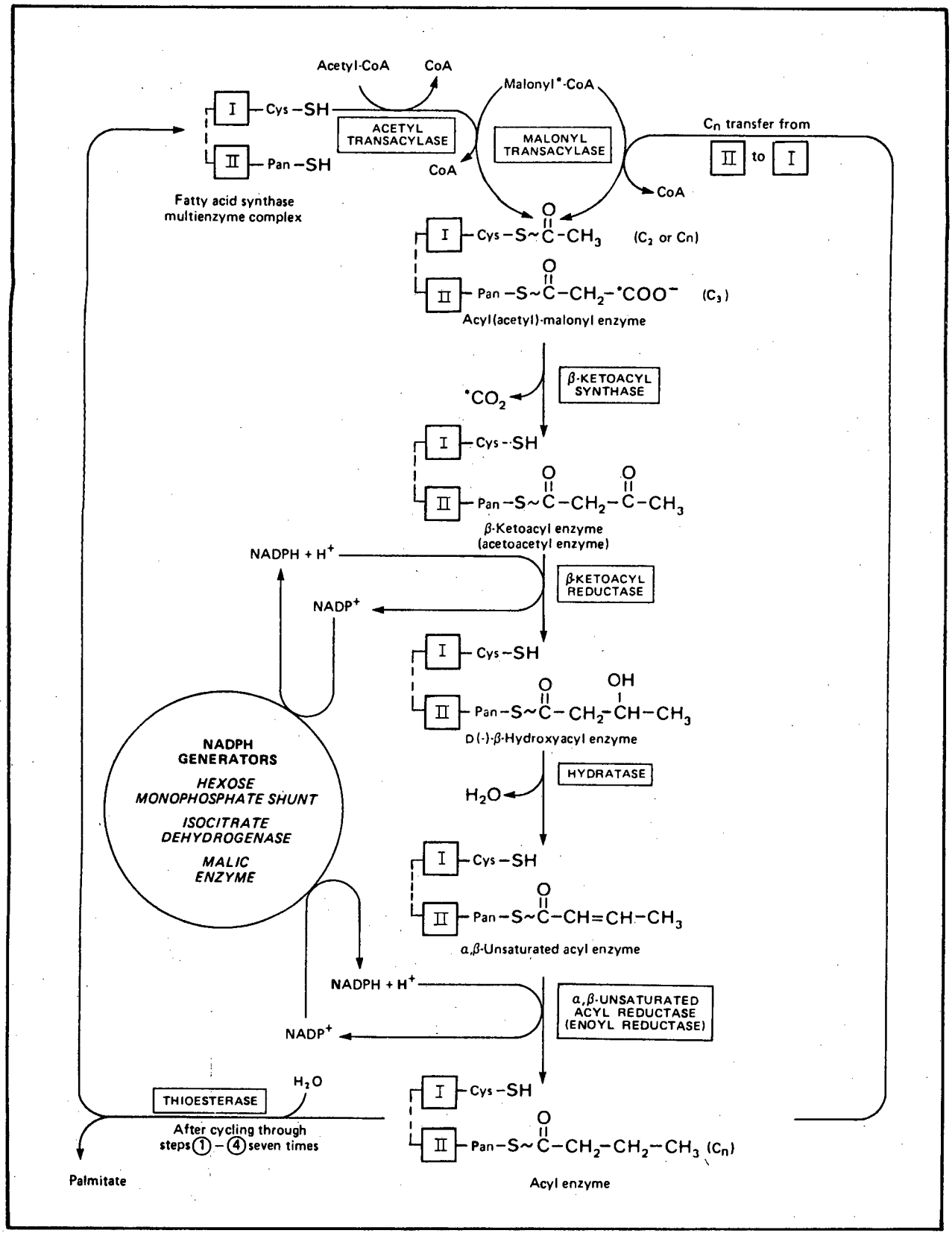

Fig 2.11 NADPH generators: Hexose monophosphate shunt, isocitrate dehydrogenase and malate dehydrogenase.

Mannose chains, some of which are shown below (Fig 2.12) are found in cell membranes.

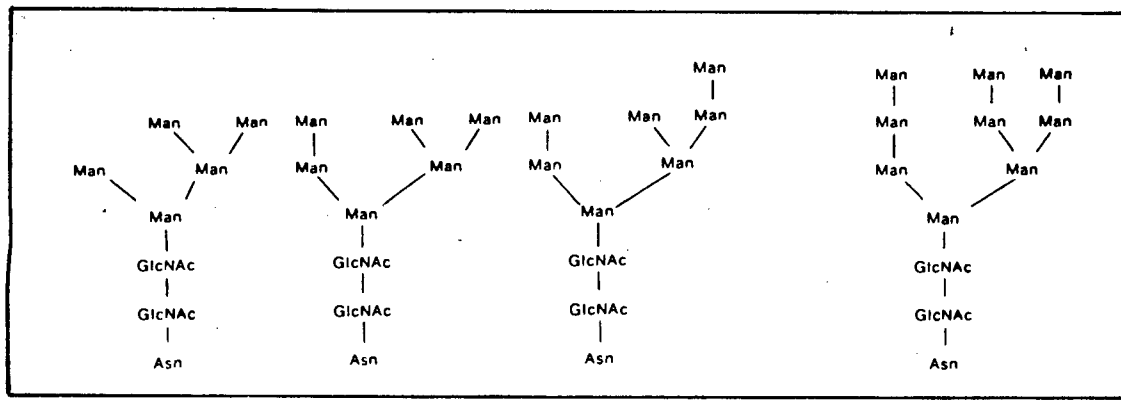

Fig 2.12 Structures of high mannose chains. Mannose (Man), Glucose (Glc), N-acetylglucosamine (GalNac), Asparagine (Asn).

Mannose phosphates originate from the glycolytic intermediate glucose-6-P through the action of two enzymes, phosphoglucose isomerase (PGI) and phosphomannose isomerase (PMI) (142, 143) as indicated below in (Fig 2.13).

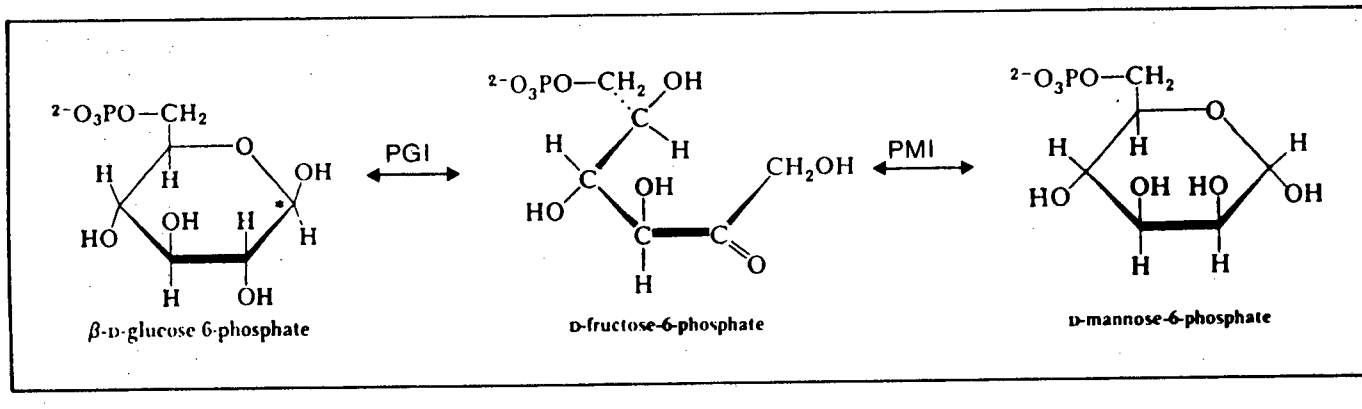

Fig 2.13 Interconversion of glycolytic intermediates by the action of PGI and PMI.

Phosphomannose mutase (PMM) catalyzes the interconversion of mannose-6-P and mannose-1-P (144).

The glycolytic metabolic intermediate pathway is related to mannose residues as represented in (Fig 2.14). It enables mannose 6 phosphate to be catabolised through the action of phosphomannose isomerase, via the glycolytic pathway (145, 146, 147).

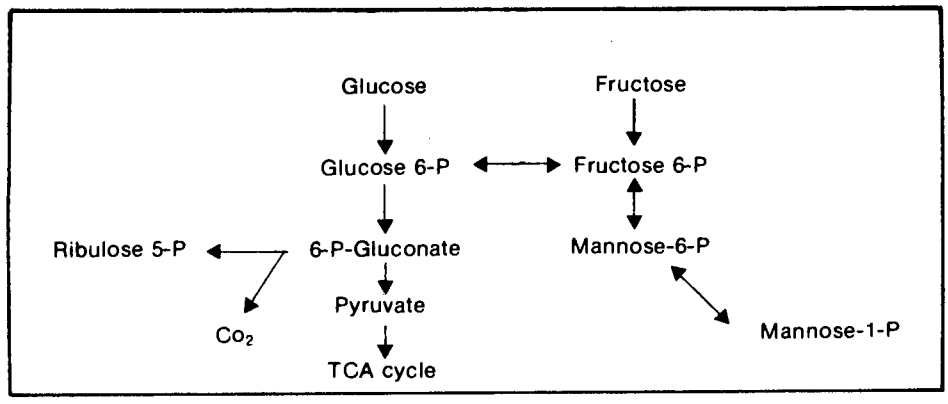

Fig 2.14 Glycolytic pathway related to mannose residues (TCA = tricarboxylic acid cycle)

2.6. Mitoxantrone an anticancer drug

There is presently a great deal of interest in combining ionizing radiation and anticancer drugs in the laboratory with the aim of providing new strategies in the clinic. It became apparent during the course of this investigation that an agent was required that would inhibit the increase in energy production seen after irradiation (Chapter 5). Neri et al (148) reported that mitoxantrone inhibited ATP production in rat heart slices. Thus this drug theoretically provides a means of inhibiting the increased energy production after irradiation, which may lead to enhanced tumour cell kill.

Mitoxantrone is an anthracenedione with structural similarities to doxorubicin, but without the daunosamine sugar group (149). The

structural formulas of mitoxantrone and doxorubicin appear below (Fig 2.15).

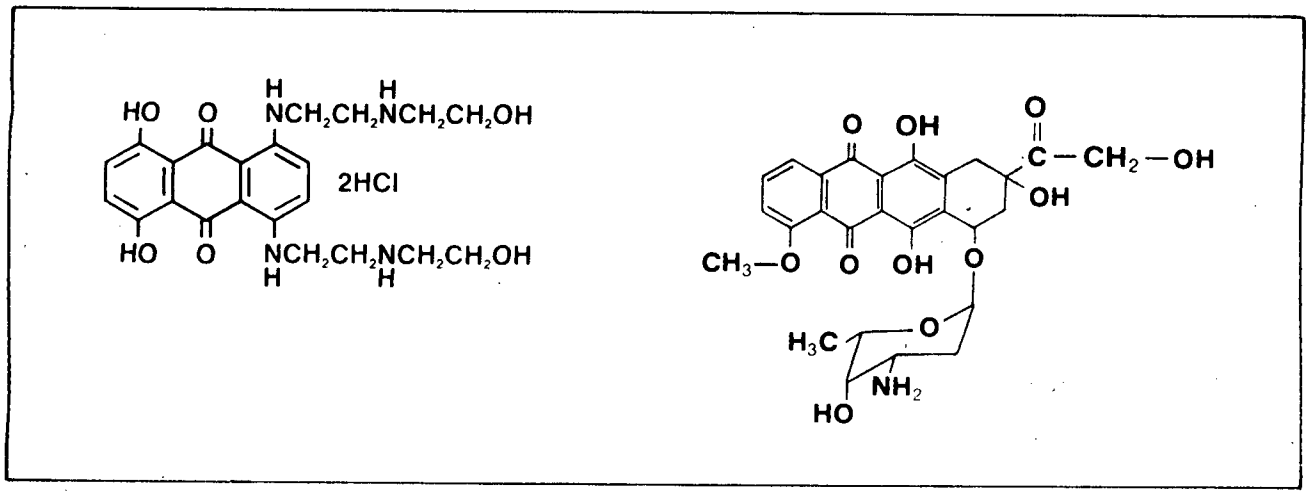

Fig 2.15 Structural formulas of mitoxantrone (left) and doxorubicin (right).

The molecular formula of mitoxantrone is $C_{22}H_{28}N_4O_6 2HCl$, its name 1,4-Dihydroxy-5,8-bis {(2-(2-hydroxyethyl)amino)-ethyl} amino-9,10-anthracenedione dihydrochloride and its molecular mass is 517.4.

The precise mechanism of action with which mitoxantrone exerts its tumoricidal effects has not been fully defined (150, 151, 152, 153). It is most likely associated with the action of mitoxantrone on chromosomal elements resulting in DNA alterations, leading to inhibition of nucleic acid synthesis and eventual death of the cell (154, 155).

Studies by a number of investigators indicate that mitoxantrone inhibits RNA and DNA synthesis and intercalates into DNA (156, 157). Mitoxantrone interacts with both double and single-stranded nucleic acids by intercalating between base pairs of the DNA helix and

distorting that structure. However the actual structure of the intercalated complex has not been fully elucidated (158).

Although the mitoxantrone molecule contains a planar aromatic chromophore, which might be expected to facilitate DNA intercalation, the presence of two extended alkyl residues on positions 1 and 4 precludes the smooth incorporation of all parts of the molecule into the intercalated compound. This consideration has led to suggestions that binding of mitoxantrone to DNA may include both, partial intercalation and external binding (159, 160). Mitoxantrone binds to DNA whether or not the cells are in active anabolism preparing for cell division. It can thus kill tumour cells irrespective of their position in the cell cycle at the time of exposure to the drug.

Leukemic cells cultured with mitoxantrone show a dramatic effect on cell progression through the cell cycle. The DNA distribution in drug treated cells showed a significant accumulation in the G_2 phase. While there is a significant increase in cell volume, for mitoxantrone treated cells, the RNA content of these cells, which are blocked by the drug, increased significantly (3 fold) in the treated cells (161). Traganos et al (162) also demonstrated that mitoxantrone treated mammalian cells in culture are blocked in the G_2 phase. This resulted in a more than 2 fold increase in RNA content. In leukemic cells treated with mitoxantrone, enlarged nucleoli and increases in levels of DNA, due to drug-induced polyploidy, are observed. Although cells are most sensitive to the bocking effects of mitoxantrone in late S phase, (manifiested as G_2-M block), cell kill is not cell cycle phase specific.

There are other metabolic effects of mitoxantrone related to its quinone functional groups (163, 164).

These quinone agents may be enzymatically activated within the cell to free radicals by a microsomal enzyme system requiring NADPH as an

electron donor. Essentially any biological system containing NADPH has the potential to reduce quinone-containing compounds to free radical semi-quinones. The important role of free radical production, as well as decreasing oxygen consumption in cell metabolism after treatment with mitoxantrone will be more fully discussed in chapter 5 in connection with the experimental results obtained in this thesis.

CHAPTER 3

MATERIAL AND METHODS

This chapter will describe the type and source of experimental mice and rats, the experimental design and the procurement of various tumour tissues. Following this section, experimental techniques will be detailed with appropriate discussion.

3.1 Experimental Animals

Three strains of mice were used in the investigations, namely CBA, BALB c and WHT. The strain of rat used was WAG/Rij.

All experimental animals were bred in the Medical School Animal Unit, University of Cape Town, 7925 Observatory, South Africa. Experimental animals were kept in the Radiobiological Laboratories, Department of Radiotherapy, University of Cape Town. Mice and rats were fed with Epol Mouse or Rat Cubes (Atlas Feeds, 392 Main Road, Wynberg, Cape). Water was allowed ad libitum.

The temperature in the animal rooms was kept at 22° ± 1°C.

3.1.1 Experimental Rodents and Tumours

3.1.2.1 CBA Mice and the CaNT Tumour

Male CBA mice were used in the experimental work (Fig 3.1). Their age at the beginning of any procedure was six weeks and their weights ranged from 18 to 24g.

The experimental CaNT tumour was originally obtained from Professor R. Berry of the Middlesex Hospital Medical School, University of London, England, and maintained by serial passage (See 3.1.3.1).

The volume of the tumours (as deduced from measurements in 3 orthogonal directions - See 3.1.2.4) used in these investigations was between 150 and 300mm^3.

Fig 3.1 Male CBA mouse with CaNT tumour (arrow)

3.1.2.2 BALB c Mice and the 3-Methylcholanthrene - Induced Transplantable Rhabdomyosarcoma.

A transplantable rhabdomyosarcoma was induced by injection of 0.1 mℓ of a 1mg/mℓ solution of 3-methylcholanthrene in arachis oil subcutaneously into the right thigh region of six 6 week old male BALB c mice (Fig 3.2). It was found that a rhabdomyosarcoma developed in all mice in approximately 3 to 4 months. Male BALB c mice used in the studies described hereunder were 6 weeks old, with a weight range of 18 to 22g, before any procedure took place. The rhabdomyosarcoma was maintained by serial passage in the upper right leg of the BALB c mice (see 3.1.3.1), which was also the position used in the experiments. The volume of the tumours (as deduced from measurements in 3 orthogonal directions - see 3.1.2.4) used in the investigations was between 150 and 300 mm^3.

Fig 3.2 Male BALB c mouse with a transplantable rhabdomyosarcoma (arrow)

3.1.2.3 WHT Mice and the Fib/t Tumour.

Male WHT mice were used whose age before any procedure was 6 weeks. The weight range was 18 to 23g. The transplantable Fib/t murine fibrosarcoma was grown on the sternum region of the WHT mice. This tumour was obtained from Dr N. McNally of the Gray Laboratories of the Cancer Research Campaign, Mount Vernon Hospital, Northwood, Middlesex, England, and maintained by serial passage (see 3.1.3.1).

Again, the volume of the tumour as calculated from measurements in 3 orthogonal directions used in the experiment was between 150 and 300 mm^3 (see 3.1.2.4).

3.1.2.4 Measurement of Volume of Experimental Mouse Tumours.

Mouse tumours were measured in 3 orthogonal directions using Vernier calipers. The following formula was used to calculate the volume:

$$\text{Volume} = \left(\frac{L + B + H}{6}\right)^3 \frac{4\pi}{3}$$

This assumed the experimental tumours to be of spherical shape.

3.1.2.5 WAG/Rij Rats and the R1 Tumour

Male WAG/Rij rats were used. The age of the rats was 8 to 10 weeks and the weight ranged from 160 to 220g (Fig 3.3). The transplantable rat rhabdomyosarcoma R1 was grown on the flank of these WAG/Rij rats, and maintained by serial passage (see 3.1.3.2). This tumour was obtained originally from Dr G.W. Barendsen, Radiobiological Laboratories, Rijswijk, The Netherlands.

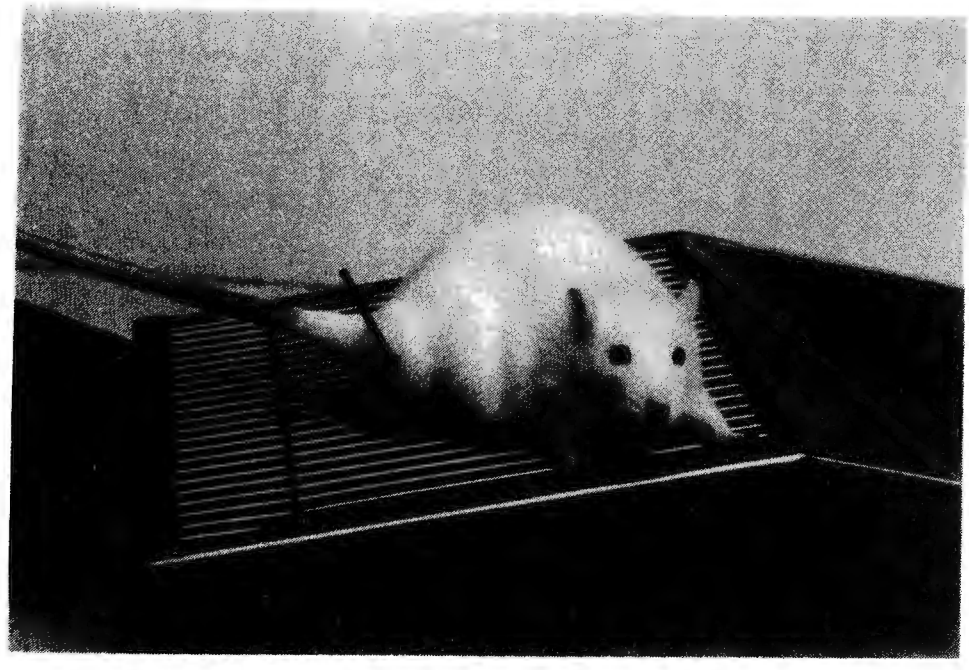

Fig 3.3 Male WAG/Rij rat with rhabdomyosarcoma R1 (arrow)

3.1.3.1 Propagation of Tumours in CBA, BALB c and WHT mice.

Tumour-bearing mice were killed by prolonged exposure to ether, then tumours removed by surgical excision. Approximately 5 mℓ of McCoy's 5A medium with L-Glutamine and $NaHCO_3$ to adjust the pH to between 7.2 and 7.4 was put in a 65x15mm Falcon Plastics petri dish, and tumours from 3 animals added. Tumour specimens were chopped finely in small pieces using sterile blades.

After chopping the total preparation was aspirated through a 12x38mm size needle into a sterile syringe (B-D plastipak). The supernatant containing tumour cells was then placed into a plastic test tube (Falcon) and the preparation was allowed to settle for a few minutes.

Subsequently 0.1 mℓ of the upper layer of the preparation was inoculated using 0.45x13mm needle by subcutaneous injection.

The CaNT and Fib/t tumour cell suspensions were injected subcutaneously into the sternal region of respectively CBA and WHT mice, and 3-methylcholanthrene induced rhabdomyosarcoma cells into the outside right upper leg of BALB c mice.

The experimental tumours appeared 10 to 20 days after inoculation.

3.1.3.2 Propagation of Tumour in WAG/Rij Rats

Tumour-bearing rats were killed by prolonged exposure to ether and the tumours excised. Tumours were placed in medium as described in 3.1.3.1 above. Afterwards

the tumour specimens were chopped up with surgical blades and a cube of tissue of size about $2mm^3$ was inserted with forceps into a small incision in the posterior right lateral mid-thigh region of WAG/Rij rats. The experimental tumour appeared about 20 days after the inoculation of the tumour.

3.1.3.3 Clamping of the CaNT tumours in CBA Mice.

The procedure adopted to clamp the CaNT tumours grown on the sternum of CBA mice was to retract the tumour and associated skin away from the body of the ether-anaesthetized mouse and tie a thin string firmly around the skin flap between the host and tumour. This clamp should in principle prevent blood from flowing through the blood vessels into the tumour.
The clamp was left in place for up to 2h.

3.2.1 Tissue Culture Techniques

3.2.1.1 Cell Line and Cell Culture Conditions

The B16 mouse melanoma cell line is an established line and can be cultured in vitro using essentially the method outlined by Puck and Marcus (165). The cells were cultured in $25cm^2$ plastic tissue culture flasks (Falcon Plastics) using McCoy's medium (Gibco) supplemented with 10% foetal calf serum and the antibiotics neomycin, penicillin, and streptomycin. The final concentrations of the latter in the medium were respectively 0.5U/mℓ, 0.25U/mℓ and 0.25U/mℓ.

Cells were grown at 37°C and in a humidified atmosphere containing 5% CO_2.

3.2.1.2 Sub-culture of B16 Cells

Reagents

(a) EDTA in phosphate buffered saline was made up to 10 times the required concentration. A solution was made up containing NaCl, 82g; Na_2HPO_4, 12.78g; $NaH_2PO_4.2H_2O$, 2g and EDTA disodium salt, 2g in 1ℓ. The pH was adjusted to 7.4 with concentrated NaOH solution, and the reagent was filter sterilized through a sterile 0.22 μm Millipore filter. The stock EDTA solution was stored frozen in 10 mℓ aliquots. The stock solution was diluted 10 fold with sterile water before use.

(b) Trypsin in phosphate buffered saline was also made up as a 10 times concentrated stock solution. The trypsin solution was prepared thus: NaCl, 82g; Na_2HPO_4, 12.78g; $NaH_2PO_4.2H_2O$, 2g; EDTA disodium salt, 1g and trypsin (Difco 1:250) 5g were dissolved in 1ℓ of water, the pH adjusted to 7.4 with concentrated NaOH, then filter sterilized through a sterile 0.22 Millipore filter. This stock solution was also stored frozen at -20°C in 10 mℓ aliquots. The stock trypsin solution was diluted 10 fold with sterile water before use.

Procedure

Medium was poured off the cells (stock B16 cell cultures), then the cells were rinsed twice with 3 mℓ 0.02% EDTA in phosphate buffered saline. Cell cultures were then trypsinized by the addition of 2 mℓ 0.05% trypsin solution, which was left in contact with the cells for 4 to 6 min at 37°C in a CO_2 incubator. The

cells became detached from the bottom of the culture flasks by this procedure, then the contents of the flasks were transferred to plastic centrifuge tubes. Two mℓ of McCoy's growth medium conaining 10% foetal calf serum and antibiotics were added to each tube, then tubes were centrifuged at 1000 rpm for 5 min in a Runne bench-top centrifuge. The supernatants were discarded and the cell pellets resuspended in 5 mℓ growth medium. The cell concentrations were obtained by counting a sample of the cell suspensions in a haemocytometer, then the volumes containing $2x10^5$ cells were pipetted into clean sterile 25 cm^2 Falcon flasks. Growth medium was added to result in a total volume in each flask of 5 mℓ.

Flasks were placed in a humidified CO_2 incubator at 37°C, then periodically checked with an inverted microscope (Wild) to monitor growth. Medium was changed when colour changed to yellow. Cells were cultured until they became confluent, when they were either further sub-cultured or used in experiments.

3.3.1 Irradiation Techniques - Ionizing Radiation

3.3.1.1 Restraining Device for Mice.

The CBA, WHT and BALB c mice with experimental tumours and which were to be subjected to irradiation were positioned on a jig made of Perspex (acrylic plastic). The mice were immobilized on the jig with rubber bands on the front and back legs as shown in Fig 3.4 (CBA mice). Mice were not anaesthetized during irradiation.

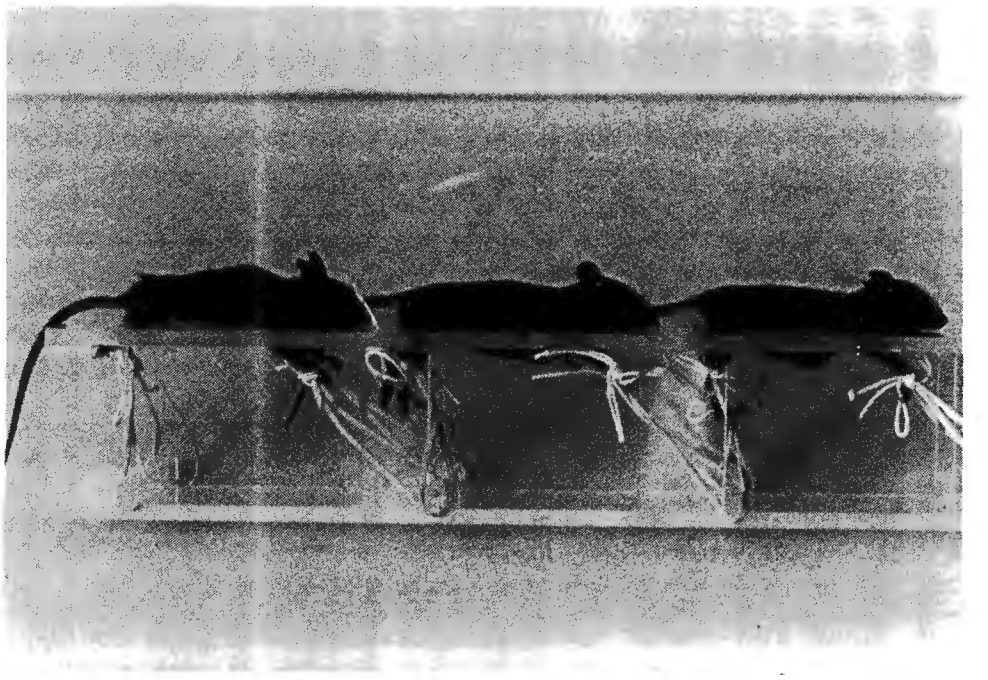

Fig. 3.4 Restraining device for mice during irradiation

3.3.1.2 Medium Voltage X-ray Unit.

A large proportion of the x-irradiations in this investigation was performed with a Philips RT100 X-ray unit, 100 kVp, 3.0mm Al HVL, 8mA. A source to surface distance (SSD) of 12.5cm was used with a circular field of diameter 2.5cm.

3.3.1.3 Dosimetry of the 100 kVp X-ray Unit.

The x-ray unit was calibrated with a flat (small volume - $0.3cm^3$) ionization chamber connected to a Baldwin-Farmer substandard dosimeter and placed at the end of a circular applicator, diameter 2.5cm, SSD 10cm. The dose rate at this distance in the centre of the

field was measured to be 7.36 Gy min^{-1} when the output of the machine was 65 Roentgens min^{-1}, measured at 30cm SSD using a circular applicator, diameter 5cm. The output was measured weekly at 30cm SSD with the circular 5cm diameter applicator, and changes in output were corrected for in the calculation of dose given to the experimental tumours. Tumours on the sternum were irradiated in such a way that half the dose was given from one side and half the dose from the other. This aided dose homogeneity. The variation in x-ray dose across the tumour was calculated to be not more than 17.02% (166). All parts of the mice apart from tumour were shielded with 3mm thick lead.

3.3.1.4 Irradiation of R1 Rat Tumours with 8MV X-rays

WAG/Rij rats were immobilized using a jig as shown in Fig 3.5. Rats were not anaesthetized during x-irradiation. The rat sarcoma was irradiated with 8 MV x-rays from a Philips SL75-20 linear accelerator, using a 5x5cm field. Two cm thick blocks of acrylic plastic were positioned in front of the tumour as build-up material. Lead blocks 7.5cm thick shielded all parts of the rat apart from the tumour.
The tumour dose given was 10Gy. Calibration of the 8 MV x-rays was with an ionization chamber positioned in the same position as the tumour, and connected to a Baldwin-Farmer dosimeter.

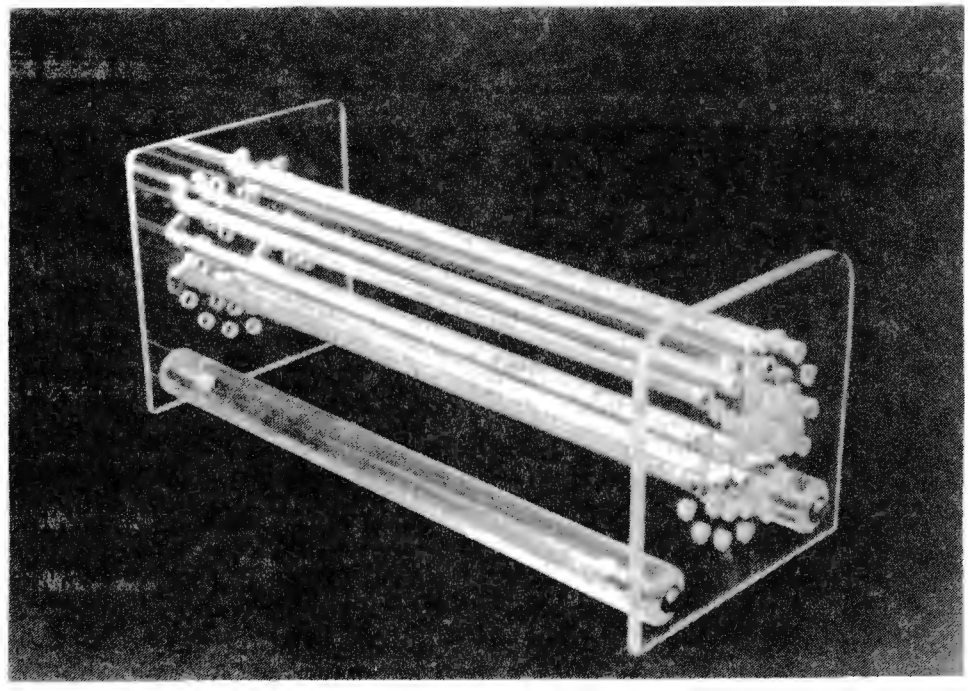

Fig 3.5 Restraining device for rats during irradiation.

3.3.1.5 Irradiation of Experimental Mouse Tumours with ^{60}Co gamma rays

Mice were restrained in acrylic plastic jigs. Irradiation was using a Picker model V4M/60 unit which emitted gamma radiations of 1.17 and 1.31 MeV. All parts of the mice were shielded with 7.5cm thick lead blocks, apart from the tumour. Blocks of acrylic plastic 0.5cm thick were placed in front of the tumours for build-up.

Dose in February 1986 was 1.1906 Gy min^{-1} for this unit.

3.3.1.6 Irradiation of B16 Mouse Melanoma Cells

Cells were grown to confluence in 25 cm^2 Falcon flasks. Medium was changed, then the cells were irradiated using an Eldorado 6 ^{60}Co unit (Fig 3.6).

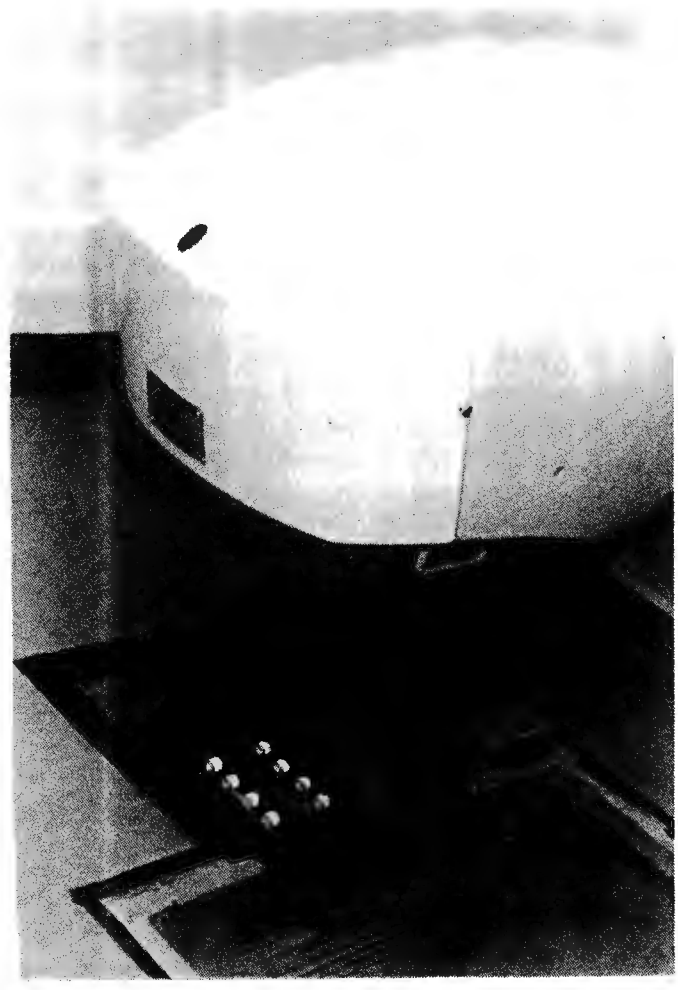

Fig 3.6 Irradiation of B16 mouse melanoma cells with ^{60}Co gamma rays.

The distance from the source to the cell layers at the bottom of the flasks was 80cm. A sheet of acrylic plastic (Perspex) 0.5 cm thick was placed on the upper surface of the flasks to provide build-up.

The output of the ^{60}Co unit was measured to be 0.598 Gy/min on 6 June 1986 at a source to surface distance of 80.63 cm using an 0.5 cm^3 ionization chamber connected to a substandard Baldwin-Farmer dosimeter.

In order to calibrate the Eldorado 6 for irradiating cells in the geometric set-up described above, a flat

ionization chamber was placed underneath and against the bottom surface of a Falcon flask containing the cells and medium. Care was taken to maintain a distance of 80 cm from the source to the bottom of the Falcon flask. A sheet of acrylic plastic 0.5 cm thick was placed on top of the flasks, then dose was measured by connecting the ionization chamber to a substandard Baldwin-Farmer dosimeter.

3.3.2.1 Clonogenicity Assays

Confluent cells were treated by exposure to x-irradiation, mitoxantrone or both. After the medium was poured off, cells were trypsinized as described in 3.2.1.2, the cell concentrations obtained by counting in a haemocytometer, then volumes containing 400 cells were pipetted into clean sterile 25 cm^2 Falcon flasks. Growth medium was added to result in a volume of 5 mℓ, then flasks were placed in a humidified CO_2 incubator. Colonies were stained after 11 days incubation by removing the medium and adding about 2 mℓ gentian violet solution (1% in water). The stain was left in contact with the cells for 12-15 minutes, removed and the flasks were washed thoroughly with water. Flasks were dried overnight and the number of colonies counted. The surviving fraction was calculated by comparison of the number of colonies in experimental flasks with those in untreated or control flasks, and response curves could then be constructed (182).

3.4.1 Exposure to Magnetic Fields.

3.4.1.1 Positioning of Mice in a Magnetic Field.

CBA mice with experimental CaNT tumours subjected to exposure in magnetic fields were kept in a non-magnetic mouse cage and fed with Epol Mouse Cubes. Water was allowed ad libitum (Fig 3.7). Control mice were also kept in these conditions, but away from artificial magnetic fields.

Fig 3.7 CBA mice with CaNT tumours exposed to magnetic fields.

3.4.1.2 Magnetic Resonance Imaging Unit (MRI).

The MRI unit used was a Gyrex S.5000 system which employs a superconducting magnet. It has a resistance of no more than $4x10^{-11}$ ohms which generates a field intensity of 0.5 Tesla. The unit can also employ a radiofrequency (RF) component of 20 MHz.

The magnet dimensions are: height - 249cm; depth - 250cm; width - 215cm and its mass is 5 000 kg.

Temperature in the MRI laboratories was regulated between 20°C and 22°C. Relative humidity was regulated at 40% to 60% (non condensing). This equipment is the first to be installed in South Africa and the Southern Hemisphere and is located in the Research Institute for Medical Biophysics of the South African Medical Research Council (MRC), Tygerberg (Fig 3.8).

Fig 3.8 Operator's console of the MRI.

3.4.1.3 Measurement of the Spin-Lattice (T1) and Spin-Spin (T2) Relaxation Times in Proton Magnetic Resonance Imaging (MRI) in the CaNT Murine Tumour

Male CBA mice with the CaNT tumour in the sternal region (see 3.1.2.1) were held in a perspex jig. Two such jigs holding two mice each were placed into the head coil of the MRI system.

A sealed perspex cube containing 1.7ℓ of a calibration solution of $NiCl_2$ (20 mM) was also inserted into the head coil in order to supply sufficient electromagnetic wave absorption necessary for the radiofrequency calibration of the resonance signals. The ensemble in the head coil was located so that it would be situated within the volume of greatest homogeneity at the centre of the static magnetic field (Fig 3.9).

A rectangular region of interest (ROI) was defined on the computer for each of the CaNT tumours. The dimensions of the ROI were such as to include each tumour, without extending beyond its boundaries. In turn this enabled one to calculate the average T1 and T2 values for each tumour (167).

The Elscint Gyrex 5000 NMRI system was used for these measurements of T_1 and T_2 at 21°C and 20 MHz.

A map of T_1 values was constructed from two spin-echo images in which the repetition time (TR) was varied but the echo time (TE) kept constant. The times used were:

TR_1 = 200ms TE = 40ms

TR_2 = 800ms TE = 40ms

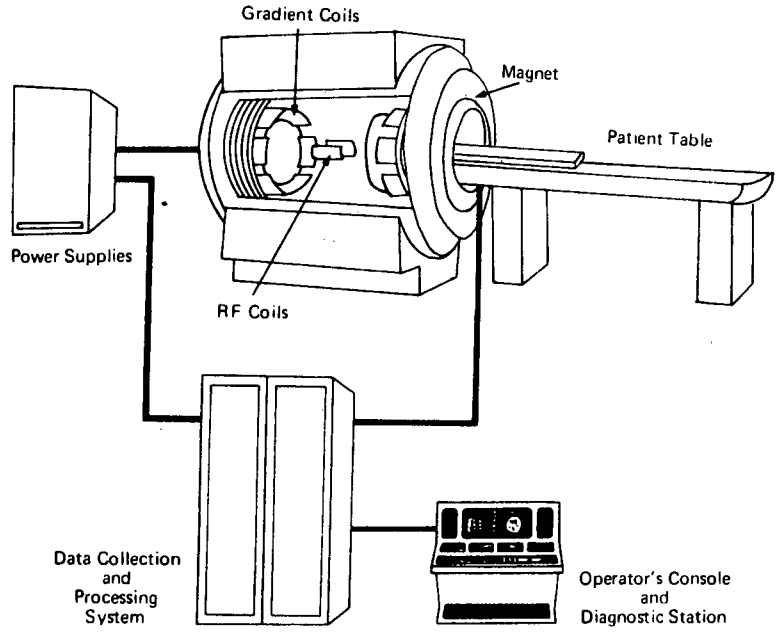

Fig 3.9 A schematic layout of an NMRI system.

A map of T_2 values was also constructed from two spin-echo images in which the TR was kept constant but the TE varied. Times used were:

TR = 800ms TE_1 = 40ms TE_2 = 160ms

3.5.1 Preparation of Tumour Tissue

The tumours from CBA and WHT mice and WAG/Rij rats were treated in two different ways as detailed in 3.5.1.1 and 3.5.1.2 immediately following their removal by surgical excision after the animals were anaesthetized with ether.

3.5.1.1 Tumour tissue preparation for Glucose-6-Phosphate Dehydrogenase (G-6-PDH), Isocitrate Dehydrogenase (ICDH), Phosphomannose Isomerase (PMI) and Tissue Sulphydryl Levels.

Tumour tissue was weighed out and homogenised 1:5 w/v with ice cold homogenizing medium, which consisted of physiological saline (0.9% NaCl w/v) which was 0.66 mM with respect to EDTA. A Potter-Elvehjem homogenizer was used. The sample was centrifuged (Sorvall RC-5B centrifuge) for 20 minutes at 17540g at 4°C. The clear supernatant fluid was removed from the centrifuge tube with a disposable Pasteur pipette. The homogenate was stored under ice for a maximum of 1 hour before any of the assays.

3.5.1.2 Tumour tissue preparation for ATP Assay

Mice were anaesthetized with ether, and the skins and tissue surrounding the tumour were removed, as was obviously necrotic tissue. Tumour was cut away and immediately dropped into liquid nitrogen. Frozen tumours were quickly weighed, then pulverized in a mortar with frequent additions of liquid nitrogen. One mℓ perchloric acid (6% w/w) was added and the tissue was ground to powder, again with further additions of liquid nitrogen. The liquid nitrogen was allowed to evaporate, the mixture liquefied and was homogenized in a Potter type glass homogenizer. The homogenate was centrifuged at 17500g for 20 minutes at 4°C, the supernatant removed and the pH adjusted to between 7.4-7.5 with 5M K_2CO_3. This was centrifuged at 17500g for 20 minutes, and the supernatant was used for ATP determinations.

3.5.1.3 Preparation of Cells for ATP Determination

Following irradiation or other treatments, flasks were replaced in the incubator at 37°C and exposed to a humidified atmosphere containing 5% CO_2 for up to 2.5h following irradiation. Cells were then trypsinized as detailed in 3.2.1.2 and resuspended in 5 mℓ serum-free McCoy's medium. Cells were counted in a haemocytometer, then the volume containing $1x10^6$ cells was placed in a plastic tube. One mℓ perchloric acid (6% w/v) was added, then the sample was freeze-thawed three times by immersion of the closed tube into liquid nitrogen followed by warming at 37°C in an incubator.

After the last thawing, the preparation was centrifuged at 17500g for 20 min. at 4°C in a Sorvall RC-5B centrifuge. The supernatant was removed, made up to 20 mℓ with water and the pH adjusted to 7.5 with 5M potassium carbonate. This was followed by recentrifugation at 17500g for 20 min. at 4°C.

The volume of supernatant was measured, and this was used for determination of cellular ATP levels using the highly sensitive luciferin-luciferase system (see 3.6.1.5 below).

3.6.1 Biochemical Assay Techniques

Methods used for the assay of the following will be discussed:

(1) Glucose-6-phosphate dehydrogenase (G-6-PDH) activity;

(2) Isocitrate dehydrogenase (ICDH) activity;

(3) Phosphomannose isomerase (PMI) activity;

(4) Adenosine-5'-triphosphate (ATP) levels;

(5) Tissue sulphydryl levels;

(6) Protein determinations.

Each of the experimental techniques used will be presented in the following format:

(a) Principles of the particular assay will be discussed.

(b) A detailed account of materials and methods will be given.

(c) The assay procedure will be succinctly described.

(d) Comments on any particular assay will be made when necessary.

The methods for calculation of results from the experimental data as well as statistical methods are given in Appendix B.

3.6.1.1 Glucose-6-Phosphate Dehydrogenase (D-Glucose-6-phosphate-NADP 1-oxidoreductase, EC 1.1.1.49)

Principles of Assay

Glucose-6-phosphate dehydrogenase (G6P-DH) was first isolated from erythrocytes and from fermenting yeast by Warburg et al. The molecular weight of the enzyme is 128000. G6P-DH was determined as described by Lohr and Waller (168). Blood cells, adipose tissue and lactating mammary gland are especially rich sources of the enzyme. Less occurs in liver, pancreas, kidney, lung, brain and gastric mucosa, while only traces are found in skeletal and heart muscle and virtually none in serum. Some human and animal tumours contain high activity of the enzyme. The first reaction of the phosphogluconate pathway is the enzymatic dehydrogenation of glucose-6-phosphate by glucose 6-phosphate dehydrogenase, also known as Zwischen ferment, to form 6-phosphogluconate. Under the conditions of the assay, the reaction involved is shown in Equation 3.1.

$$\text{Glucose-6-phosphate} + NADP^{+} \overset{\text{G6P-DH}}{\rightleftharpoons} \text{6-Phosphogluconate} + NADPH + H^{+} \qquad \text{(Equation 3.1)}$$

Dehydrogenation of glucose 6-phosphate by G6P-DH forms 6-phosphogluconate. This enzyme, which is not present in mitochondria is specific for NADP as electron acceptor. It carries out dehydrogenation of carbon atom 1 of the pyranose form of glucose 6-phosphate to yield the corresponding 6-phosphoglucose-δ-lactone.

Materials and Methods

The sample of the experimental mouse tumours was freshly prepared as detailed in 3.1.6.1 and kept under ice, ready to utilize for the enzymatic assay.

The different reagents used to prepare the solutions had the following concentrations:

(a) Triethanolamine 50 mM, buffered to pH 7.5 with 1 N NaOH

(b) Nicotinamide-adenine dinucleotide phosphate (β-NADP): 30 mM.

(c) Glucose-6-phosphate (G-6-P): 40 mM.

The rate of formation of NADPH was used as a measure of the enzyme activity and followed by means of the increase in extinction at 340 nm using a Pye Unicam 5P8-400 UV/V15 double beam spectrophotometer.

Assay Procedure

The total volume of 1.2 mℓ was contained in 1.5 mℓ quartz glass cuvettes. For the measurement, the reference cuvette contained: Triethanolamine buffer: 57.12 µmol (pH 7.5), 0.010 mℓ tumour sample.

The sample cuvette contained triethanolamine 52.20 µmol (pH 7.5), nicotinamide-adenine dinucleotide phosphate (β-NADP): 10 nmol, glucose-6-phosphate: 13.4 nmol, 0.010 mℓ tumour sample.

Absorbance change at 340 nm was monitored at 25°C for 3 min.

Comments

The enzymatic reaction kinetics were linear using between 0.005 and 0.025 mℓ of tissue homogenate from the experimental mouse tumours.

3.6.1.2 Isocitrate Dehydrogenase (Threo-Ds-isocitrate: $NADP^+$ oxidoreductase-decarboxylating-EC 1.1.1.42).

Principles of assay

Isocitrate dehydrogenase (ICDH) is widely distributed in nature. The enzyme is a component of the Krebs tricarboxylic acid cycle, and has been studied in bacteria, protozoa, fungi, yeasts, higher plants, insects and mammals including man.

ICDH activity was determined as described by Bernt and Bergmeyer (169). In mammalian tissues there are two NADP-specific ICDH isoenzymes located in the mitochondria and cytoplasm respectively (170). The isoenzymes of these two cell compartments are under independent genetic control. In mammalian cells, the heart and skeletal muscle contain predominantly the mitochondrial NADP-specific isoenzyme, whereas the liver contains mainly the cytoplasmic NADP-specific isoenzyme (171). Mammalian NADP-specific ICDH enzymes generally have a molecular weight less than 96000 and consist of a single polypeptide chain, or have a dimeric structure. The reaction that involves ICDH is shown in Equation 3.2.

$$\text{Threo-Ds-Isocitrate} + NADP^+ \xrightarrow[Mn^{2+}]{ICDH} \text{2-oxoglutarate} + NADPH + CO_2 + H^+$$

(Equation 3.2)

The NADP-specific isocitrate dehydrogenase requires Mn^{2+} for its activity. The reaction proceeds with a large decrease in Gibbs free energy because of the simultaneous loss of the beta-carboxyl group as CO_2 in the highly exergonic reaction.

Materials and Methods

The sample of the experimental tumours was freshly prepared as detailed in 5.1.6.1 and kept under ice for not more than one hour before starting the assay.

The different reagents used to prepare the solutions had the following concentrations:

(a) Triethanolamine buffer 38.6 mM (pH 7.3)

(b) DL isocitrate 1.70 mM

(c) NaCl 19.32 mM

(d) β-NADP 0.12 mM

(e) $MnSO_4.H_2O$ 1.56 mM

The rate of formation of NADPH was used to measure the enzyme activity. A Pye Unicam 5P8-400 UV/V15 spectrophotometer with a thermostatted cuvette holder (25°C) was used to measure the increase in absorbance at 340 nm.

Assay Procedure

The total assay volume of 1.2 mℓ was contained in 1.5 mℓ quartz cuvettes for the measurement of ICDH activity, the reference (control) cuvette contained triethanolamine buffer 95.6 µmol (pH 7.5), DL-isocitrate 4.42 µmol, NaCl 50.19 µmol and 0.005 mℓ tumour sample.

The sample cuvette contained triethanolamine 92.4 µmol (pH 7.5), DL-isocitrate 4.27 µmol, NaCl 78.51 µmol, nicotinamide-adenine dinucleotide phosphate (β-NADP) 12.8 nmol, $MnSO_4$ 0.15 µmol and 0.005 mℓ tumour sample.

Absorbance changes were measured in isothermic conditions, at 25°C for 3 minutes.

Comment

Bernt et al (169) observed that ICDH lost 30% of activity after 3 days at 4°C.

In this study the activity of the ICDH, was always measured within 1 hour of preparation of the sample.

3.6.1.3 Phosphomannose Isomerase (D Mannose-6-phosphate Ketol-isomerase, EC 5.3.1.8)

Principles of assay In 1947 Gottschalk (172) suggested that the conversion of glucose-6-phosphate and mannose-6-phosphate to the common intermediate, fructose-6-phosphate, is catalyzed by two separate and specific enzymes which he designated Isomerase I and II.

Glucopyranose-6-P $\underset{\text{Isomerase I}}{\rightleftarrows}$ Fructofuranose-6-P $\underset{\text{Isomerase II}}{\rightleftarrows}$ Mannopyranose-6-P

Isomerase I had been identified in 1933 by K Lohmann (142) as phosphoglucose isomerase. It was not until 1950 that the existence of Isomerase II, Phosphomannose isomerase (PMI), as a separate enzyme was positively demonstrated by Slein (173). PMI activity was determined in this research work, using the method described by Gawhn (174).

The reactions that involve PMI are shown in the following equations (3.3, 3.4 and 3.5).

$$\text{Mannose-6-P} \xrightarrow{\text{PMI}} \text{Fructose-6-P} \qquad \text{(Equation 3.3)}$$

$$\text{Fructose-6-P} \xrightarrow{\text{PGI}} \text{Glucose-6-P} \qquad \text{(Equation 3.4)}$$

$$\text{Glucose-6-P} + \text{NADP}^{+} \xrightarrow{\text{G6P-DH}} \text{Gluconate-6-P} + \text{NADPH} + \text{H}^{+} \qquad \text{(Equation 3.5)}$$

The assay for PMI (Equation 3.3) is performed indirectly in the following way. The two enzymes PGI and G6P-DH are added in excess to Mannose-6-P and the final reaction (Equation 3.5) is observed using a spectrophotometer to measure the absorbance of NADPH at 340nm. In this way the activity of PMI is determined, since its action is the rate limiting step in Equations 3.3, 3.4, 3.5.

Materials and Methods

The sample to measure phosphomannose isomerase (PMI) activity in the experimental tumours was freshly prepared as detailed in 3.5.1.1 and stored under ice. The various reagents used in the assay had the following concentrations:

(a) Triethanolamine buffer: 50 mM (pH 7.6)

(b) Mannose-6-P, K salt: 3.2 mM

(c) β-NADP: 11 mM

(d) Phosphoglucose isomerase (PGI) 560 U/mg

(e) Glucose-6-Phosphate dehydrogenase (G6P-DH) 400 U/mg

A Pye-Unicam SP8-400 UV/V15 dual beam spectrophotometer with a thermostatted cuvette holder (25°C) was used to measure the absorbance change at 340 nm.

Assay Procedure

The total volume of 1.2 mℓ was contained in 1.5 mℓ quartz glass cuvettes. The reference cuvette contained:

triethanolamine buffer 96.24 µmol (pH 7.6)

mannose-6-phosphate, K salt, 32 nmol and 0.010 mℓ tumour sample.

The sample cuvette contained:

triethanolamine buffer 91.12 µmol (pH 7.6),

mannose-6-phosphate, K salt 32 nmol, NADP, Na salt 20 nmol, PGI 16 Units, G6P-DH 195 units and 0.010 mℓ tumour sample.

Absorbance changes were monitored at pH 7.6 and 25°C for 3 minutes.

3.6.1.4 Adenosine-5'-Triphosphate

Principles of assay

Of all the naturally occurring phosphates, adenosine-5'-triphosphate, is the most widely distributed. This energy-rich nucleotide serves as an "energy pool" to meet the energy requirements of cellular metabolism.

The enzymatic determination of adenosine-5'-triphosphate (ATP) by a spectrophotometric method as developed by Lamprecht and Trautschold (175) and used in this present work makes use of the following reactions:

Hexokinase (HK) (ATP : D-hexose-6-phosphotransferase, EC 2.7.1.1) phosphorylates glucose with ATP in the presence of Mg^{2+} to glucose-6-phosphate (G-6-P). G6P-DH (D-Glucose-6-phosphate NADP1-oxidoreductase, EC 1.1.1.49) catalyses the dehydrogenation of G-6-P with NADP to give 6-phosphoglucono-δ-lactone. The reaction scheme is given in Equation 3.6.

$$\text{ATP} + \text{Glucose} \xrightarrow{\text{HK}} \text{G-6-P} + \text{ADP}$$

$$\text{G-6-P} + \text{NADP}^{+} \xrightarrow{\text{G-6-PDH}} \text{6-Phosphoglucono-5-lactone} + \text{NADPH} + \text{H}^{+} \quad \text{(Equation 3.6).}$$

For each mole of ATP present, 1 mole of NADPH is formed, and can be determined spectrophotometrically at 340 nm.

Materials and Methods

The tissue sample of the experimental mouse tumours was freshly prepared as detailed in 3.5.1.2 and kept in ice.

The reagents required for the assay were:

(a) Triethanolamine buffer: 50 mM (pH 7.4)

(b) Nicotinamide-adenine dinucleotide phosphate (β-NADP): 10 mM.

(c) Magnesium chloride ($MgCl_2$): 0.1 M

(d) Glucose 6-phosphate dehydrogenase (G-6-PDH): 400 U/mg

(e) Hexokinase (HK): 480 U/mg

(f) Glucose: 0.5 M.

The absorbance changes at 340 nm were monitored with a Pye-Unicam SP8-400 UV/V15 dual beam spectrophotometer.

Assay Procedure

Spectrophotometer sample cuvettes contained triethanolamine 32 µmol, NADP 1.32 nmol, $MgCl_2$ 533 nmol and 0.1 to 0.12 mℓ tumour sample containing ATP and water in a total volume of 1.075 mℓ at pH 7.4.

Initial absorbance readings were made at 340 nm against a reference cuvette containing all reagents listed for the sample cuvette, with the exception of NADP.

Glucose-6-phosphate dehydrogenase suspension 14.5 units was added to both sample and reference cuvettes, the absorbance at 340 nm was monitored until a constant reading was obtained, then 6 µmol glucose contained in a volume of 0.12 mℓ was added to both cuvettes. An absorption reading at 340 nm was made, then 6 units of hexokinase preparation were added. The absorbance change at 340 nm was monitored for 20 minutes, and a final reading made.

Comment

It was essential that tissue samples were very quickly frozen to preclude further metabolism of ATP. It is known that the metabolite concentration in a tissue depends on the

speed with which the tumour was removed and on the manipulations during the sacrifice of the animal.
A sample of ATP deteriorates, because it is hydrolysed when standing in solution. Storage at 0°C, freezing or lyophilization generally leads to a decrease in the ATP values. For this reason in this investigation, the ATP levels in tumour samples were determined immediately after sample preparation.

3.6.1.5 Determination of ATP using Luciferin-Luciferase Assay

Principles of Assay

A highly sensitive method for the determination of ATP has been developed using luciferase from the American firefly, Photinus pyralis. This enzyme catalyses a chain of reactions, where firstly luciferin is activated by adenylation followed by oxidation with atmospheric oxygen. On decarboxylation, oxyluciferin is formed in the excited singlet state, which returns to the ground state by emission of a photon. This reaction has a very high quantal yield, of the order of 90%, so that the system is eminently suitable for making highly sensitive measurements of ATP concentrations (176).

Materials and Methods

Reagents required for the assay were:

(a) Luciferin-luciferase (Sigma Chemical Company, St Louis, U S A) dissolved in deionized water to result in a concentration of 8mg/mℓ. This solution was wrapped in aluminium foil and stored in the dark at 4°C for between 5 and 24h before use.

(b) Tris-acetate buffer was prepared by adjustment of the pH of tris-(hydroxymethyl) aminomethane solution to 7.75 with glacial acetic acid. The final concentration of the buffer was 0.25M.

(c) A stock solution of ATP (0.5mM) was prepared by dissolving 27.56mg ATP (from equinine muscle, Sigma Chemical Company, St Louis, U S A) in 100 mℓ deionized water. Stock solution was diluted 1:1000 just prior to the start of the assay.

Bioluminescence was measured using a Beckman Liquid Scintillation Counter, Model LS 1801, which was programmed to make use of the single photon monitor. Samples were counted for 0.1 minutes. Individual samples were counted immediately after preparation, and it was found that good reproducibility was achieved if sample preparation time and exposure to light were limited to the shortest possible periods.

Assay Procedure

Luciferin-luciferase solution 0.01 mℓ was added to tris-acetate buffer and from 0.01 to 0.02 mℓ ATP preparation contained in a plastic scintillation counting vial. The final assay volume was 0.5 mℓ. The sample was gently shaken to ensure good mixing of the reagents, then taken immediately to the scintillation counter and counted.

With each set of ATP determinations, a calibration curve was prepared. It was found convenient to add 0.003, 0.005, 0.0075, 0.010 and 0.020 mℓ of the 1:1000 dilution of the stock ATP solution (corresponding to 1.5×10^{-13}, 2.5×10^{-13}, 3.75×10^{-13}, 5×10^{-13} and 1×10^{-12} moles ATP) to tris-acetate buffer in a test tube to result in a volume of

0.49 mℓ. Luciferin-luciferase solution (0.01 mℓ) was then added before samples were counted. The counts obtained were plotted against ATP content on a log-log scale, and the line of best fit was obtained by regression analysis. The concentration of ATP in the "unknown" samples could then be ascertained from the calibration plot. The ATP content was then expressed as moles ATP per cell.

It should be noted that ATP in each sample was assayed in duplicate at two different concentrations, namely using 0.01 mℓ and 0.02 mℓ of sample in the manner described above. Results at these two concentrations were found to be consistent within experimental error, (showing no variation in the assay of ATP content of the sample). The mean ATP content of each sample was calculated from the mean of the four separate determinations.

3.6.1.6 Tissue Sulphydryl Levels

Principles of Assay

The most ubiquitous and important thiol present in tissues accepted to be glutathione (γ-glutamylcysteinylglycine). Its apparent involvement in a multitude of biological functions (177) have generated a continual interest in methods of analysis of this cellular component, ever since its discovery and isolation nearly 60 years ago. Although the tripeptide can exist in both a reduced (sulphydryl) and an oxidized (disulfide) form it is maintained in vivo predominantly in the former state through the action of the equally ubiquitous enzyme glutathione reductase (Equation 3.7).

$$GSSG + NADPH + H^+ \xrightarrow[\text{reductase}]{\text{Glutathione}} 2G\text{-}SH + NADP^+$$

(Equation 3.7)

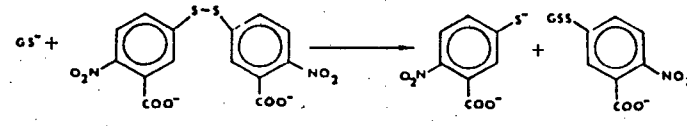

(Equation 3.8)

Tissue sulphydryl levels can be very conveniently determined using the reaction with 5,5'-dithiobis-(2 nitro) benzoic acid) (Ellmans reagent) (Equation 3.8).

The chromophore product resulting from the reaction can be determined spectrophotometrically by measurement of absorbance at 412 nm. Thiols were assayed using a modified version of the method described by Deakin (178) with 5,5'-dithiobis(2-nitro)benzoic acid (DTNB).

Materials and Methods

The tissue samples of the experimental rat tumours (rhabdomyosarcoma R1) and mouse tumours (CaNT) were freshly prepared as detailed in 3.5.1.1 and stored in ice for not longer than one hour before starting the assay procedure.

The reagents used in the assay were:

(a) Sodium phosphate buffer 0.08M, pH 8.0.

(b) Ethylenediaminetetra-acetate disodium salt ($EDTA\text{-}Na_2H_2$) 1.32 mM.

(c) 5,5'-dithiobis 2-nitrobenzoic acid (DTNB) 0.1 M.

(d) Reduced glutathione (GSH) 0.4 mM.

The absorbance of the chromophore resulting from the reaction of glutathione with DTNB was measured in a Pye Unicam SP8-400 UV/V15 dual beam spectrophotometer at 412 nm.

Assay Procedure

Spectrophotometer sample cuvettes contained sodium phosphate buffer 232 µmol (pH 8.0) 0.010 to 0.1 mℓ sample containing GSH, 5,5'-dithiobis-2-nitrobenzoic acid (DTNB) 10 µmol and water to a total volume of 3 mℓ. The contents of the reference cuvette was the same except that the GSH - containing sample was replaced by water.

After allowing 15 minutes for the reaction between GSH and DTNB, the absorbance of the sample cuvette was measured against the reference cuvette at 412 nm at 25°C.

Concentrations of all thiols in tissue homogenates were determined by comparison against a standard curve.

This latter was prepared as in the above assay, but 0.02 to 1.0 µmol GSH was substituted for tissue homogenate.

3.6.1.7 Glutathione

Principles of Assay

Glutathione in its oxidised or reduced state can be very specifically determined by the method of Tietze (179). This method allows the analysis of nanogram quantities of glutathione and is based on the catalytic action of GSH or GSSG in the reduction of Ellman reagent (DTNB) by a mixture of NADPH and yeast glutathione reductase. The catalytic action of glutathione in this system resides in the continual enzymic regeneration of GSH, present initially or formed enzymatically from GSSG, following its interaction with the sulfhydryl reagent.

Materials and Methods

The tumour samples of the CaNT tumours were homogenized as indicated in 3.5.1.1. A volume of 5% TCA equal to that of the homogenizing medium was added, and following further homogenization the preparation was centrifuged at 17540g for 20 minutes at 4°C. The supernatant was used in the determination of glutathione levels.

The reagents used in the assay were:

(a) Sodium phosphate-EDTA buffer 0.1 M, pH 7.5.

(b) Glutathione reductase, 150 U/mg.

(c) 5'5'-dithiobis-(2-nitrobenzoic acid) (DTNB), 0.1 M.

(d) Reduced glutathione (GSH), 0.033 mM.

(e) Reduced nicotinamide-adenine dinucleotide phosphate (NADPH), 11 mM.

Assay Procedure

For the standard glutathione assay system, quantities of the compounds required are shown in Table 3.1. Components were dissolved in phosphate-EDTA buffer, pH 7.5 and were added in the amounts and in the order indicated in this table. Final volumes were 1.0 mℓ. The rate of reaction at 25°C was expressed as the change in absorbancy per minute at 412 nm.

TABLE 3.1: Protocol for standard glutathione assay

Test cuvette	Amount	Blank cuvette
DTNB	600 nmol	DTNB
Deproteinized sample	1-100 ng GSH	-
Glutathione reductase	10 µg	Glutathione reductase
NADPH	200 nmol	NADPH

Glutathione levels in the tumour homogenates were determined by comparison against a standard curve prepared when tissue sample in the standard assay was replaced by 10 to 100 ng reduced glutathione. Ten microliters of supernatant was diluted in 1 mℓ of sodium phosphate-EDTA buffer 0.1 M, pH 7.5 and volumes between 10 and 50 µℓ were used in the assay.

3.6.1.8 Protein Determination

These were made by the method of Lowry et al (180) using bovine serum albumin, fraction V as a standard. All protein determinations were made so that the amounts measured ranged from 0.05 mg to 0.25 mg, thus falling within the linear range of concentration as measured spectrophotometrically at 750 nm.

3.7.1 Electron Microscopy

Results from electron microscopy formed part of this project. This work was performed in the Research Institute for Medical Biophysics, Medical Research Council, and methods used in these studies will be described briefly.

3.7.1.1 Electron Microscopy Techniques

Tumour tissue was fixed in 2.5% glutaraldehyde in 0.1 M cacodylate buffer, pH 7.4, rinsed in buffer and post-fixed in 1% osmium tetroxide. Tissue was dehydrated in ethanol and embedded in EBL (Spurr's) low viscosity resin. Sections were cut on a Reichert Om U3 microtome using glass knives and stained with uranyl acetate added to lead citrate. Sections were viewed with a Philips 420 transmission electron microscope at an accelerating voltage of 60-80 kV.

CHAPTER 4

RESULTS

4.1 Some Biological Effects of Ionizing Radiation

4.1.1 ATP levels

ATP levels were investigated in the following mouse tumours:

1. CaNT murine tumour in CBA mice.
2. Fib/t murine fibrosarcoma in WHT mice.
3. Rhabdomyosarcoma tumour in Balb C mice.

The ATP content of tumours was determined:

(a) under normoxic conditions.

(b) after clamping the tumours (hypoxic conditions).

(c) under normoxic conditions following ionizing radiation.

(d) after clamping the tumours following ionizing radiation.

(e) following treatment with mitoxantrone (an anthraquinone drug).

(f) Under treatment with mitoxantrone and x-rays.

4.1.2.1 ATP content in CaNT, Fib/t and Rhabdomyosarcoma tumours in normoxic conditions

ATP content and changes of Gibbs free energy of formation (ΔG_{ATP}) were measured under normoxic conditions at 25°C. The results are presented in Table 4.1.

TABLE 4.1: ATP concentration in normoxic tumours and levels of Gibbs free energy of formation

Tumour Type	Number of determinations	Concentration (nmol/mg)	ΔG_{ATP} (J/mg)x10^{-3}
CaNT	68	3.42 ± 0.47	125
Rhabdomyosarcoma	13	2.78 ± 0.34	102
Fib/t	17	2.64 ± 0.39	97

Entries represent mean ± SEM.

4.1.3.1 ATP content after clamping CaNT tumours (hypoxic condition)

Adenosine-5'-triphosphate concentration in the CaNT tumour in CBA mice was measured at 15 minutes and 2 hours after clamping the tumours.

A tumour ATP concentration decrease below the control value was observed 15 minutes and 2 hours after clamping. The measured concentrations were 0.78 times and 0.75 times respectively that of the controls ($P < 0.001$).

The depletion of ATP concentration is shown in Fig 4.1.

The Gibbs Free energy change in tumour ATP after clamping is presented in Table 4.2.

TABLE 4.2: Gibbs Free energy changes in tumour ATP after clamping CaNT tumours

Experimental Conditions	Time of tumour clamping	ΔG_{ATP} (J/mg)x10^{-3}
Unclamped (normoxic control)	-	125
Clamped (hypoxic condition)	15 minutes	101
Clamped (hypoxic condition)	2 hours	98

The value of ΔG_{ATP} were calculated at pH 7.4 and 25°C.

4.1.4.1 Tumour ATP content in normoxia following ionizing radiation

Adenosine-5'-triphosphate levels in CaNT, Fib/t and Rhadomyosarcoma tumours in normoxic conditions were measured after x-ray irradiation (100 KVp).

CaNT tumours were irradiated with the following doses:

5 Gy, 10 Gy, 15 Gy, 30 Gy, 100 Gy and 200 Gy.

Fib/t murine fibrosarcoma and Rhabdomyosarcoma were x-irradiated with 10 Gy.

4.1.4.2 Levels of ATP in CaNT tumour

(a) Effects of x-rays (5 Gy)

Adenosine-5'-triphosphate concentrations in CaNT murine tumours in normoxic conditions have been determined at various times after an x-ray irradiation of dose 5 Gy was given. An increase in tumour ATP content was noted one hour after irradiation. A considerable augmentation was observed 4 hours after giving the x-rays, which was 1.70 times that of controls. The ATP concentration returned to the control levels 13 hours after x-irradiation. This is represented in the Fig 4.2.

The Gibbs free energy change (ΔG_{ATP}) of 213 $x10^{-3}$J/mg in tumour ATP content 4 hours after x-irradiation was increased by 1.70 times compared with the control value.

(b) Effects of x-rays (10 Gy)

ATP levels in the CaNT-tumour in CBA mice at different times after x-irradiation using 10 Gy were measured and are shown in Fig 4.3.

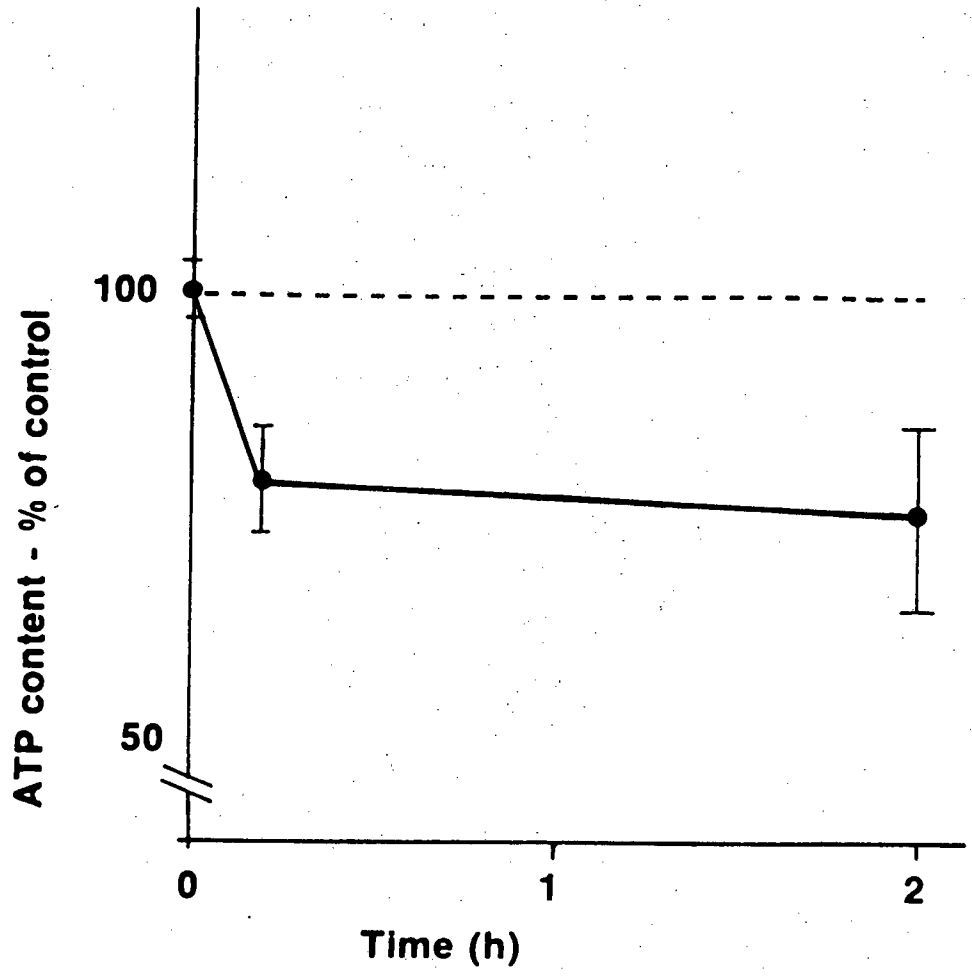

Fig 4.1 ATP levels after clamping CaNT tumours.

Each point represents the mean of not less than 4 values and SEM is indicated by the vertical bars.

An increase in tumour ATP content was first noted 45 minutes after irradiation. The maximum increase was observed 2.5 hours after receiving the x-rays. This was 3.76 times that of the control, then a decrease to 1.31 times that of the controls was observed up to 13 hours after irradiation. This is represented in Fig 4.3. The Gibbs free energy change in tumour ATP yield 2.5 hours after the x-ray dose, when ATP levels were maximal, was 473 x 10^{-3} J/mg.

(c) Effects x-rays (15 Gy).

The variation of ATP concentration in the CaNT tumour in CBA mice was measured at different times, after an x-ray irradiation of 15 Gy was given.

The value of the ATP content after 45 minutes increased by 1.39 times that of control level. It continued to increase up to a maximum value of 2.09 times that of control at 2.5 hours after irradiation. Then ATP levels decreased almost to the control level 13 hours after irradiation. This result is shown in the Fig 4.4.

The Gibbs free energy changes in tumour ATP synthesis, 2.5 hours after the x-ray, dose of 15 Gy has its maximum value of 263 x 10^{-3} J/mg.

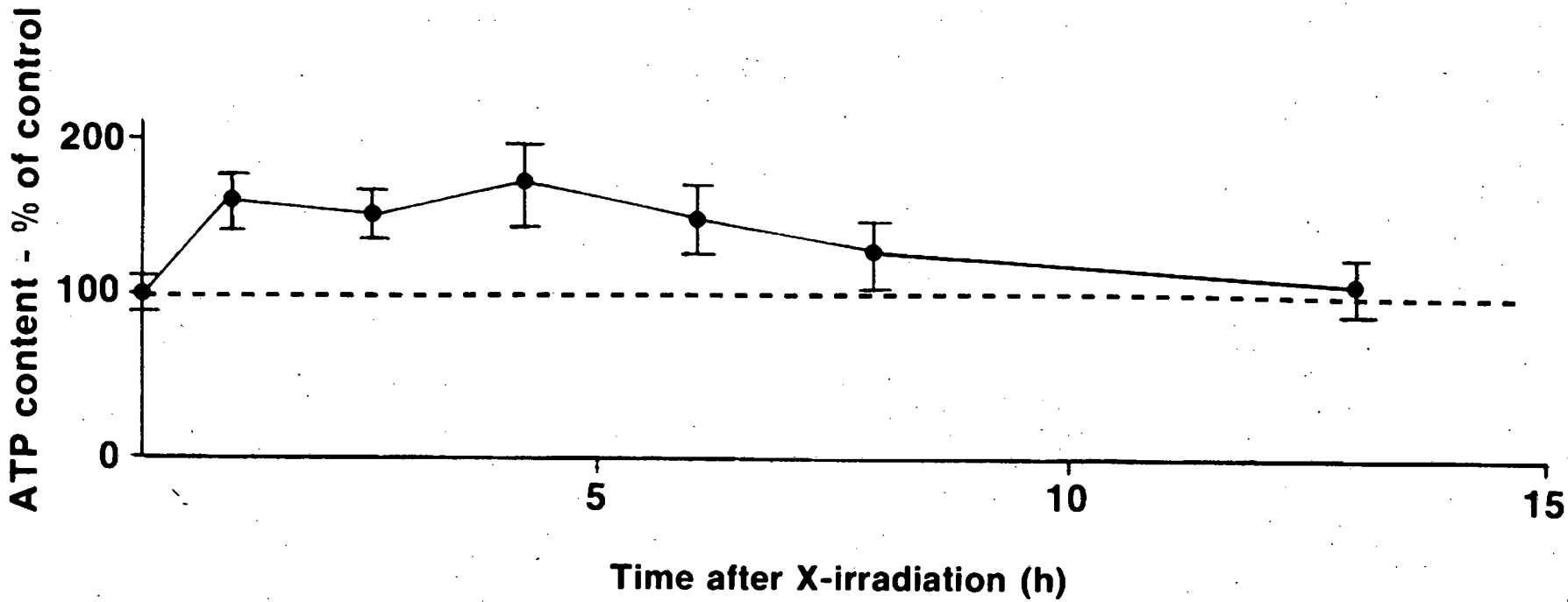

Fig 4.2 ATP levels in the CaNT tumours at various times after receiving an x-ray dose of 5 Gy.

Each point represents the mean of not less than 3 values and SEM is indicated by the vertical bars.

(d) Effects of x-rays (30, 100 and 200 Gy).

The variation of ATP concentration in the CaNT tumours was measured after the above x-ray doses, 2.5 hours after x-irradiation.

The values of ATP content after the doses of 30 Gy, 100 Gy and 200 Gy increased by 1.69 times, 1.17 times and 1.05 times respectively compared with the controls.

The Gibbs Free energy changes in tumour ATP content 2.5 hours after x-irradiation doses of 5 Gy, 10 Gy, 15 Gy, 30 Gy, 100 Gy and 200 Gy are presented in the Table 4.3.

TABLE 4.3: Gibbs Free energy changes in tumour ATP after x-irradiation

Dose (Gy)	ΔG_{ATP} (J/mg) x 10^{-3}*
5	187
10	473
15	263
30	210
100	146
200	131

* The values of ΔG_{ATP} were calculated at pH 7.4 and 25°C.

The variation of ATP content in CaNT tumours 2.5 hours after doses of 5 Gy, 10 Gy, 15 Gy, 30 Gy, 100 Gy and 200 Gy x-rays is shown in the Fig 4.5.

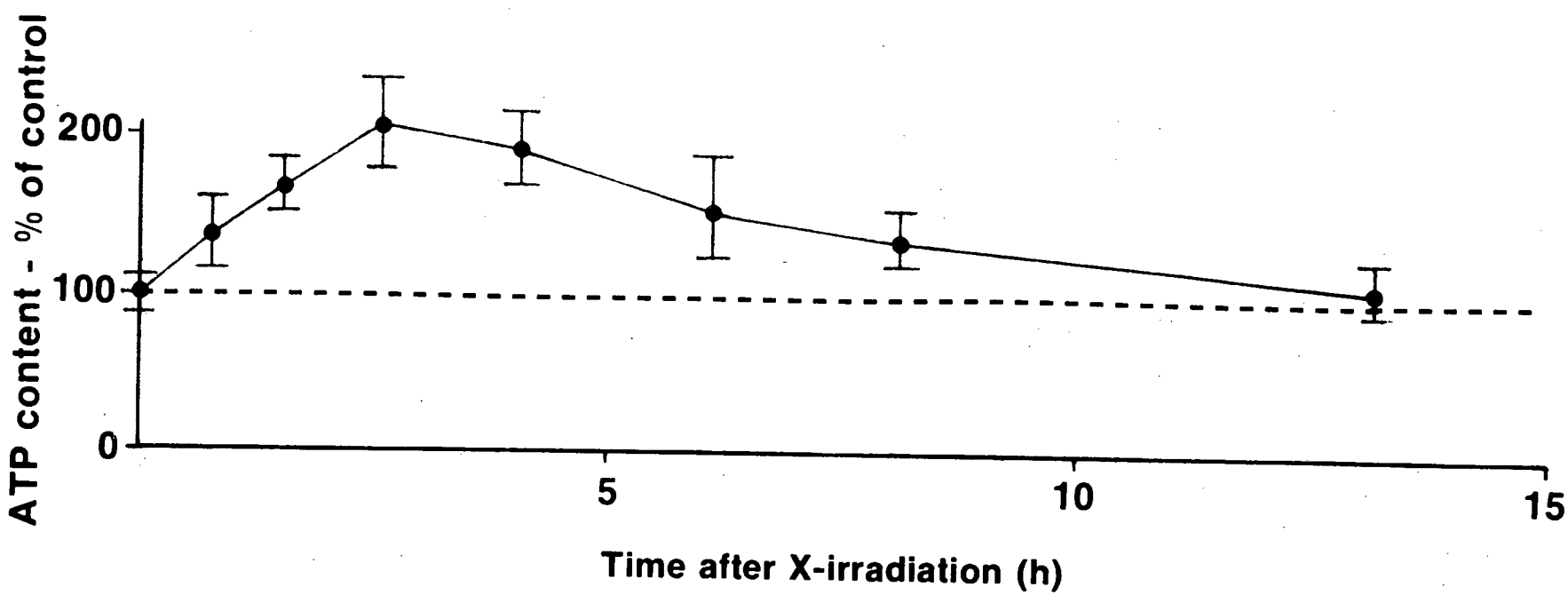

Fig 4.4 ATP levels in the CaNT tumours at various times after receiving an x-ray dose of 15 Gy.

Each point represents the mean of not less than 3 values. SEM is indicated by the vertical bars.

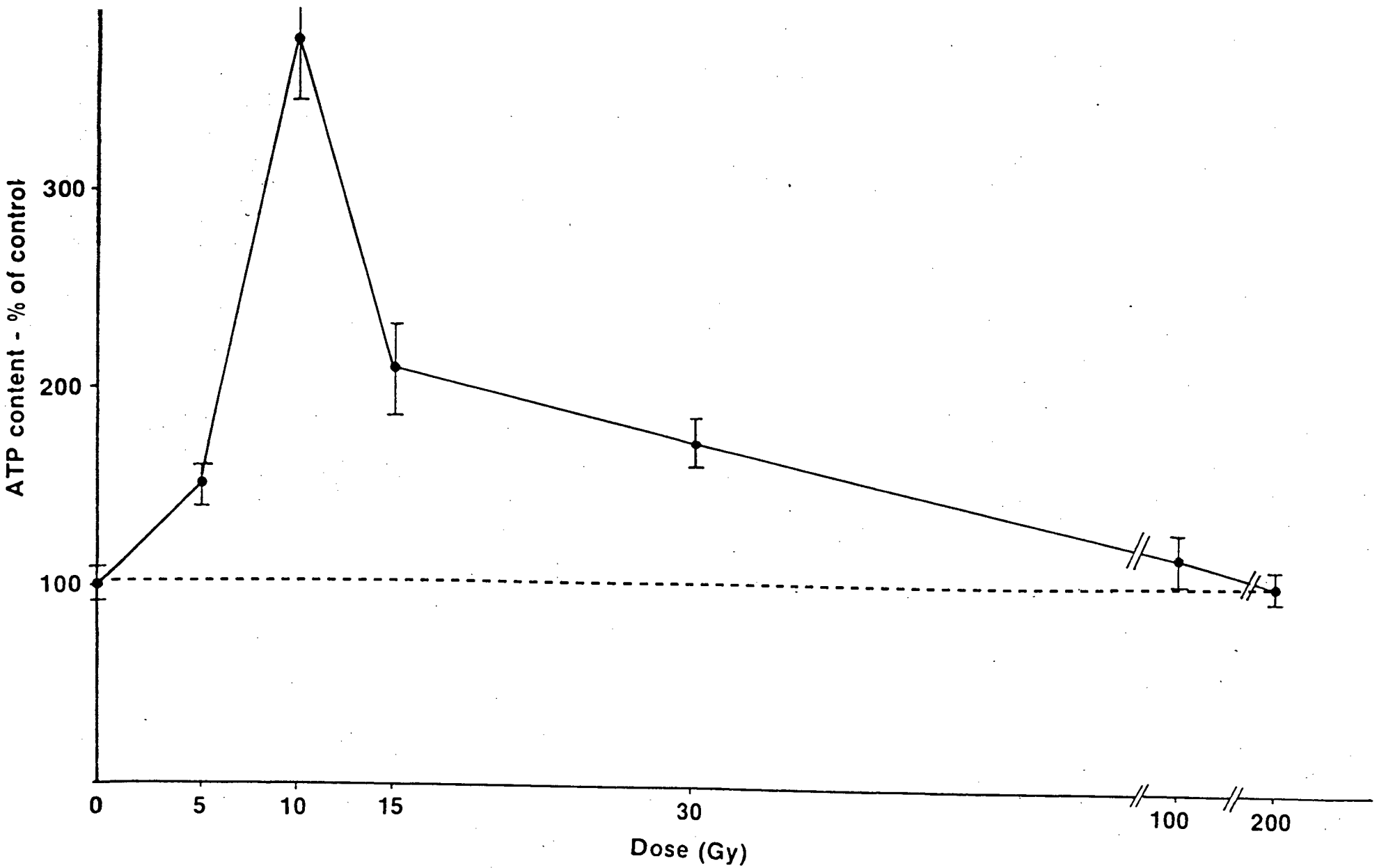

Fig 4.5 Variation of ATP concentration in the CaNT tumours 2.5 hours after x-ray doses of 5 Gy, 10 Gy, 15 Gy, 30 Gy, 100 Gy and 200 Gy. Each point represents the mean of not less than 4 values. SEM is indicated by the vertical bar.

4.1.4.3 Levels of ATP in Fib/t and Rhabdomyosarcoma tumours after x-irradiation (10 Gy).

The levels of ATP were measured, 2.5 hours after x-irradiation.

An increase in ATP Levels to 1.48 times and 1.43 times that of controls ($P < 0.025$) respectively in Rhabdomyosarcoma and Fib/t was noted. Therefore the ΔG_{ATP} yield at 25°C was 186×10^{-3} J/mg and 179×10^{-3} J/mg respectively.

4.1.4.4 ATP levels after clamping CaNT tumours following x-irradiation.

Measurements were made after clamping the tumour by using a string tourniquet for 15 minutes, followed by a radiation dose of 10 Gy and maintaining the tourniquet for a further 2.5 hours. Then ATP levels were determined in 12 CaNT mice tumours. The decrease of ATP content to 0.86 times ($P < 0.005$) that of controls was observed. Consequently the ΔG_{ATP} yield at 25°C was 107×10^{-3} J/mg.

4.1.5.1 ATP content in CaNT tumours after treatment with mitoxantrone

ATP intracellular concentration was reduced by 0.89 times, compared to controls ($P < 0.05$), after both intraperitoneal injection of 200 µl of mitoxantrone, and a local administration of 45 µl inoculated directly into the tumour of the CBA mice.

ATP content was measured 1 hour after treatment with this anthroquinone drug.

4.1.5.2 ATP levels after treatment with mitoxantrone and x-rays

ATP levels were measured after the following procedures:

1) Treatment with 200 µl of mitoxantrone by intraperitoneal administration plus local mitoxantrone injection of 35 µl into the CaNT tumour;
2) After 1 hour the tumours received 10 Gy of 100 kVp x-rays.
3) After a further period of 2.5 hours the ATP determination was made.

The ATP yield was increased (by 1.37 times, $P < 0.05$) compared to control values. This is represented in Fig 4.6.

4.1.6.1 Levels of ATP in CaNT tumours after different qualities of ionizing radiation.

The levels of ATP in the transplantable CaNT murine tumours were measured 2.5 hours after receiving 10 Gy of different photon energy: 100 KVp x-rays, 250 KVp x-rays, ^{60}-Co γ-rays (1.17/1.33 MeV) and 8 MeV x-rays. The resulting measured ATP concentrations with respect to unirradiated controls were 3.78 times with 100 KVp, 1.56 times greater with 250 KVp and 1.23 times greater with 1.17/1.33 MeV ($P < 0.05$). With 8 MeV radiation, the tumour ATP concentration remained unchanged to within the experimental uncertainty.

These results are shown in the Fig 4.7.

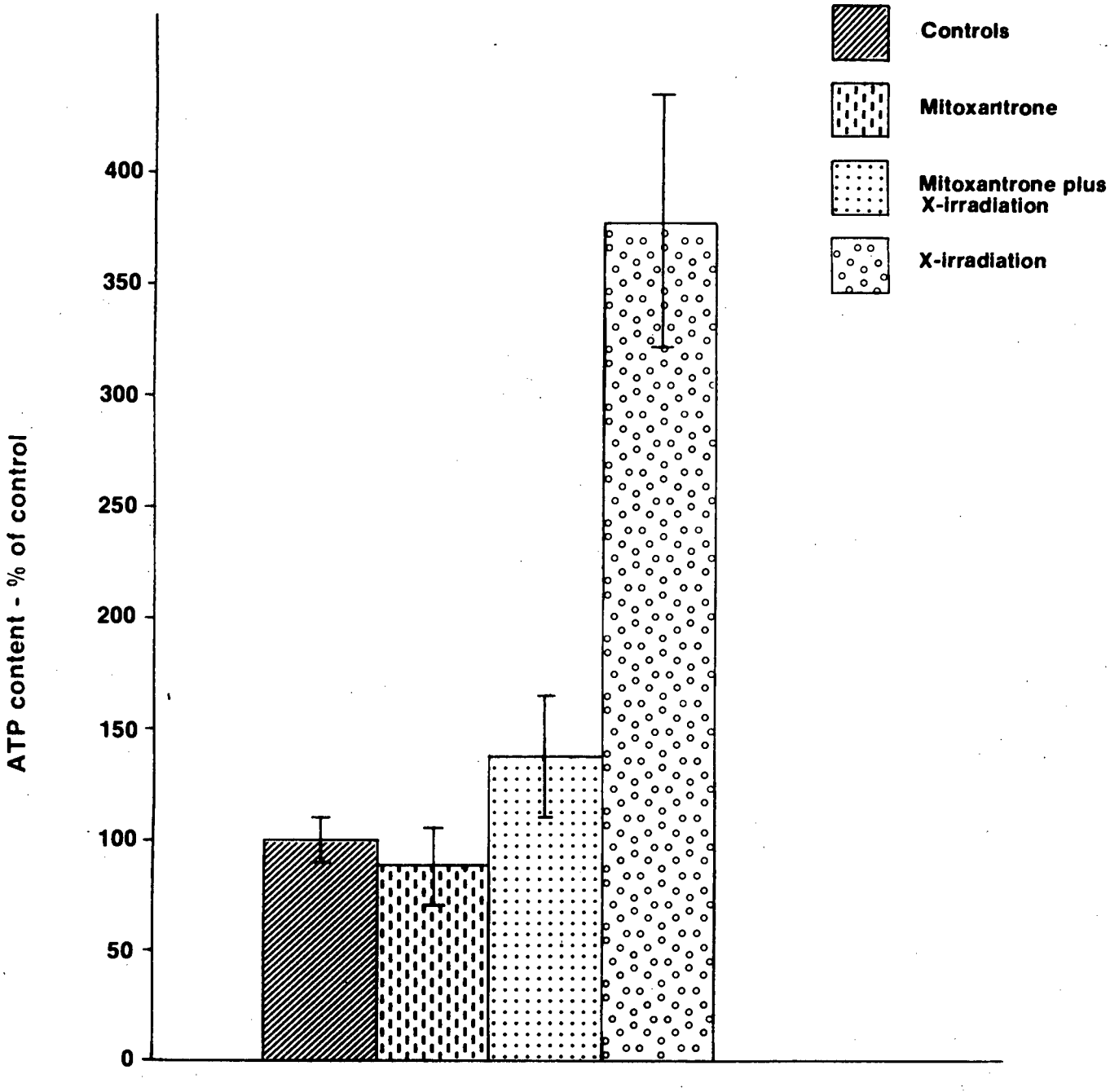

Fig 4.6 ATP content after treatment with mitoxantrone and x-rays.
The heights of the histogram compartments represent the mean of not less than 6 determinations. The error bars shown represent the SEM.

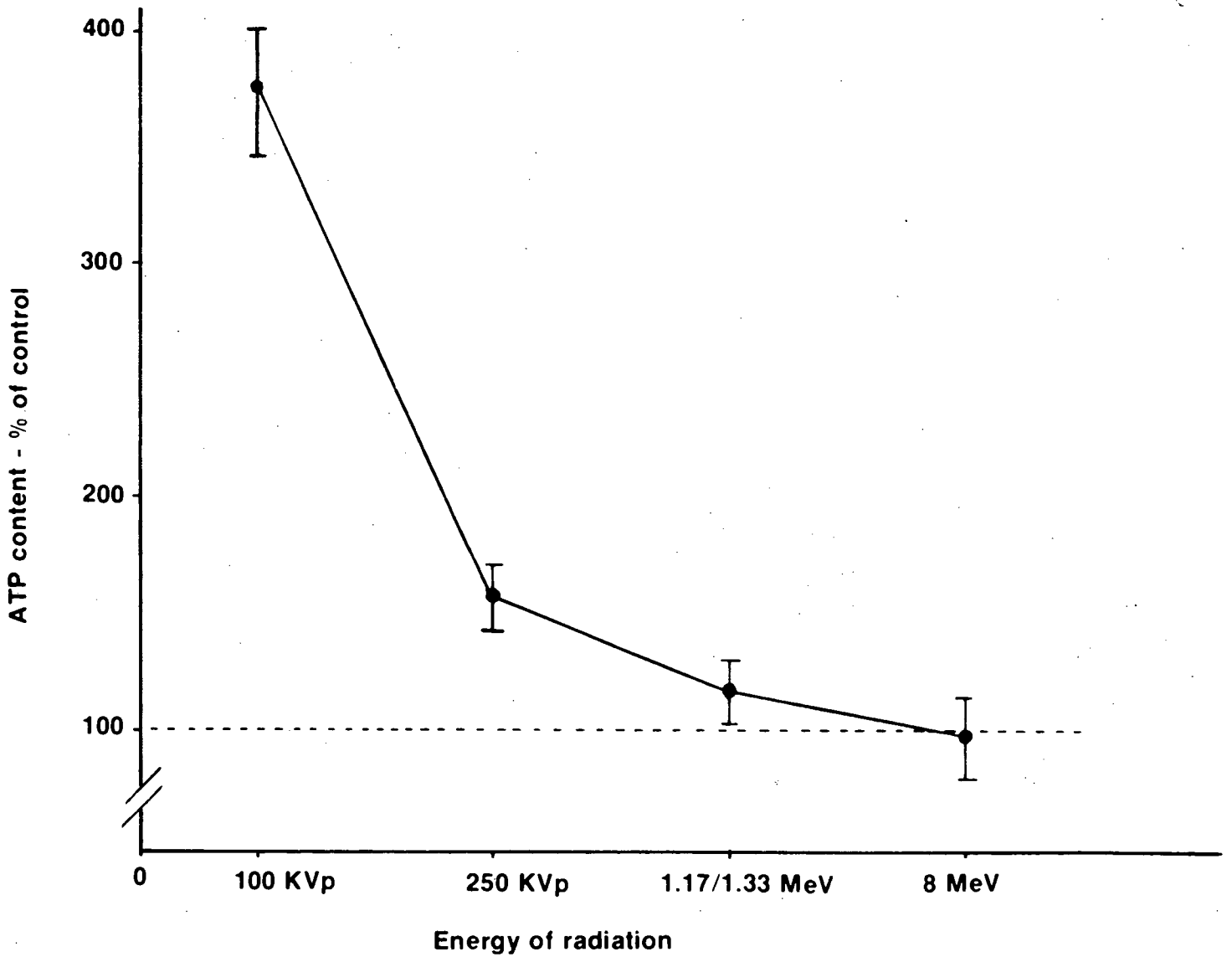

Fig 4.7 Levels of ATP in CaNT tumours after different photon energies. Each point represents the mean of not less than 4 values and vertical bars represent SEM.

The Gibbs Free energy change in tumour ATP in normoxic conditions with different photon energy is presented in Table 4.4.

TABLE 4.4: Gibbs Free energy changes in tumour ATP with different photon energy

Photon energy	ΔG_{ATP} (J/mg) x 10^{-3}
100 KVp	473
250 KVp	195
1.17/1.31 MeV	151
8 MeV	125

4.1.7.1 Levels of ATP in B16 mouse melanoma cells following ^{60}Co-gamma rays

The levels of ATP in the B16 mouse melanoma cell line were measured 3 hours following 2, 4, 6, 8 and 10 Gy of gamma radiation from a ^{60}Co source. Maximal ATP level increases occurred with the 6 Gy dose (2.3 times that of unirradiated controls which is $(6.05 \pm 0.71) \times 10^{-16}$ moles/cell, $P < 0.05$). The result is presented in Fig 4.8.

4.1.7.2 ATP content in B16 mouse melanoma cells after treatment with mitoxantrone

ATP concentrations were determined 3 hours after adding 5.6 μg/ml of mitoxantrone to the incubation medium of B16 mouse melanoma cells. Intracellular ATP content

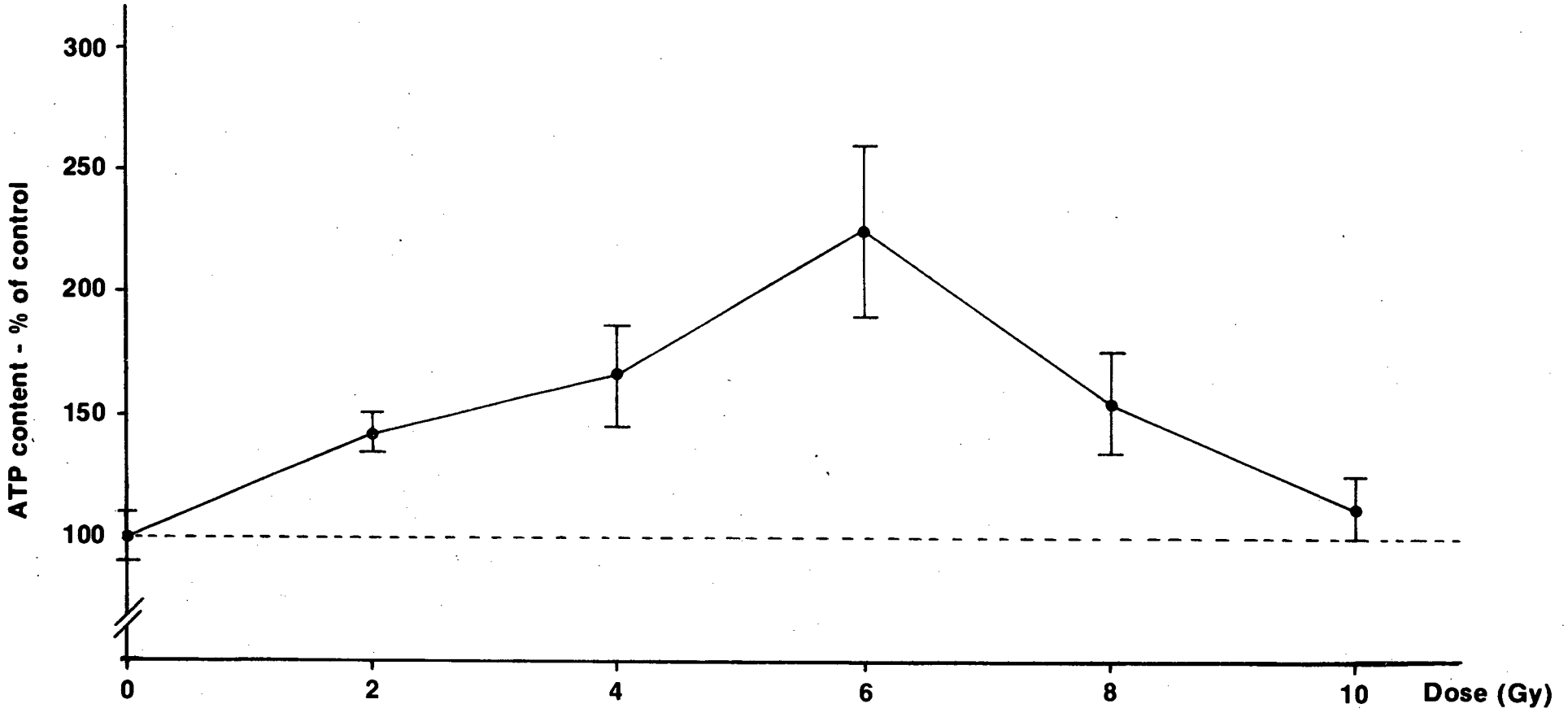

Fig 4.8 Variation of ATP levels in B16 mouse melanoma cells after ^{60}Co-gamma rays.

Each point represents the mean of not less than 5 values. SEM is indicated by the vertical bars.

was reduced by 0.84 times ($P < 0.025$), compared to control values. This is represented in Fig 4.9.

4.1.7.3 ATP concentration after treatment with mitoxantrone and ^{60}Co gamma rays

Mitoxantrone (5.6 µg/mℓ final concentration in the medium) was added to B16 cells immediately before they received 2, 4, 6, 8 and 10 Gy of gamma radiation. Cellular ATP levels were determined after a further 3 hour incubation period.

There was significant difference ($P < 0.05$) in the ATP levels of the irradiated cells compared to the untreated controls. These results are shown in Fig 4.10.

4.1.7.4 Effect of exposure of B16 mouse melanoma cells to varying concentrations of mitoxantrone

In order to construct radiation dose response curves, when cells were exposed to both mitoxantrone and radiation, it was considered expedient to investigate firstly the effect that varying concentrations of mitoxantrone have on the survival levels of the B16 cells, as determined by cell clonogenicity.

Cells were exposed to mitoxantrone contained in the medium, at concentrations varying from 10^{-4} to 0.5µg/mℓ. Exposure to the drug was for 4 hours, followed by washing out of the mitoxantrone and plating out of the cells. Flasks containing the cells and growth medium were placed in the incubator and after 11 days colonies were stained and counted.

As can be seen from Fig 4.10(a) a threshold dose of approximately $5x10^{-3}$µg/mℓ was apparent, after which there was an approximately linear relationship with surviving fraction, on a log-log plot.

Because of the extremely low surviving fractions expected at concentrations of mitoxantrone used in prior experiments (Section 4.1.7.3), it was considered desirable to use a mitoxantrone concentration of 0.5µg/mℓ in the remainder of the dose response studies. It was also considered useful to determine ATP levels following exposure to a mitoxantrone concentration of 0.5µg/mℓ for 4 hours. These levels were compared with those of unirradiated cells and also cells receiving a dose of 6 Gy of ^{60}Co-gamma rays (Table 4.5).

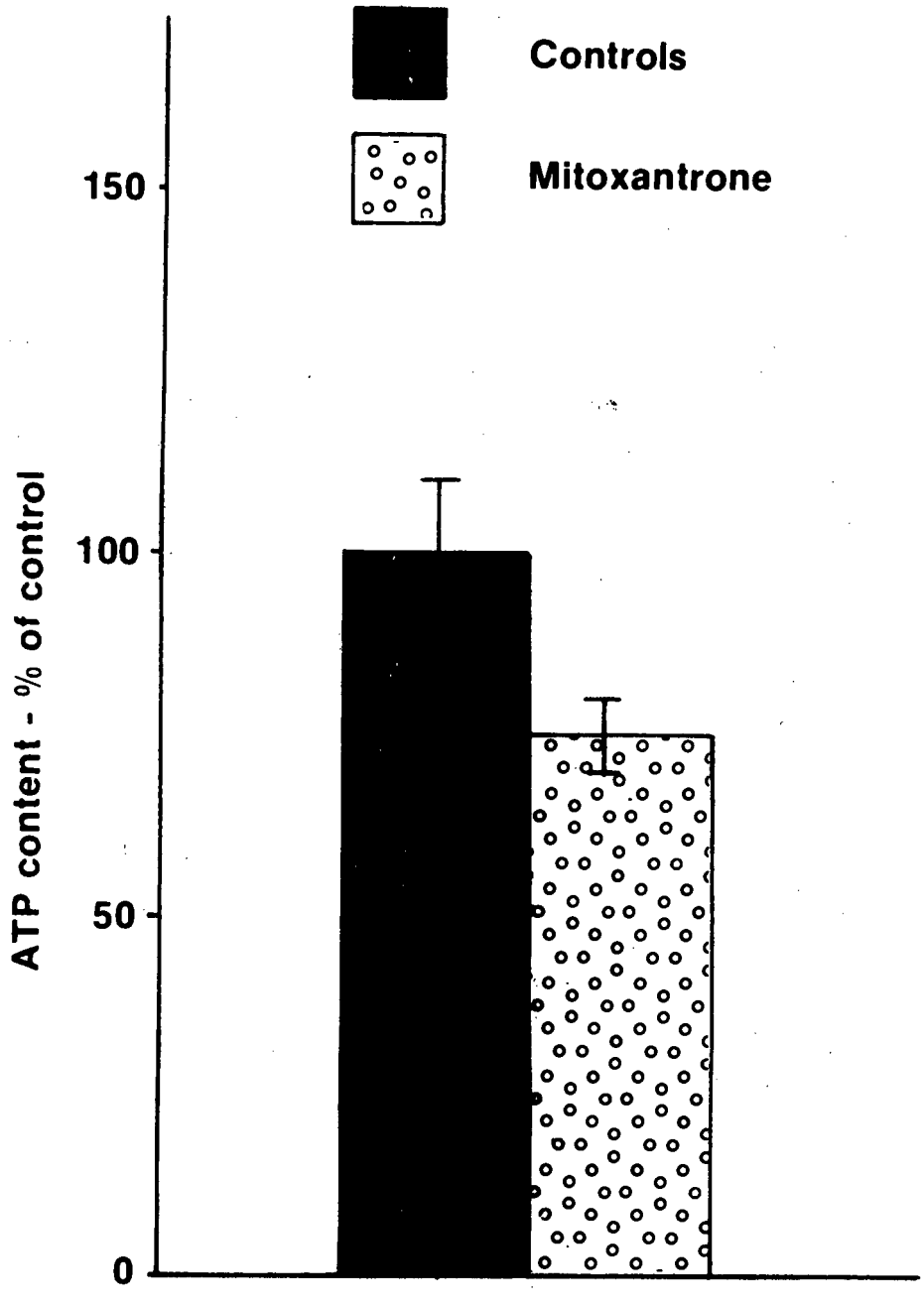

Fig 4.9 ATP concentration in B16 mouse melanoma cells after treatment with mitoxantrone.

The heights of the histogram compartments represent the mean of 7 determinations. The error bars shown represent the SEM.

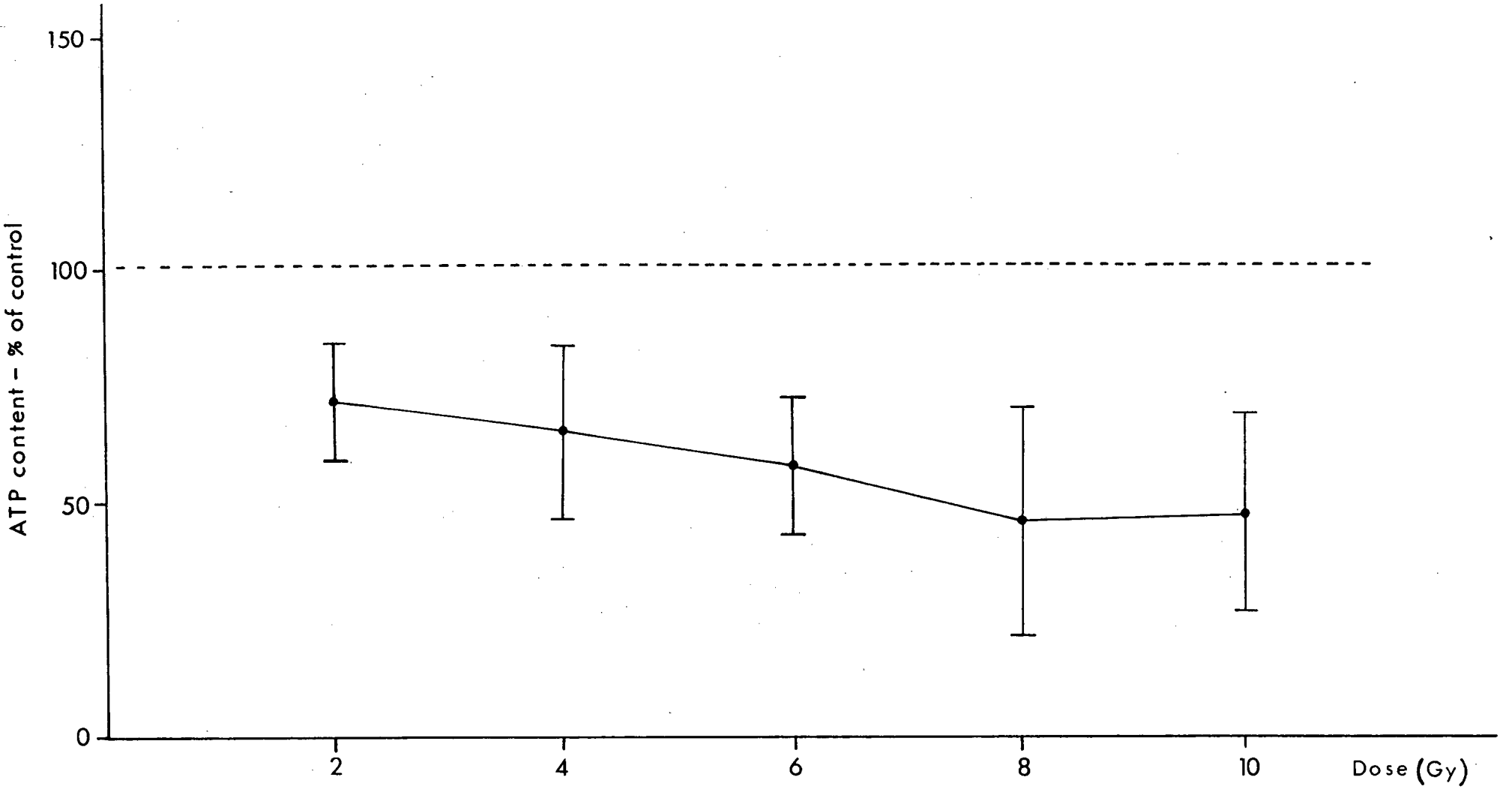

Fig 4.10 Levels of ATP in B16 mouse melanoma cells after treatment with mitoxantrone and ^{60}Co-gamma rays.

Each point represents the mean of not less than 6 values. SEM is indicated by the vertical bars.

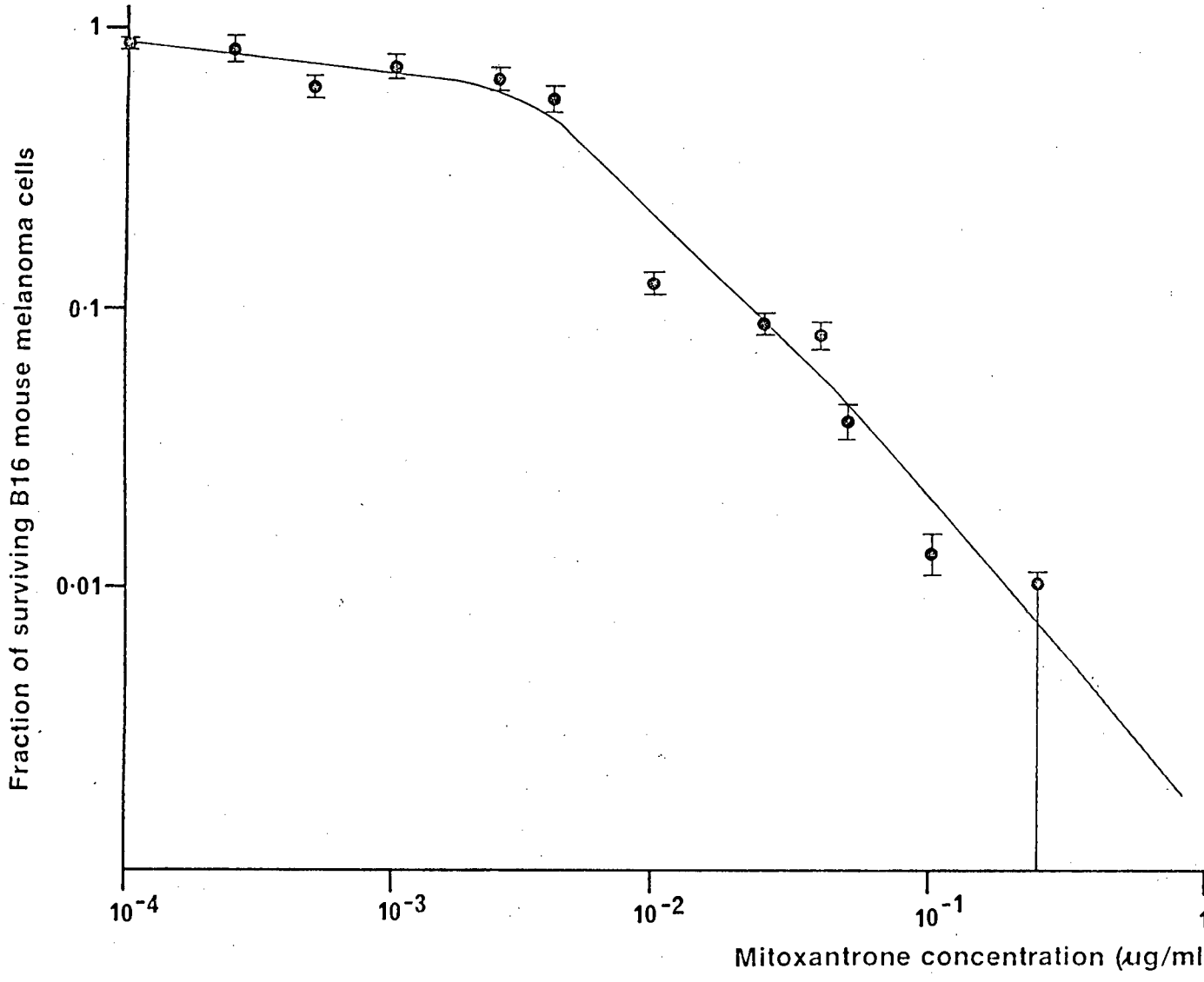

Fig 4.10(a) Dose response curve for B16 melanoma cells exposed to mitoxantrone in the medium for 4 hours.
Each point represents the mean of 4 values, with SEM indicated by the vertical bars.

TABLE 4.5: ATP levels in B16 melanoma cells after treatment with ^{60}Co-gamma rays and mitoxantrone.

Treatment	f moles ATP/cell ($\pm$ SEM)
Controls	1.67 $\pm$ 0.19
^{60}Co-gamma rays (6 Gy)	2.47 $\pm$ 0.30
Mitoxantrone (0.5 µg/mℓ)	2.59 $\pm$ 0.23
^{60}Co-gamma rays (6 Gy) plus mitoxantrone (0.5 µg/mℓ)	2.70 $\pm$ 0.27

As can be seen from Table 4.5, a somewhat unexpected finding was that mitoxantrone at a concentration of 0.5µg/mℓ did not cause a significant decrease in ATP levels, compared with the case of mitoxantrone at a concentration of 5.6µg/mℓ (see Section 4.1.7.2). This might be because mitoxantrone at the lower dose (0.5µg/mℓ) might cause repairable damage to cells, which can lead to increased energy demand, i.e. increased ATP. In this situation, it may therefore be expected that no decrement of ATP following mitoxantrone and gamma-irradiation applied together may occur, as was described above.

4.1.7.5 Radiation response curves after treatment with mitoxantrone

Radiation dose response curves were constructed in the presence and absence of mitoxantrone (0.5 µg/mℓ). Cells were exposed to the drug (a) for 10 minutes before and for 4 hours after irradiation, (b) for 4 hours after irradiation, the drug added immediately

after irradiation. After the 4 hour period, cells were washed and plated out. Because of the very low plating efficiency observed at a dose of 0.5μg/mℓ mitoxantrone, it was necessary to plate out 10^4 cells per flask at doses up to 4 Gy, and 10^5 cells per flask at doses up to 8 Gy.

In both cases there were a left shift of the curves towards lower radiation doses, the greatest shift being in the case of mitoxantrone added before irradiation (Fig 4.11). The dose modifying factor of the mitoxantrone added before and after irradiation at survival levels of 0.37 were 3.15 and 1.80 respectively. At a survival level of 0.1, the dose modifying factors of the mitoxantrone added before and after irradiation were 1.82 and 1.39 respectively.

The experimentally determined response curves of B16 melanoma cells exposed to ^{60}Co-gamma rays and to ^{60}Co-gamma rays where mitoxantrone was added either before or after radiation were analysed according to the linear quadratic model, $S = \exp\{-p(\alpha D+\beta D^2)\}$ using a curve fitting programme. The values of $p\alpha$ and $p\beta$ were computed to be as follows:

(a) ^{60}Co-gamma irradiation only,

$p\alpha = 0.0335\ Gy^{-1}$, $p\beta = 0.0692\ Gy^{-2}$

(b) ^{60}Co-gamma irradiation with mitoxantrone added after irradiation

$p\alpha = 0.5509\ Gy^{-1}$, $p\beta = -\ 0.0005\ Gy^{-2}$

(c) ^{60}Co-gamma irradiation with mitoxantrone added before irradiation

$p\alpha = 0.7214\ Gy^{-1}$, $p\beta = -\ 0.0088\ Gy^{-2}$.

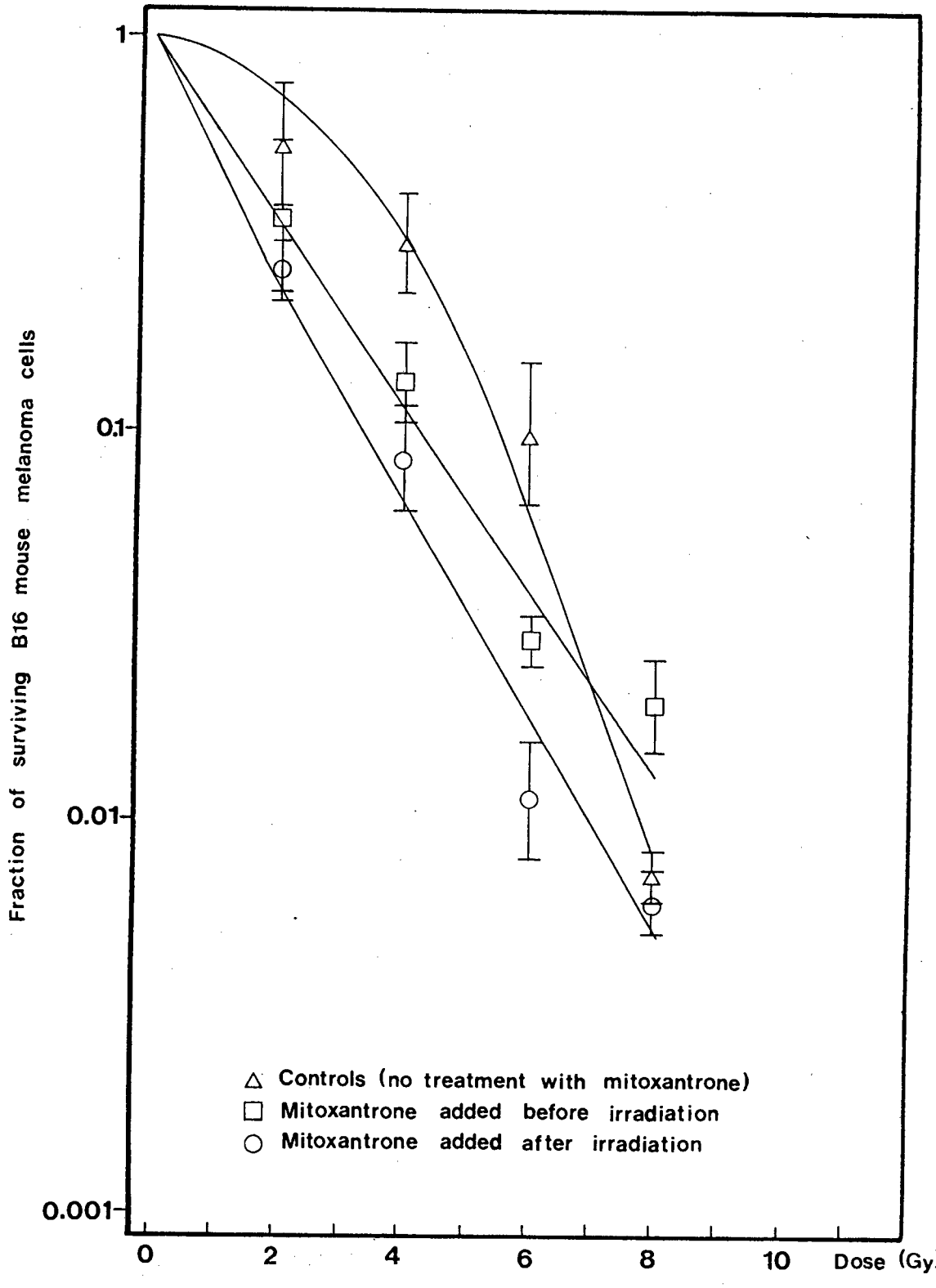

Fig 4.11 Response curve for B16 melanoma cells exposed to ^{60}Co-gamma rays and mitoxantrone.

Each point represents the mean of not less than 3 values. SEM is indicated by the vertical bars. Curves were fitted by making use of the linear quadratic equation, $S = \exp\{-p(\alpha D+\beta D^2)\}$.

4.1.8.1 Relationship between ATP content and volume of the CaNT tumours

Adenosine-5'-triphosphate levels have been measured in CaNT tumours having the following ranges of volumes: 50-150 mm^3, 150-250 mm^3, 250-350 mm^3, 350-450 mm^3 and 450-550 mm^3. The measurements of ATP content within the entire removed tumours always were made immediately after sacrifice of the animals. The result is presented in Fig 4.12.

4.2.1 Glucose-6-phosphate dehydrogenase activity

Glucose 6-phosphate dehydrogenase activity in the CaNT tumour in CBA mice was measured:

(a) in normoxic conditions.

(b) in normoxic conditions after starvation for 72 hours.

(c) in normoxic conditions following x-irradiation.

(d) after clamping the tumours (hypoxic conditions).

(e) after clamping the tumours following x-irradiation.

Glucose-6-phosphate dehydrogenase was measured as well in Fib/t murine fibrosarcoma in WHT mice:

(a) in normoxic conditions.

(b) in normoxic conditions following x-irradiation.

4.2.2 Glucose-6-phosphate dehydrogenase activity in CaNT tumours

4.2.2.1 Glucose-6-phosphate dehydrogenase activity in CaNT tumours in normoxic conditions

In the normoxic control tumour the mean activity from 35 determinations was 0.028 $\pm$ 0.003 µmol glucose-6-phosphate converted/min/mg protein.

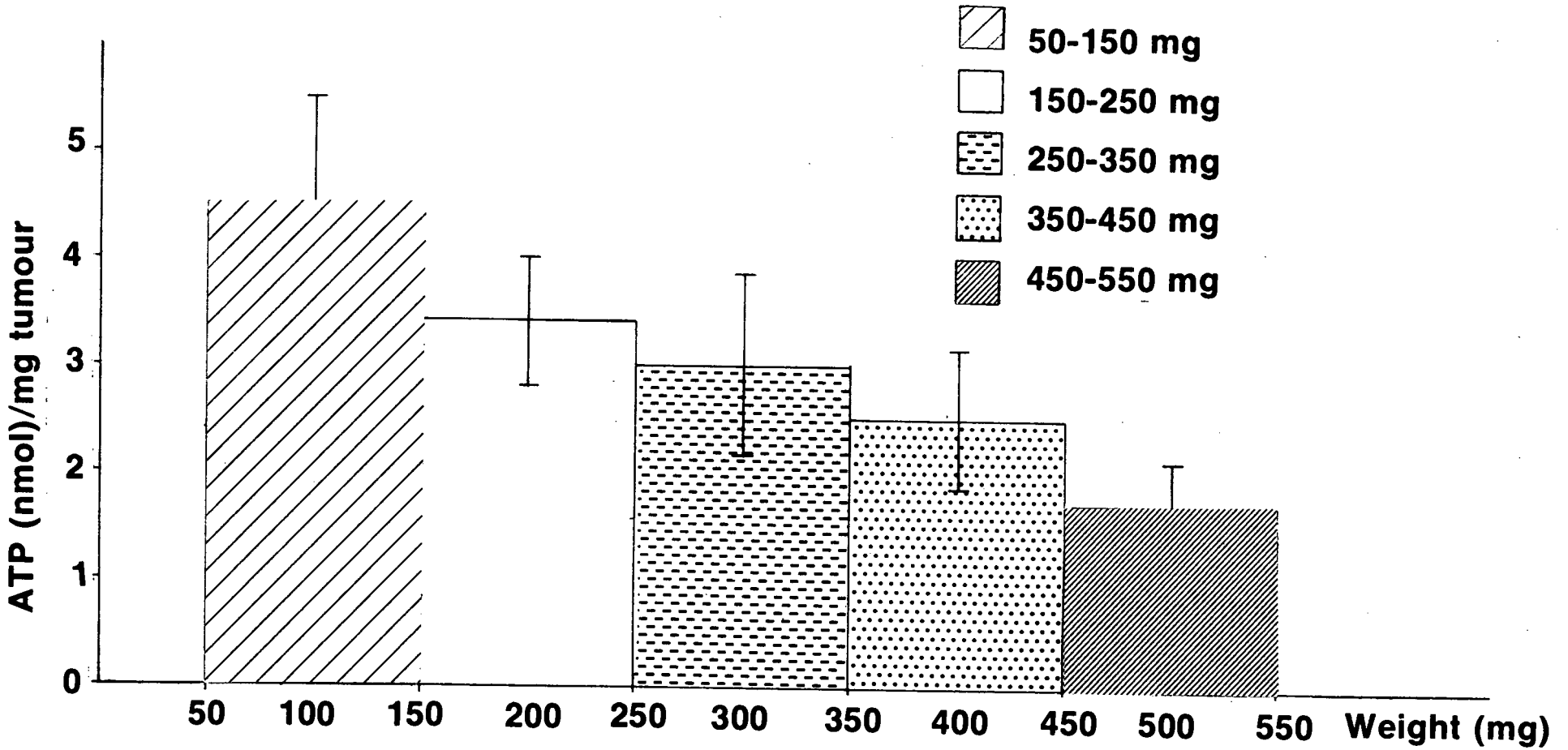

Fig 4.12 ATP levels in different masses of CaNT tumours.

Each point represents the mean of not less than 9 values. SEM is indicated by the vertical bars.

4.2.2.2 Glucose-6-phosphate dehydrogenase activity in CaNT tumours in normoxic conditions after 72 hours of starvation

The mean activity of the enzyme determinations was 0.026 ± 0.004 μmol glucose-6-phosphate converted/min/mg protein. This was not significantly different from the value obtained in the normoxic control tumour ($P > 0.7$).

4.2.2.3 Glucose-6-phosphate dehydrogenase activity in normoxic conditions following x-rays

The effect of ionising radiation on Glucose-6-phosphate dehydrogenase activity was measured at 30 minutes, 1, 3, 4, 18, 20 and 48 hours after a dose 10 Gy x-rays.

An enzyme activity increase was noted by 30 minutes after x-irradiation which was statistically significant ($P < 0.05$). The maximal increase was observed 1 hour after the x-ray dose of 10 Gy. This is shown in the Fig 4.13.

4.2.2.4 Glucose-6-phosphate dehydrogenase activity after clamping CaNT tumours

The enzyme activity after 15 minutes of clamping the tumours showed an increase of 1.36 times compared with the normoxic unirradiated control tumours ($P < 0.025$). Nine determinations were made.

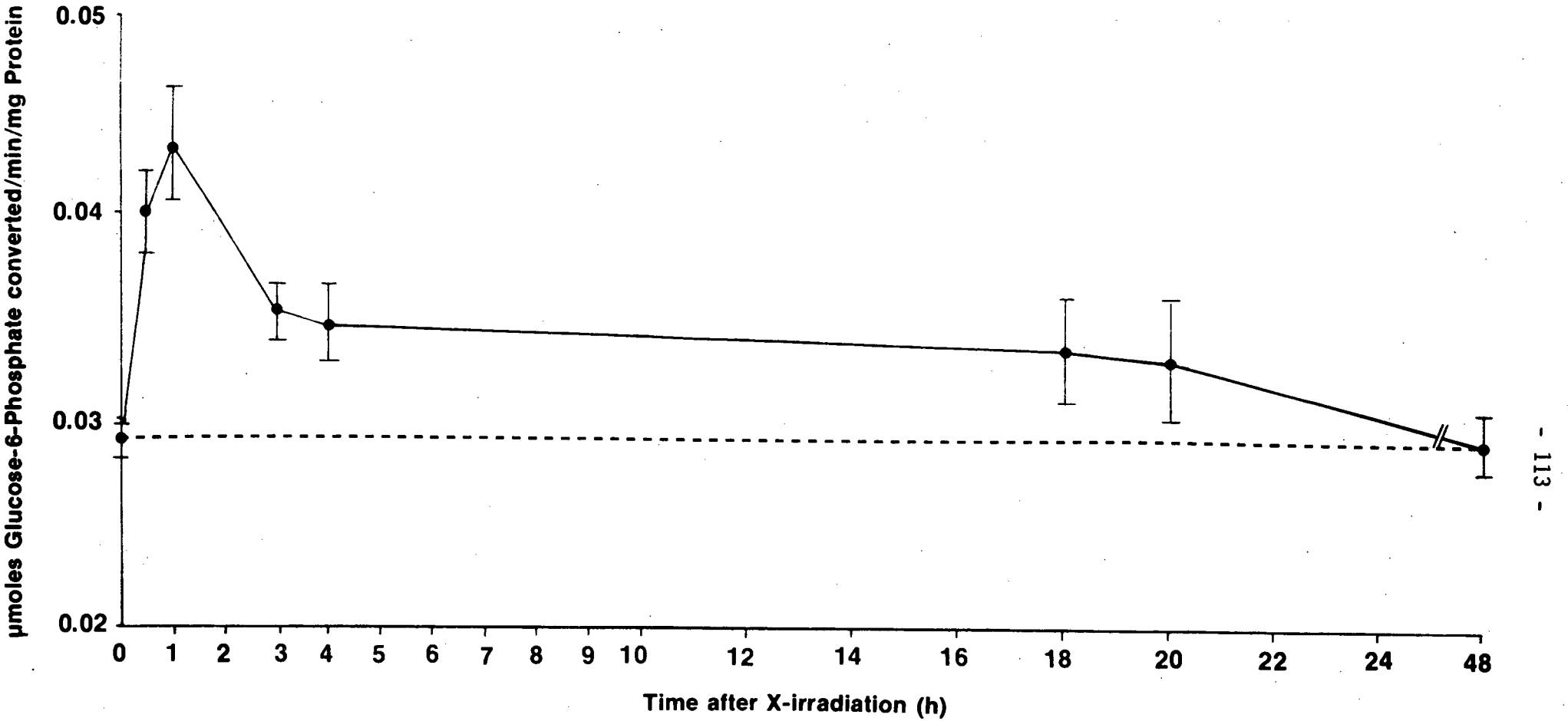

Fig 4.13 Glucose-6-phosphate dehydrogenase activity was measured at various times after a dose of 10 Gy.

Each point represents the mean of not less than 7 values and SEM is indicated by the vertical bars.

4.2.2.5 Glucose-6-phosphate dehydrogenase activity after clamping the tumours following x-irradiation

The activity of the enzyme remained unchanged after 15 minutes of clamping the tumour, following x-irradiation (10 Gy), when the activity was compared with CaNT tumours clamped without radiation.

4.2.3 Glucose-6-phosphate dehydrogenase activity in Fib/t tumours

4.2.3.1 Glucose-6-phosphate dehydrogenase activity in Fib/t murine fibrosarcoma tumours in normoxic conditions

In the normoxic control Fib/t murine fibrosarcoma tumours the mean activity from 5 determinations was 0.029 $\pm$ 0.003 μmoles of glucose-6-phosphate converted/min/mg of protein.

4.2.3.2 Glucose-6-phosphate dehydrogenase activity in normoxic conditions following x-irradiation

The specific activity of G6P-DH activity was measured 1 hour after x-ray administration (100 kVp, 10 Gy). The activity of the enzyme increased. This was statistically significant ($P < 0.001$) and is shown in Fig 4.14.

4.3.1 Phosphomannose isomerase activity

Phosphomannose isomerase activity was measured in liver tissue and tumour tissue of CBA and WHT mice in normoxia, and results are presented in Table 4.6.

TABLE 4.6: Phosphomannose isomerase activity in CBA and WHT mice

Strain of Mouse	Organ/tissue	Specific activity of extract (Units/mg/protein)
CBA	Liver	0.017 ± 0.002
WHT	Liver	0.015 ± 0.001
CBA	CaNT tumour	0.019 ± 0.003
WHT	Fib/t tumour	0.013 ± 0.002

Units are expressed as μmol mannose 6-phosphate converted per minute at 25°C under standard assay conditions.
The mean value ± SEM for 4 determinations of Phosphomannose isomerase activity in different tissue is given above.

4.4.1 Isocitrate dehydrogenase activity

The enzyme activity was measured under the different conditions of:

(a) normoxia,

(b) normoxia following x-irradiation (10 Gy),

(c) after clamping the tumours (hypoxic conditions),

(d) after clamping the tumours and then giving x-irradiation (10 Gy).

4.4.2.1 Isocitrate dehydrogenase activity in normoxia

The mean activity of the enzyme was 0.46 ± 0.07 µmoles isocitrate converted/min/mg protein, as determined in 31 tumours.

4.4.2.2 Isocitrate dehydrogenase activity in normoxia following x-irradiation

As is shown in Fig 4.15, the activity of isocitrate dehydrogenase in normoxic conditions increased after x-irradiation. The maximum increase was observed 3 hours after receiving the 10 Gy x-irradiation. This was 1.46 times that of the control ($P < 0.05$).

4.4.2.3 Isocitrate dehydrogenase activity after clamping the tumours with and without x-irradiation

In both conditions the specific activity of the enzyme in CaNT tumours, which was determined at 25°C, remained unchanged which compared with the control (unirradiated and normoxic conditions)($P > 0.8$). Eleven determinations in each experiment were made (Fig 4.16).

4.5.1 Tissue sulphydryl levels

Tissue sulphydryl levels were determined in CaNT tumours in CBA mice and Rhabdomyosarcoma R1 tumours in WAG/Rij rats. Tissue sulphydryl levels of tumours was measured under:

(a) normoxic conditions

(b) after mice had been exposed to 8% and 12% oxygen for 72 hours

(c) normoxic conditions following x-irradiation (100 KVp and 8 MV), with a dose of 10 Gy.

(d) after clamping the tumours for 15 minutes.

(e) after clamping the tumours followed by x-irradiation.

4.5.2.1 Tissue sulphydryl levels in CaNT Tumours

The results of the tissue sulphydryl levels are illustrated in Fig 4.17. No significant changes in tissue sulphydryl levels compared with controls ($P > 0.8$ in both cases) were observed when mice were exposed to 8% or 12% oxygen in nitrogen for 72 hours prior to assay. Also, no significant changes were observed after clamping of tumours, or x-irradiation with 10 Gy, or after 10 Gy x-irradiation and clamping ($P > 0.8$).

4.5.2.2 Tissue sulphydryl levels in Rhabdomyosarcoma R1 tumours

Tissue sulphydryl levels were measured in Rhabdomyosarcoma R1 tumours, in normoxia and in normoxia 1 hour after a dose of 10 Gy 8MV x-rays using a Philips SL 75-20 linear accelerator.

There was no significant difference between tumour tissue sulphydryl levels following the x-ray dose and controls ($P > 0.7$) as shown in Fig 4.18.

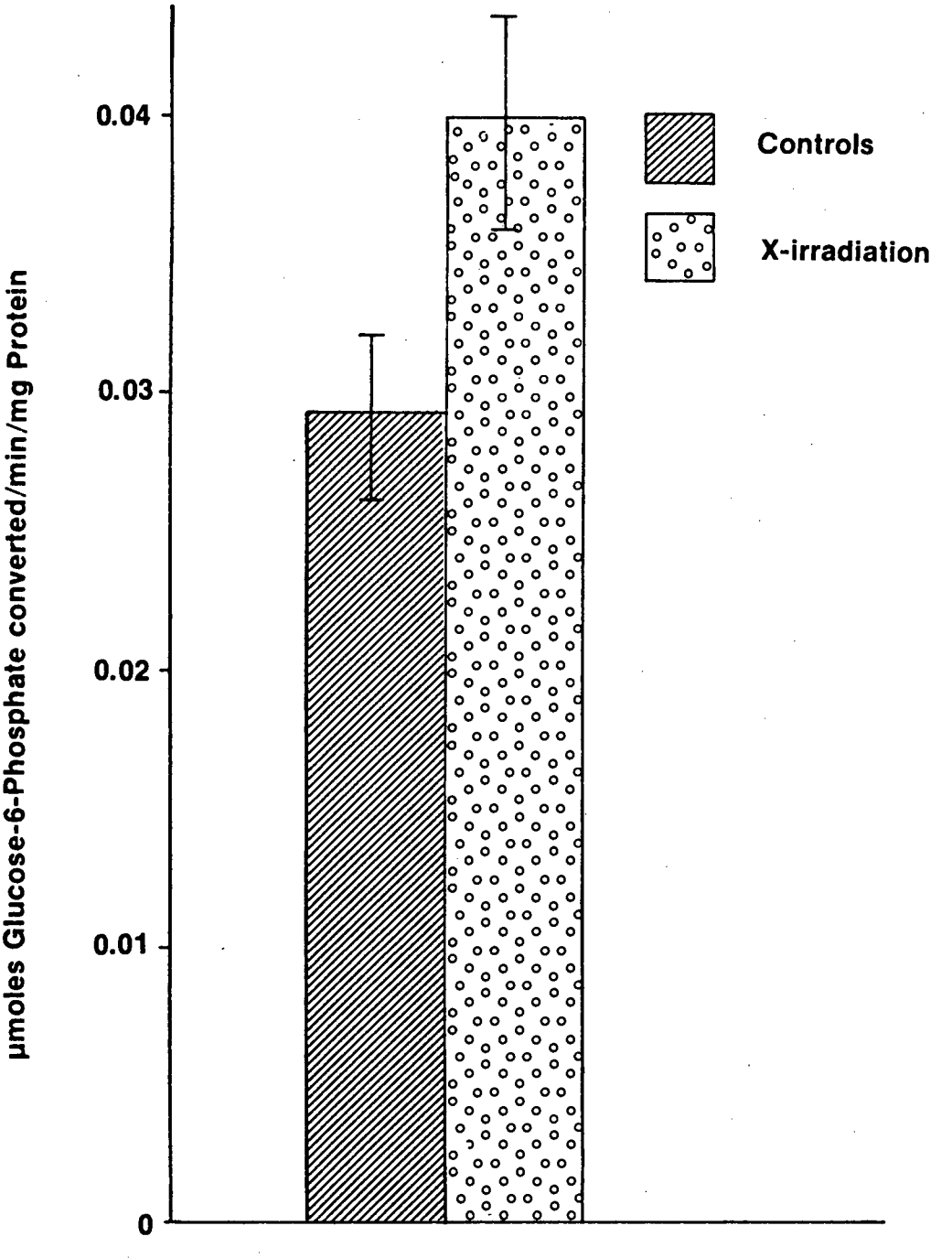

Fig 4.14 Glucose-6-phosphate dehydrogenase activity in Fib/t murine fibrosarcoma following x-irradiation.

The heights of the histogram compartments represent the mean of not less than 7 determinations. The error bars shown represent the SEM.

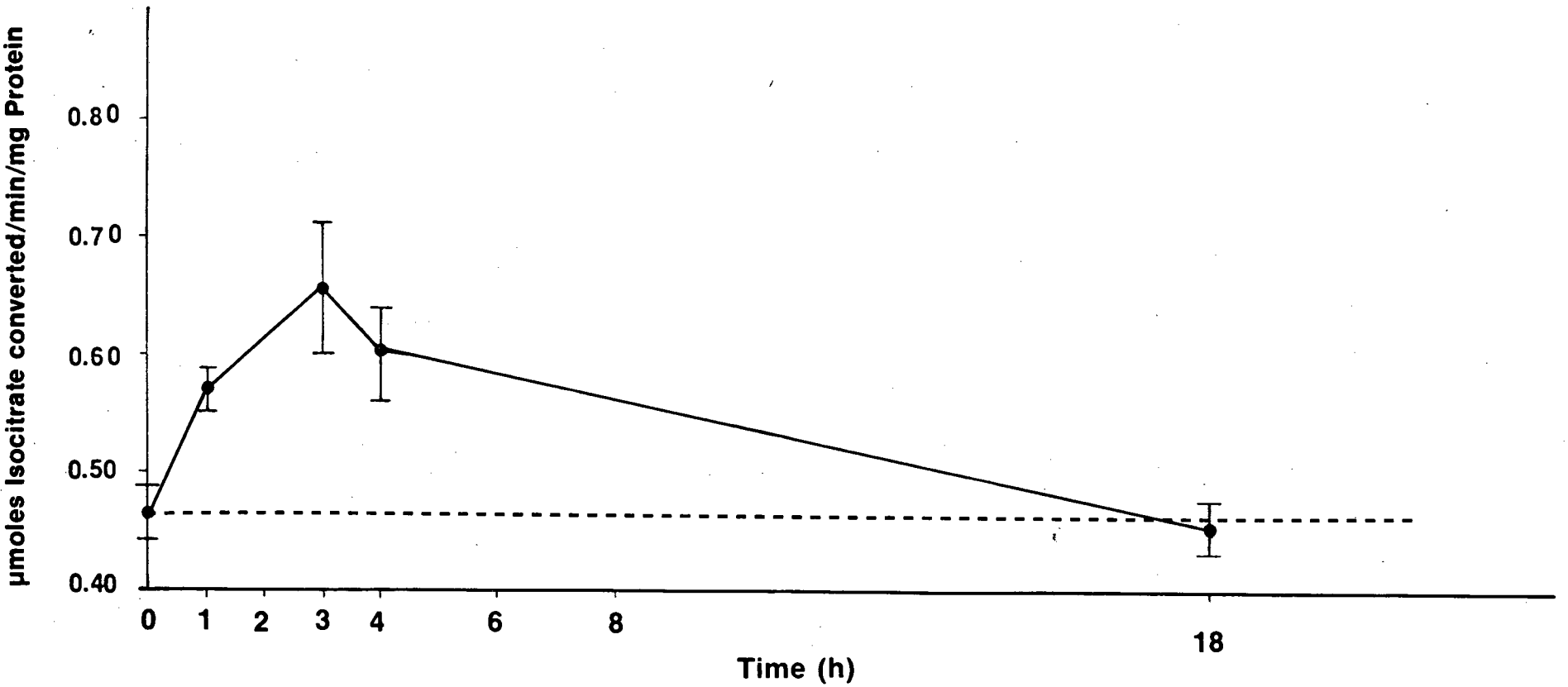

Fig 4.15 Isocitrate dehydrogenase activity in CaNT tumours following x-irradiation.

Each point represents the mean of not less than 5 values and SEM is indicated by the vertical bars.

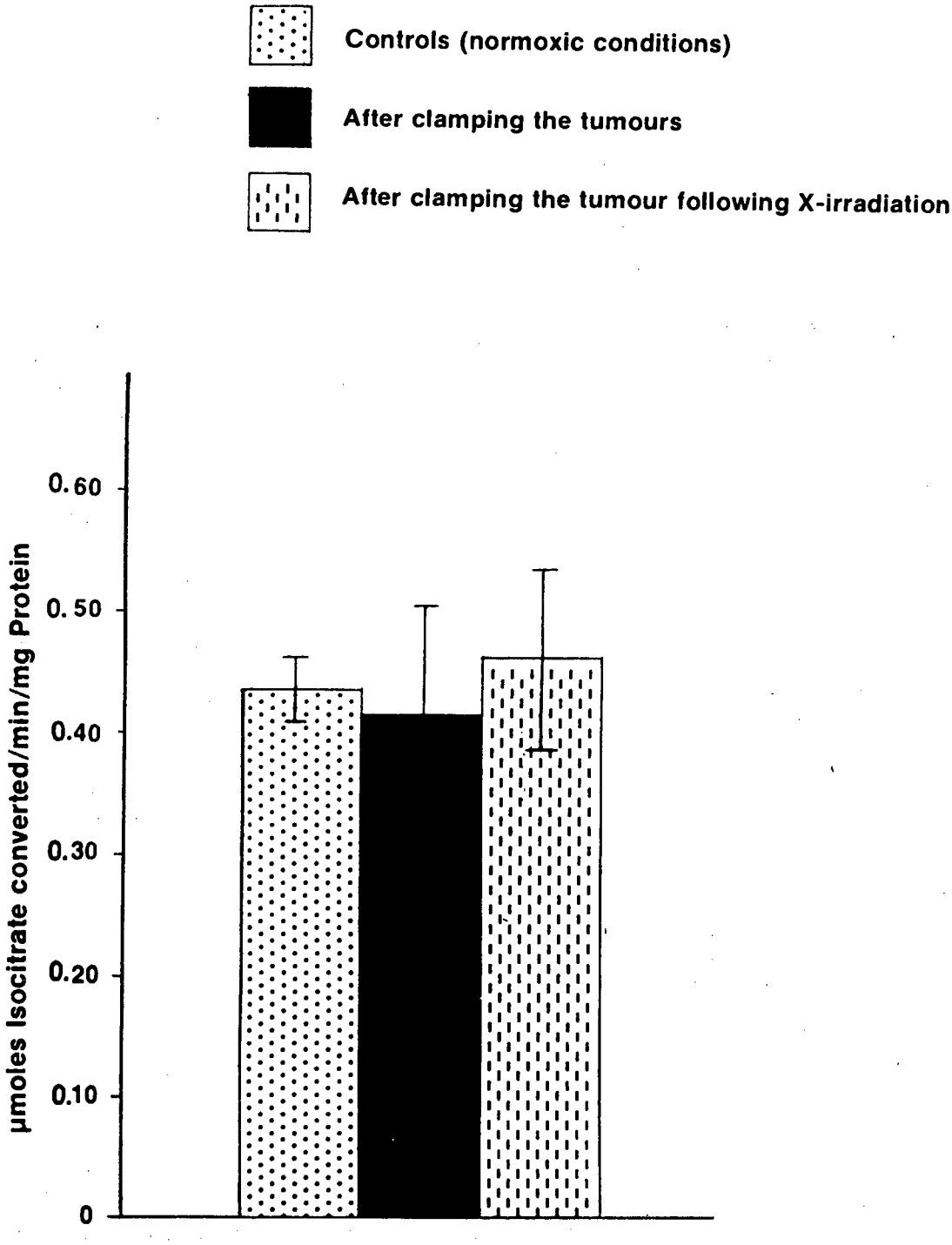

Fig 4.16 Isocitrate dehydrogenase activity after clamping the tumours with and without x-irradiation.

The heights of the histogram compartments represent the mean of not less than 11 determinations. The error bars shown represent the SEM.

4.5.2.3 Glutathione (GSH) levels in deproteinized samples of CaNT tumours

By using the enzymatic method of Tietze (179) for quantitative determination of the amounts of total and oxidized glutathione, its level was measured in CaNT tumours. The mean ± SEM of the GSH levels in 4 unirradiated control tumours and in 4 tumours after 10 Gy x-irradiation, in deproteinized samples were 1571 ± 0.082 ng GSH/mg tissue and 1633 ± 0.054 ng GSH/mg tissue respectively. This result showed no significant difference ($P > 0.8$) in the levels of GSH between unirradiated tumour controls and irradiated tumours. The finding of no difference in glutathione levels between irradiated and non-irradiated tumours using a specific assay is similar to the finding where total thiols were assayed (4.5.2.1).

4.5.2.4 Exogenous GSH added to CaNT samples and its quantitation

To establish that glutathione extraction from tissue was quantitated, a fixed amount of GSH was added to the samples immediately after initial homogenization. Two different concentrations of GSH were added to the tumour samples: 500 ng and 1000 ng of GSH/mg tissue. The following procedures were performed and then the GSH levels assayed:

(i) The CaNT tumours were removed from the CBA mice and cut into two pieces.

(ii) Tumour tissue was weighed out and homogenized 1:5 w/v with ice cold homogenizing medium, which consisted of physiological saline (0.9 NaCl w/v) in 0.66 mM of EDTA.

(iii) To the homogenate of one piece of tumour tissue was added 500 ng of GSH/mg of tissue. The other piece of the tumour was homogenized without adding extra GSH. The same procedure using a concentration of 1000 ng of GSH/mg tissue was followed in another tumour, similarly cut in two.

(iv) To deproteinize all the samples 1 mℓ of 5% TCA was added.

The results indicated that the GSH levels in the samples with exogenously added GSH (2279 and 2377 ng GSH/mg tissue) were equivalent to those added to the initial homogenates plus the endogenous GSH content (1773 and 1382 ng GSH/mg tissue). Thus the differences were 506 and 995 ng GSH/mg tissue respectively. These values are 101.2% and 99.5% of the added amounts of 500 and 1000 ng GSH/mg tissue.

4.5.2.5 Stability of glutathione in non-deproteinized homogenates

A tumour extract was prepared as described in 3.5.1.1. Immediately after preparation the glutathione level was determined in 50 mℓ of a 1 in 100 dilution of the preparation, using the method described in 3.6.1.7. The preparation was stored on ice and glutathione levels were determined again at 0,1 and 4 hours. No detectable change in glutathione levels were measured

over the 4 hour period, indicating that glutathione remains stable in tissue homogenates over at least a 4 hour period.

4.6 Some Biological Effects of Magnetic Fields

4.6.1 Growth rate

The effects on growth rate of CaNT murine tumours in CBA mice, when exposed to magnetic fields of a Nuclear Magnetic resonance imager have been studied. Measurements were made with the tumours subject to:

(a) Single exposure and split exposures in static magnetic field (0.5 Tesla).

(b) Split exposure in static magnetic field (0.5 Tesla) plus a varying magnetic field 5×10^{-3} Tesla/m.

4.6.2 Determinations of the growth rate with exposure to magnetic field

Tumour diameters were measured in three perpendicular directions using Vernier calipers, and the tumour volume was calculated assuming tumours to be spherical. Mean tumour volumes at the beginning of each of the treatments were 170 $\pm$ 29 mm^3. CBA mice with CaNT tumours in the thorax were divided into 4 groups:

Group 1 - Controls; Group 2 - Single exposure in static magnetic field for 62 hours; Group 3 - Split exposure in static magnetic field for 16 hours per day over 7 days and Group 4 - Split exposure in changing magnetic field (superimposed on static field 0.5 Tesla) for 16 hours per day over 7 days.

Retardation of the tumour growth was observed after exposure to static and dynamic magnetic gradient fields. The result is represented in Table 4.7.

Significantly different tumour growth was seen in Groups 3 and 4 when compared with Group 1 ($P < 0.0010$ and $P < 0.0015$ respectively). Group 2 showed no significant difference compared with the controls.

4.6.3 Evaluation of the volume doubling time when exposed to a magnetic field

The mean tumour volume doubling time in controls (no exposure to magnetic field) was 71 ± 8.1 hours ($n = 12$). In Groups 2, 3 and 4, when compared with Group 1 (controls), it was noted that longer times were required to attain twice the initial tumour volume. This result is shown in Fig 4.19.

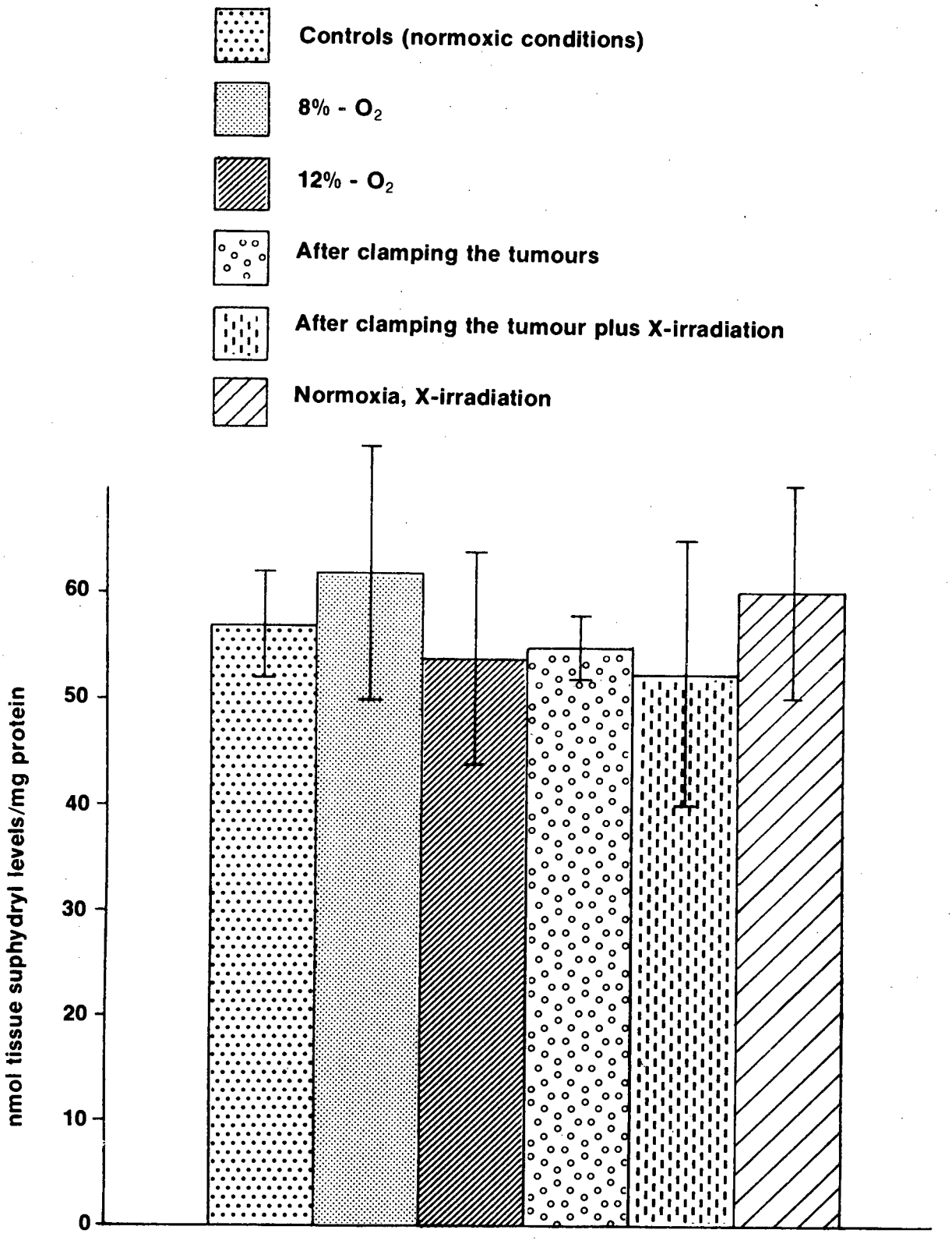

Fig 4.17 Tissue sulphydryl levels in CaNT tumours.

The heights of the histogram compartments represent the mean of not less than 9 determinations. The error bars shown represent the SEM.

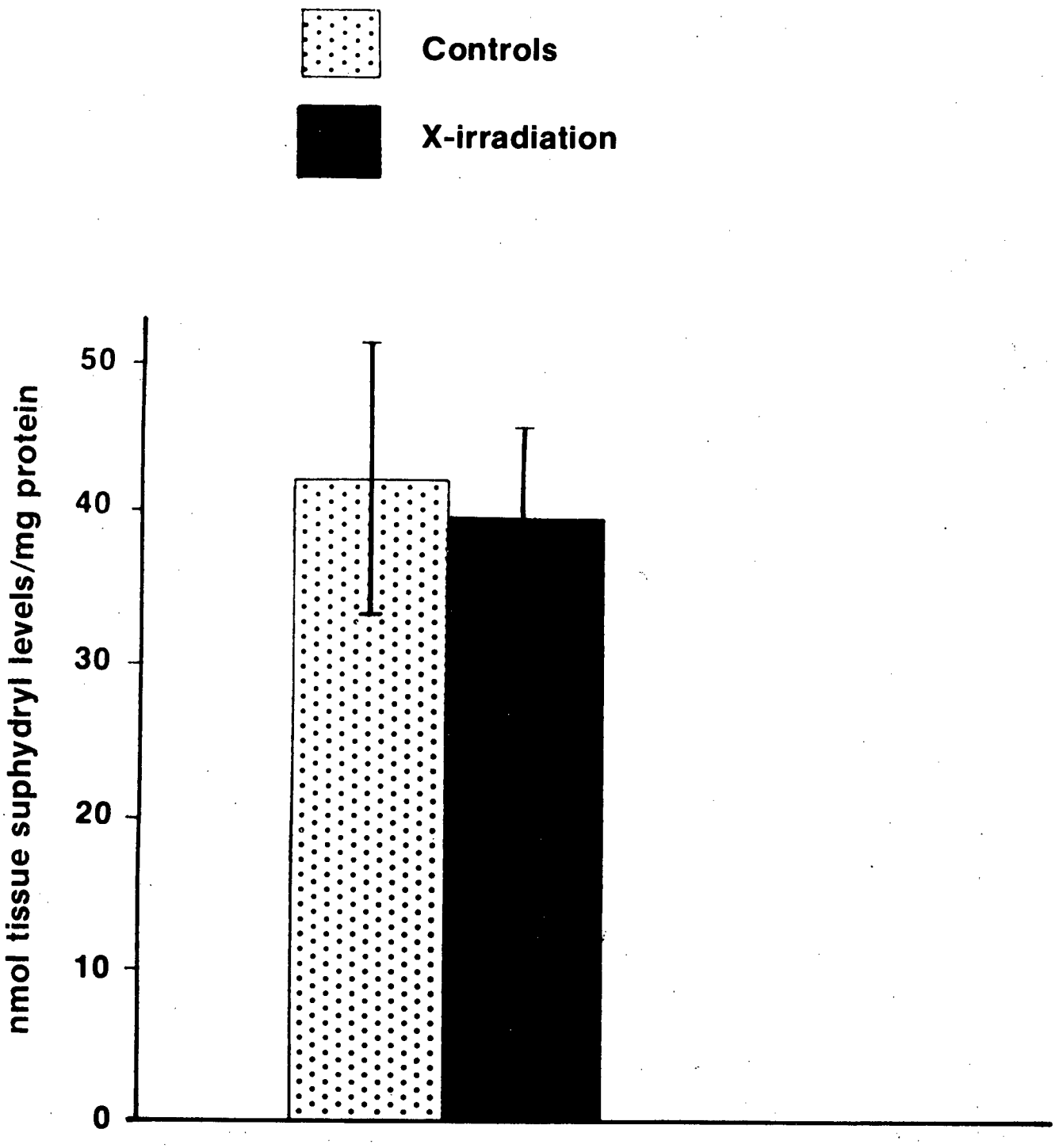

Fig 4.18 Tissue sulphydryl levels in Rhabdomyosarcoma R1 tumours after x-irradiation.

The heights of the histogram compartments represent thé mean of not less than 5 determinations. The error bars shown represent the SEM.

TABLE 4.8

Biomagnetic effects on growth rates			
Ca NT tumour	**n**	**Magnetic Induction**	**Effects observed after 7 days**
Group 1	12	—	Controls
Group 2	7	Static magnetic field	13.7% inhibition of tumour growth
Group 3	9	Static magnetic field	43.3% inhibition of tumour growth
Group 4	9	Dynamic magnetic gradient fields	39.7% inhibition of tumour growth

4.7.1 Specific activities of Glucose 6-phosphate dehydrogenase and Phosphomannose isomerase in CaNT tumours exposed to magnetic field

The effects of magnetic fields upon specific activities of glucose-6-phosphate dehydrogenase and phosphomannose isomerase were measured after split exposures in superimposed static and pulsed magnetic field gradients (0.5 Tesla plus a varying magnetic field 5×10^{-5} Tesla/cm) for 16 hours per day over 7 days (Group 4). The activities of the enzymes show no statistically significant difference after split exposures in magnetic fields.

The result is presented in Fig 4.20.

4.8.1 Measurements of T1 the spin lattice relaxation time and T2 the spin-spin relaxation time in CaNT tumours exposed to magnetic fields

The effects of different exposures to a static magnetic field (0.5 Tesla) on T1 and T2 values of CaNT tumours in CBA mice were measured using controls and tumours exposed in the magnetic field for 16 hours per day over 7 days.

The relaxation times T1 and T2 of CaNT tumours show no statistically significant difference ($P > 0.8$) after split exposures in the nuclear magnetic resonance imager.

The following image shows the tumour in a rectangular region of interest (ROI) Fig 4.21. Centering the ROI on the tumour of each mouse in turn enabled the average of its relaxation times to be determined. The computer also calculated the standard deviation in each case (181).

The result of the measurements is presented in Table 4.8.

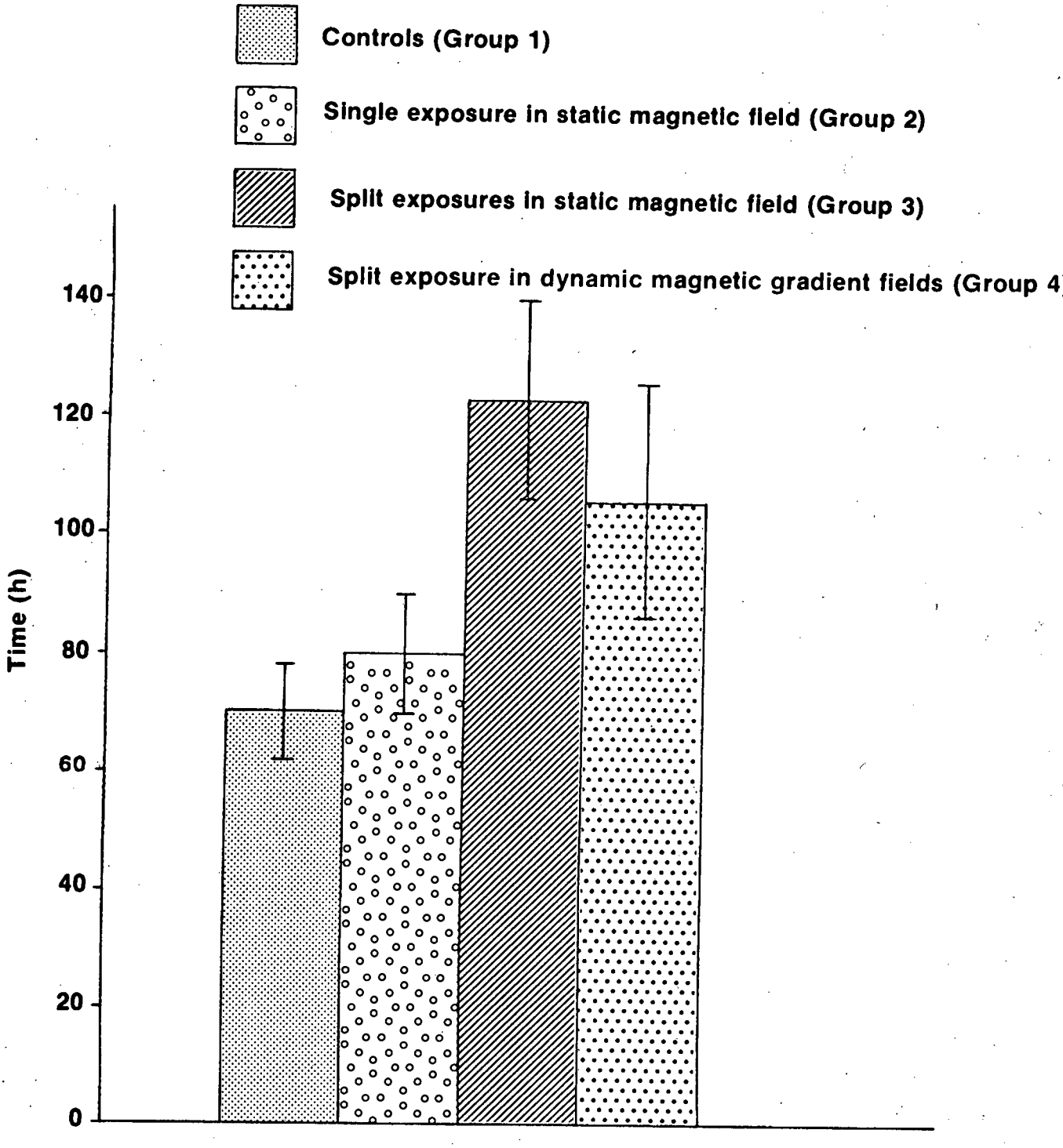

Fig 4.19 Volume doubling time in CaNT tumours when exposed to a magnetic field. Mean time (hours) ± SEM for each group of tumours to reach 2 times the initial tumour volume.

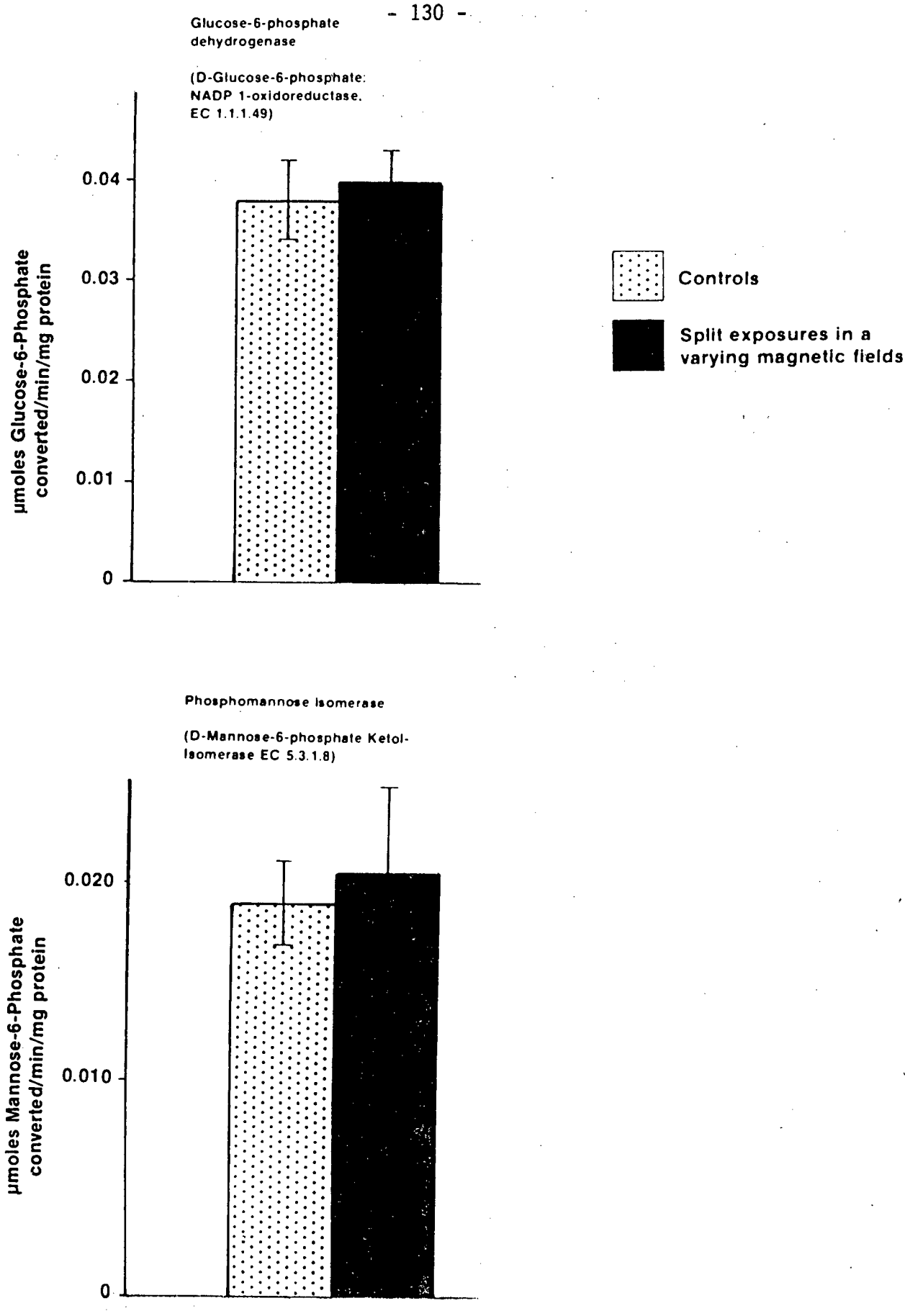

Fig 4.20 Specific activities of glucose-6-phosphate dehydrogenase and phosphomannose isomerase in CaNT tumours exposed to magnetic field. Each point represents the mean of 6 values and vertical bars represent SEM.

TABLE 4.8: NMRI: CaNT tumour in CBA mice

	Controls	Magnetic Field	n
T_1 (ms)	84.2 ± 12.6	79.5 ± 9.7	8
T_2 (ms)	2301 ± 201	2366 ± 156	8

4.9 Electron microscopy ultrastructural studies in CaNT tumours after x-irradiation

Electron microscopic ultrastructural studies were made of CaNT tumours in CBA mice before and after x-irradiation using doses of 10 and 100 Gy.

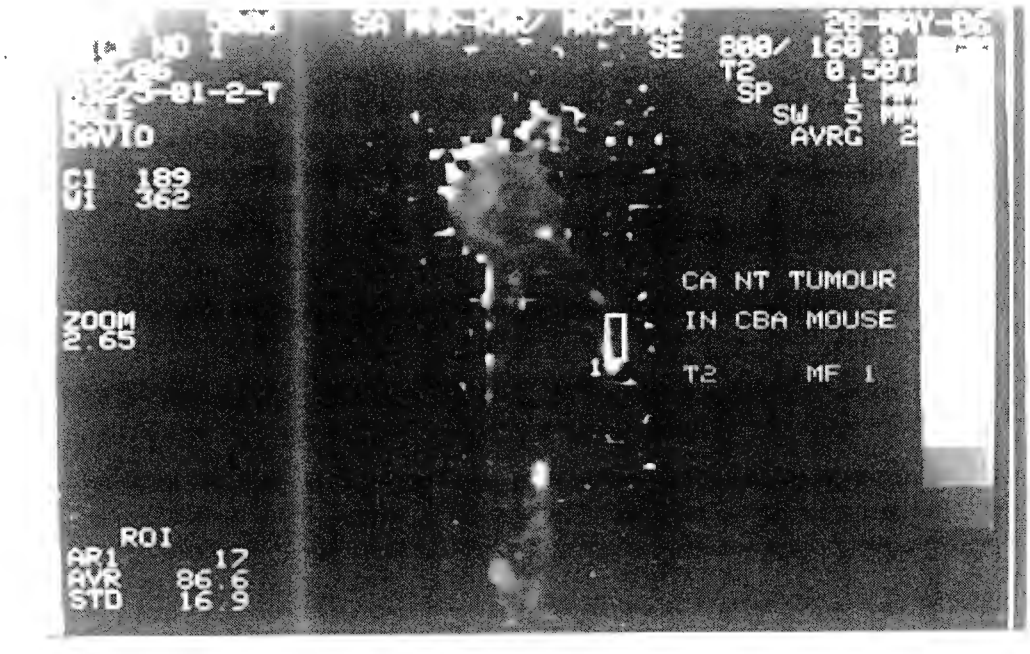

Fig 4.21 A nuclear magnetic resonance image of a CBA mouse with CaNT tumour. (This image is used to calculate quantitative relaxation times and is not intended to demonstrate morphology).

No changes in representative electron micrographs of CaNT tumours, compared with control (Fig 4.22) (non-irradiated) tumours, could be observed after irradiation with 10 Gy (Fig 4.23). However, after irradiation with 100 Gy morphological alterations were noted in the cell, with drops characteristic of lipid (Fig 4.24), probably released from rupture or disruption of organelles. There is also clear degeneration of the cristae and matrix of mitochondria in the tissue irradiated with 100 Gy (Fig 4.25) compared with the control.

Apart from cellular damage resulting from the radiation, which has been described above, another interesting feature was noted and thanks are due to Prof W Becker of the Department of Virology, University of Stellenbosch Medical School for assistance in the analysis of the micrographs. This was a series of round particles with a dense circular concentric interior region and a surrounding less dense ring (Fig 4.26).

In a control tumour about 25 such particles were seen grouped together outside the cell membrane. In irradiated cells these particles were fewer and scattered, some within cisternae and in one case budding from the cell membrane (Fig 4.27). These particles have the typical apperance of a murine leukemia type C retrovirus with a dense nucleoid. The particle observed budding from a membrane is also characteristic of such viruses. They are frequently seen and are most likely to be an associated (not causative) finding in these tumours.

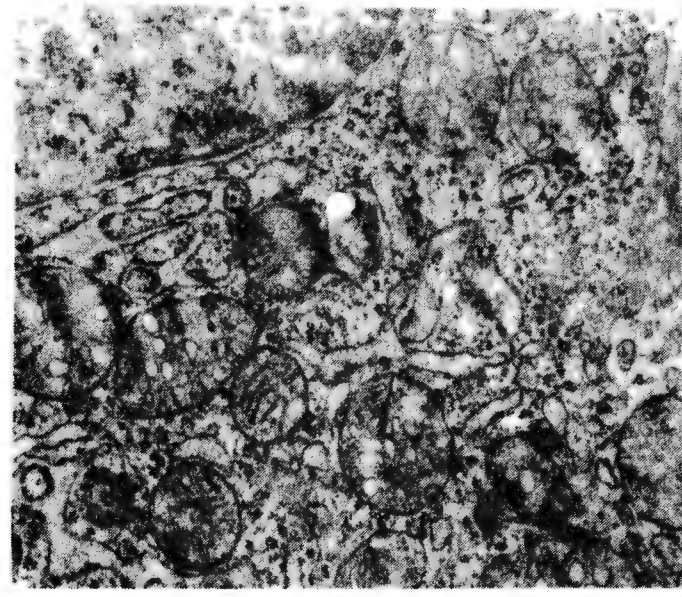

Fig 4.22 Electron micrograph of control CaNT tumour using magnification 23000X. A typical region is shown with no difference between organelles and structure of this image and those of Fig 4.23.

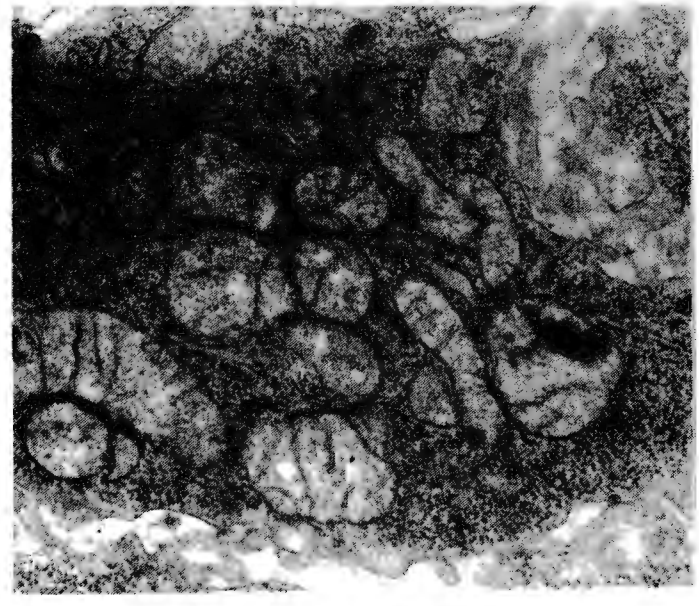

Fig 4.23 Electron micrograph of a typical region of a CaNT tumour which has received 10 Gy of x-irradiation. The magnification is 23000X. There is no significant difference from the control tumour.

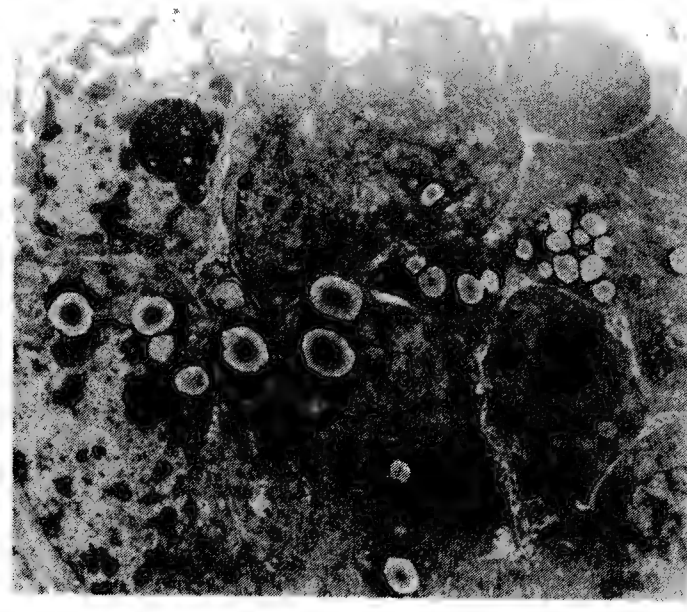

Fig 4.24 Electron micrograph of a CaNT tumour which has received 100 Gy of x-irradiation. Lipid droplets are clearly visible as described in the text. The magnification is 49000X.

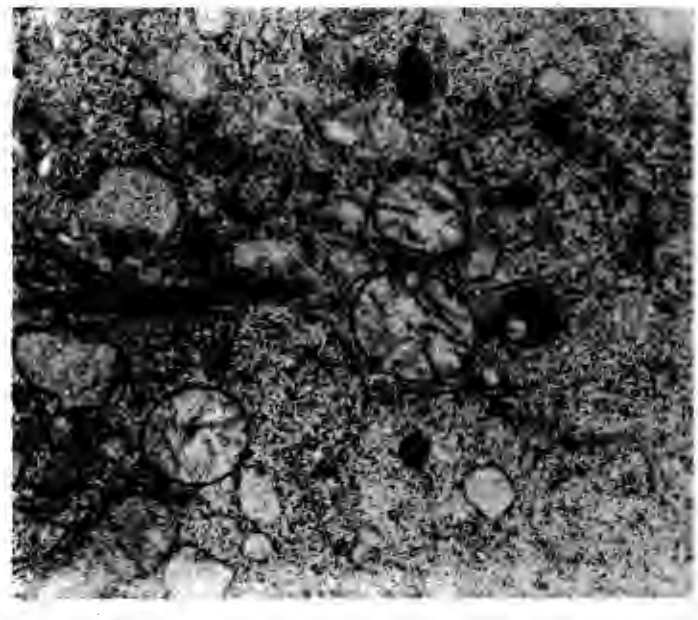

Fig 4.25 Electron micrograph as for Fig 4.24, but showing disruption of mitochondrial structure as described in the text, using magnification 23000X.

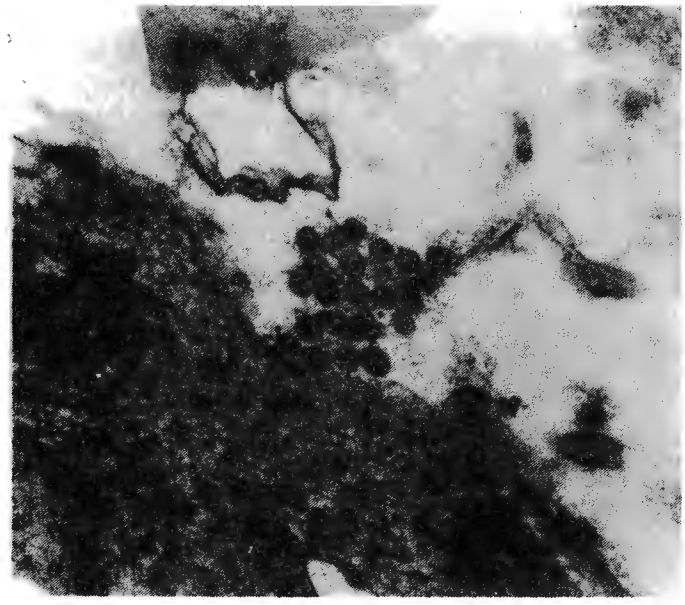

Fig 4.26 Electron micrograph of a control CaNT tumour showing viral particle inclusions, at magnification 23000X.

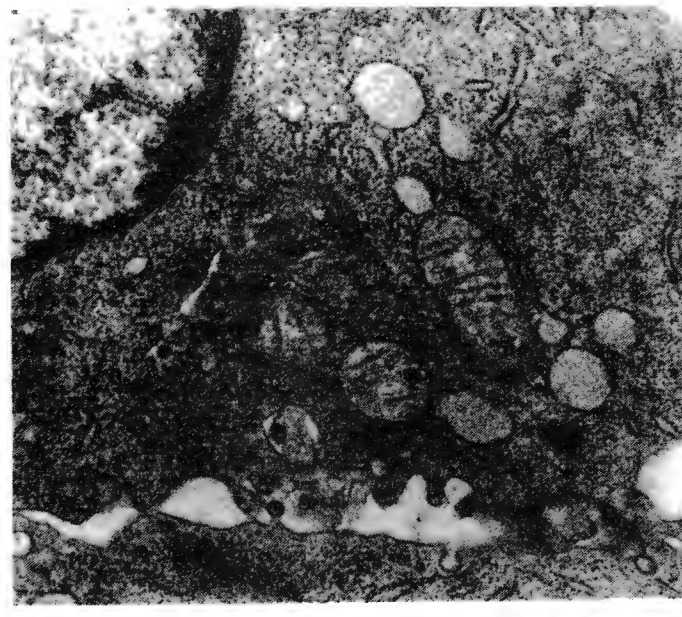

Fig 4.27 Electron micrograph of a CaNT tumour which has received 100 Gy of x-irradiation. There are fewer viral particles detectable and one particle budding from the cell membrane is clearly seen. The magnification is 23000X.

CHAPTER 5

DISCUSSION

Observable effects of radiant energy in living organisms include cell death, blockage of replication capacity, or induction of nonlethal alterations in macromolecules including enzymes and cell membranes (40, 55).

The biological effects of radiation have been investigated in depth by a great many workers with the aim of gaining a greater understanding of the mechanisms of the nature of the cell killing process and by which radiation leads to tissue breakdown.

Many studies have been in vitro, where mammalian and bacterial cells have been subjected to irradiation, and the cloning ability of survivors assessed using a conventional dose response curve (182). From these curves information can be obtained concerning radiosensitivity of various cell types, repair processes, and effects of changing physical conditions. The way in which these and other factors interact will ultimately determine the radiation response of organised normal tissues and tumours.

The radiosensitivity of the many specialized forms of cell and tissue in the body varies widely. In general, cells are sensitive to radiant energy in direct proportion to their reproductive or mitotic activity and in inverse proportion to their level of specialization.

Further information regarding the mechanism of radiation action can be obtained from biochemical studies following irradiation of biological material. In this thesis a number of metabolic parameters have been investigated following irradiation, with particular emphasis on energy production and energy utilizing processes in tumour cells.

In particular this study investigates the possible interrelationship of adenosine-5'-triphosphate, glucose-6-phosphate dehydrogenase, isocitrate dehydrogenase, phosphomannose isomerase and glutathione in normoxic and hypoxic conditions following irradiation.

Neoplasms, which obviously include the tumours used in this study, viz CaNT, Fib/t, 3-MC-induced and R1, consist of a complicated heterogeneous population of dividing cells, non-dividing cells, oxic cells, hypoxic cells and necrotic cells.

As a result the radiation sensitivity of the tumour will vary with the different cell populations. For example Gray et al (183) provided experimental evidence to show that hypoxic cells are about three times more resistant to x-rays than oxygenated cells.

In addition, it should be noted that during clonal amplification in tumours, a series of additional phenotype changes (184) occur which are related to the regulation of growth and differentiation as well as to the continual environmental and physiological changes, which may lead to inhibition of intercellular communication and modification of biochemical response (185). Therefore the heterogenous tumour cell population consequently undergoes a disturbance of homeostatically regulated growth. These phenomena are multifactorial and not fully understood (186).

It is of interest to note that several in vitro studies have suggested that radiation sensitivity can be altered by modification of the energy state of the cell (187, 188). Although as discussed above, the tumour is a more complicated system, the potential does exist for changing the energy state of tumours, an approach which may lead to the development of novel strategies for tumour radiosensitization.

Adenosine-5'-triphosphate appears to play an important role in repair mechanisms including cellular repair following radiation damage (189, 190). The relationship between ATP yield and repair processes remains unclear in cell metabolism.

A very important and relevant repair process is that of DNA. A general mechanism for repair involves removal of a segment of a damaged strand, with the gap then filled by the action of DNA polymerases, followed by the action of DNA ligases (191).

The key to all the repair or recombination processes is the initial recognition of the defect. One or more enzymes will combine with a DNA strand containing deletions, strand crosslinks or other abnormal base constituents and hydrolyze the polynucleotide backbone adjacent to the defect. After the DNA strand is broken, exonucleases remove the defective residues. The gap is then filled by DNA polymerases and finally closed by DNA ligases (192, 193). These enzymes participate in DNA replication and repair pathways in both prokaryotes and eukaryotes. The 3'-5' phosphodiester bond generated by DNA ligase restores the integrity to DNA strands following replication and repair.

The relationship of ATP to DNA repair has been studied by several workers who have shown that some of the enzyme steps require ATP, e.g. normal diploid human fibroblasts (AG 1518), xeroderma pigmentosum fibroblasts group G (194, 195), Escherichia coli and calf thymus cells.

It has been suggested by some authors that ATP is associated with cell membrane repair following ionizing radiation (18, 19). For example, conformational changes in the cytoplasmic membrane due to ATP-dependent polymerising proteins have been described (17).

Adenosine-5'-triphosphate has also been shown to modify the ionizing radiation response in several situations. Tikhomirova et al (196) have demonstrated that ATP protects against high energy protons. The survival of CBA and CS7B1 hybrid F1 mice treated with ATP and irradiated throughout the whole body with 9 GeV protons was reported to have been increased from 63 to 80%.

Nikolov et al (197) also have shown that ATP administration provides protection for monkeys (Macaca mulatta) against a dose of 8.3 Gy gamma irradiation (^{137}Cs). The survival in control groups was only 5% and after ATP administration (two injections of 37 mg kg^{-1} body weight) was 50%. (The previous two references (196, 197) were available only in the form of abstracts).

Nishīzawa et al (23) investigated the effect of ATP deprivation by 2,4 dinitrophenol (DNP) in murine melanoma cells in culture on the x-radiation response of these cells. The survival curves were changed as a result of post

irradiation treatment with DNP, with a diminished shoulder (implying less radiation damage repair) and also a decreased extrapolation number (n). Experiments were conducted concerned with the protection of C57BL male mice from genetic radiation damage in germ-cell genetic structures, using a combination of adenosine-5'-triphosphate, aminoethylisothiuronium Br-HBr (AET) and serotonin (188, 189). Such a combination was found to reduce, by a factor of 2, the metaphases with translocations observed after 3 and 4 Gy x-rays to mouse spermatogonia compared with irradiated mice not receiving the combination. Removal of ATP from the combination led to a significant reduction (59%) in protective effect. These findings indicate that there might be a role for ATP in repair systems. The authors emphasize that this high energy phosphate compound should be considered as an essential component in selecting combinations of agents intended to protect against genetic radiation injuries. There are several examples which show the ATP pool increases in cell metabolism after different types of radiation both "in vitro" and "in vivo". Barbe et al (198) have reported that UV-irradiation of Escherichia coli induces a two fold increase in the ATP pool. The ATP augmentation is dependant on exonuclease activity, which suggests there exists a relationship between DNA damage repair and the increase in ATP levels. Passarella et al (199) have shown that there is an increase of proton electrochemical potential and ATP synthesis in Wistar rat liver mitochondria, irradiated in vivo by a helium-neon laser. Irradiation was carried out with a power of 15 mW to give an energy dose of 5J/cm^2. An explanation was given in terms of the radiation-induced electron transfer giving rise to proton translocation and changes in the redox state of mitochondrial coenzymes and subsequently increases in ATP yield. Sijens et al (200) have reported a study of the response of a murine mammary tumour after ^{60}Co gamma radiation. The effect on the implanted murine mammary carcinoma NU-82 in DBA-2 strain mice, to 10 Gy of gamma radiation was followed by an in vivo ^{31}P-nuclear magnetic resonance spectroscopy study. During the first 8h after the dose of 10 Gy, the ratio ATP/inorganic phosphate increased to a value of 120 $\pm$ 15% (SE) of

the control value. One of the authors' hypotheses is that increased ATP consumption is related to repair of radiation damage, and in particular to restore damaged membranes. In the present research work the levels of ATP in the transplantable CaNT murine tumours grown in CBA mice, rhabdomyosarcoma tumours in Balb C mice, and Fib/t fibrosarcoma in WHT mice, were increased at various times following x-rays and ^{60}Co gamma radiation as presented in Chapter 4. In fact, as well as in B16 melanoma cells in culture, the largest increase in ATP levels noted, viz 3.8 times that of controls 2.5h following 10 Gy (201) is most considerable. Nevertheless very high doses, viz 100 or 200 Gy would be expected to sterilize the tumour, with little or no resultant repairable damage. If then, ATP was involved in damage repair, it would not be expected for ATP levels to increase following these doses. Indeed this was observed in the CaNT tumour. It is suggested that the increased ATP content after irradiation may play a major role in energy provision when cellular repair processes are able to operate.

A clear montonically decreasing trend is seen in the variation of CaNT mouse tumour ATP content, as a percentage of control values, with increasing photon energy using equal doses of 10 Gy (Chapter 4, Section 4.1.6.1). It must be emphasised that the processes of interaction differ at the different photon energies, for example because the microscopic range of reaction products depends on incident photon energy. Further, as has already been explained in Chapter 2, (Section 2.2), the relative cross sections for the different interaction mechanisms vary by several orders of magnitude over the range of photon energy applied (0.1 to 8.0 MeV). Therefore with the highest incident energies used, the biochemical effects of the interactions of this ionizing radiation must differ in nature and spatial distribution from the lowest. Possibly when there is a more extensive energy deposition within the cell more damage might be suffered by the repair mechanism and the production and control responses using ATP. This may explain the tendency to lesser ATP yield in tumour tissue subject to higher photon energies.

It is interesting to note that other adenosine phosphates may be involved in DNA repair processes following ionizing radiation. For example, Vikhauskaia et al (202) showed repair of single stranded DNA breaks in CHO-K1 cells resulting from x-irradiation could be stimulated by treatment of the cells with isoproterenol. This latter treatment increased cellular cAMP. (The previous reference was available only in the form of an abstract).

Further, cAMP stimulating agents given before x-irradiation increased the survival of irradiated V-79 cells (203, 204) and thymocytes (205) in culture. In vivo studies by Langendorff et al (206) demonstrated that cAMP together with ATP provided a significant degree of protection in irradiated mice, but cAMP alone was ineffective. (Interestingly, ATP alone provided about a 44% degree of protection, compared with the combination of cAMP and ATP which gave 70%). Low dose (0.15 Gy) x-irradiation of Chinese hamster fibroblast cells has been shown to increase significantly intracellular cAMP levels without any hormonal stimulation (207). It has also been suggested that irradiation activates membrane bound enzymes which mediate conformational changes in the cell membrane structure. This may result in beta-adrenergic activation of adenylate cyclase, with subsequent augmentation of cAMP levels.

Sarkav et al (208) have exposed male Sprague Dawley rats to whole body ^{60}Co gamma radiation (4 and 10 Gy) without exogenous stimulation. The results show a significant increase in myocardial adenylate cyclase with simultaneous decrease of phosphodiesterase activity, indicating indirectly an increase in cAMP. This study indicates that even without a hormonal stimulating treatment, activation of myocardial adenylate cyclase occurs by some endogenous modulator, probably as a mechanism for radiation protection.

Cyclic AMP acts as a second messenger in conveying a signal to responsive enzymes within the cell. It is possible that radiation modifies coupling between receptors and adenylate cyclose. As a result of radiation, then there may be an amplification of the initial signal. It may be useful at this stage to consider this concept in more detail. Cyclic AMP is known to take part in

the regulation of carbohydrate metabolism by promoting glycogenolysis and glycolysis and by inhibiting glycogen synthetase. When a living organism is confronted with an emergency (e.g. stress by radiation) that may demand prompt energy production increase, it must mobilize glucose rapidly from glycogen to have the fuel available. Cyclic AMP acts as a "second messenger" conveying the signal received on the receptors of the plasma membrane which triggers an intracellular cascade of enzyme activation to accelerate formation of glucose from glycogen (209). The cell then metabolizes the glucose to supply free energy (ATP) and maintains homeostasis after injury in response to the radiation. This may be the mechanism which explains the ATP increases noted in this work. This chain of events may be controlled by a feedback mechanism that helps the cells to defend themselves against injuries. Most of ATP yield is produced in the mitochondria and is transported across the inner mitochondrial membrane to the cytosol by a carrier or antiporter translocase system (adenine nucleotide translocase).

Energy transport is one of the central problems in the thermodynamic balance in living organism. The crucial role of creatine phosphokinase in the requirement for a high flux of high energy phosphate from the inner mitochondrial membrane to the medium surrounding the mitochondria is supported by numerous physiological studies (210, 211). According to Dzeja et al (212) mitochondrial and cytoplasmic isoenzymes of adenylate kinase can act in parallel with creatine phosphokinase isoenzymes in ATP energy transmission from the mitochondria to the localized sites of energy demand in the cytoplasm. If there is a low activity of creatine phosphokinase, adenylate kinase can perform this function independently. Another function of adenylate kinase isoenzymes is to cause a decrease in the difference of the phosphate potential and Gibbs free energy of ATP hydrolysis. This implies that energy transport would proceed with an increased efficiency and reduced energy transmission losses (entropy) when adenylate kinase controls the energy flux.

The augmentation of the protons' movement from the inside to the outside of the mitochondrial membrane, due to acceleration of glucose catabolism in the Krebs cycle, may be result in a change of the redox state of mitochondrial coenzymes (213), creating an extra-electrochemical gradient which would then be involved in the generation of ATP.

Thus far, the discussion has centred on ATP changes following radiation, radiation sensitization as a result of ATP depriviation, radiation protective effects of exogenous ATP, the relationship of cAMP to ATP, and it has been suggested that perhaps ATP increases following x-irradiation may provide energy to repair radiation damage. However, it is enlightening to consider the ATP increases following radiation from a biophysical/thermodynamical point of view. The radiation processes increment the disorders by augmentation of random fluctuations in biological systems. Normally the cell is said to be in a homeostatic "steady state" able to handle physiological demands. Radiation damage may bring about a number of cellular adaptations in which a new but altered steady state is achieved, but in which the cell remains viable. One can consider the cell to have an indefinite number of steady states. Consequently when the cell is still alive and it tries to maintain order in its constituent matter, it takes negative entropy from the environment. These negentropic phenomena permit the cell to fight against the irreversible processes of increasing disorder after radiation injury. Therefore in the cells, radiation damage represents residual uncertainty about the biophysical system after an ordering effect in the number of radiation induced disturbances.

Whether specific types of stress such as ionizing radiation or magnetic field induce an adaptive response, as repairable injury, or cell death, depends on the nature and severity of the lesion, and on many other variables relating to the intrinsic state of energy metabolism. In other words repair is the capability to "capture" negentropic organization against the random variations produced at the biochemical level to obtain order. This occurs at the expense of the order

of the surrounding medium. An isolated system is subject to processes that do not violate the second principle of thermodynamics (214).

It has been shown in Chapter 4, Section 4.1.3.1 that tumour ATP levels are decreased to 78 and 75% (215) of control levels after 15 minutes and 2 hours of tumour clamping. (This procedure produces radiobiological hypoxia (216)). The sequence of events in hypoxic injury has been studied by a number of authors in experimental animals and in tissue culture sytems (217, 218, 219). The first point of attack of hypoxia is the cell's aerobic respiration i.e., oxidative phosphorylation by mitochondria (220, 221). As the oxygen tension within the cell decreases, there is a decrease of oxidative phosphorylation and of ATP generation. There is inhibition of the electron transfer system coupled to oxidative phosphorylation in the mitochondria and therefore intereference with ATP synthesis (222).

The decrease in cellular ATP and associated increase in AMP stimulates the enzyme phosphofructokinase, which results in an increased rate of anaerobic glycolysis to maintain the cell's energy sources by generating ATP from glycogen (223). Glycolysis results in the accumulation of lactic acid and inorganic phosphates from the hydrolysis of phosphate esters (224, 225). This reduces the intracellular pH (226).

Nagle et al (187) have reported the effects of 5-thio-D-glucose (5-SH-D-Glc) on cellular ATP levels and DNA rejoining in hypoxic and aerobic Chinese hamster fibroblasts. Intracellular ATP levels were measured in both hypoxic and aerobic cultures of V79 Chinese hamster cells treated with 5-SH-D-Glc. This glucose analogue, a known inhibitor of D-glucose transport and metabolism, reduced ATP in cell cultures which were allowed to become hypoxic, but not in aerobic cultures treated with this compound. Cells depleted in ATP were unable to rejoin x-ray induced DNA strand breaks. The 5-SH-D-Glc leads to reduced energy metabolism in cells dependent on glycolysis for ATP production. The inference for radiation therapy (226) is that inhibition of glucose metabolism by this

drug selectively depletes energy reserves in hypoxic cells, rendering these cells more radiosensitive and leading to a more effective tumour treatment. The requirement of glucose for the production of ATP in mammalian cells was reported by Matsudaria et al (227) who used Ehrlich ascites cells in vitro suspended in phosphate-buffered saline (PBS) with or without 5mM of glucose. When these cultures were made anaerobic by gassing with N_2, cellular ATP in the absence of glucose decreased to about 15% of that in aerobic cells. Freudenberg et al (228) reported a 90% reduction in intracellular ATP in anaerobic cultures of rabbit reticulocytes in vitro. Matsudaria et al (229) also observed that glucose-free anaerobic cultures of Ehrlich cells in PBS did not rejoin x-ray-induced DNA strand breaks, whereas rejoining did occur under N_2 when glucose was present. It appears that ATP is necessary to support rejoining of DNA. 5-thio-D-glucose effectively inhibits D-glucose metabolism and as a consequence, cellular ATP was reduced and DNA rejoining inhibited (226). The cellular dependence on ATP for the rejoining of ionizing radiation induced DNA single-strand breaks has been presumed to result from the involvement of DNA ligase (230) which requires ATP as a cofactor. Guanosine-triphosphate or other high energy phosphate compounds do not function in this capacity (231). Therefore, ligation of DNA strand breaks would not be possible in cells depleted of ATP regardless of which ligase was required for this repair. More work must be done to establish the identity of the repair DNA ligase and to quantitate further its ATP dependence in irradiated cells. The DNA degradation observed by Song et al (232) in hypoxic cells after addition of 5-SH-D-Glc, may have been a consequence of the cytotoxicity of the 5-thio-D-glucose for hypoxic cells, rather than energy deprivation. Hypoxic cells, which are most dependent on anaerobic glycolysis for energy production, were reported by Nagle et al (187), to become severely depleted in energy (ATP) when this process is inhibited by interference with glucose metabolism. The energy depleted hypoxic cells produced a deficiency in DNA repair capability. Therefore a transient inhibitor of tumour cell glycolysis combined with irradiation could selectively sensitize

the hypoxic cells, and thereby lead to therapeutic advantages. The levels of ATP following x-irradiation during experimental hypoxia in CaNT tumours were investigated. The decrease of ATP content to 78 and 75% (Chapter 4, Section 4.1.3.1) with respect to the controls can be associated with impaired nutrient blood flow and diminished oxygen consumption in the tumour. Adenine nucleotide translocase, is an antiport localized on the inner mitochondrial membrane. It is a carrier with a molecule-for-molecule exchange of ATP and ADP. In this manner it confers the specificity of oxidative phosphorylation and controls the ratio of ATP/(ADP + Pi) or phosphate potential of the cell. Any disruption, such as the diminished oxygen consumption in normally coupled mitochondria, would immediately be reflected in a lack of energy balance between the metabolic processes of the intra- and extra-mitochondrial compartments of the cells. This leads to interference with ATP synthesis. Consequently under these conditions uncoupled oxidative phosphorylation in the mitochondria with a reduced ATP yield, is unable to generate any response related to repair processes following radiation damage.

ATP content of control CaNT tumours grown in CBA mice was measured for different ranges of tumour masses. It is clear there is an inverse relation between ATP content per unit mass of tumour and total tumour mass (Chapter 4, Section 4.1.8.1). This finding most likely reflects the well-known association between tumour size and degree of necrosis (182). This correlation has been confirmed and analysed for individual rods of tumour cells using diffusion theory for oxygen penetration from capillaries and histological observations.

The effect of ionizing radiation on glucose-6-phosphate dehydrogenase activity in normoxic conditions was determined at different times after the x-irradiation in CaNT tumours in CBA mice and Fib/t murine fibrosarcomas in WHT mice. The activity of the enzyme increased after these tumours received 10 Gy x-rays and the results are described in Chapter 4, Sections 4.2.2.3 and 4.2.3.2.

Major functions of the pentose phosphate pathway are to provide NADPH for reductive synthesis outside the mitochondria and to provide ribose for

nucleotide and nucleic acid synthesis. Glucose-6-phosphate dehydrogenase catalyzes the initial and rate-limiting step of the pathway that is the principal source of cytoplasmic NADPH in the cell. Engstrom et al (233) have evaluated the early effect of local x-irradiation with moderate doses to the epiphysis of the tibial bone in rats. The activity of glucose-6-phosphate dehydrogenase was analysed and related to the morphology of the epiphyseal cartilage and metaphyseal bone in irradiated animals. Increased activity was noted for glucose-6-phosphate dehydrogenase especially after 8 and 10 Gy, and an increased number of osteoclasts was noted in morphological observation. The increased enzyme activity in the epiphyseal cartilage was suggested to correspond to a cellular demand for an increased metabolism through the pentose phosphate shunt and stimulates the proliferation and number of osteoclasts. The temporary enhancement of this enzyme might be due to a demand of restitution of a diminished cell population caused by the cell death or inhibition of cell division after irradiation.

According to an abstract obtained from a literature database, Savitsky et al (27) have shown changes in fructosediphosphate aldolase and glucose-6-phosphate dehydrogenase activity in brain, liver, myocardium and skeletal muscle after irradiation of rats with a single whole body dose of gamma irradiation (10 Gy). The activity of fructosediphosphate aldolase was mainly inhibited and that of glucose-6-phosphate dehydrogenase increased. In other words the initial step of glycolysis was significantly inhibited and the first reaction step of the pentose phosphate pathway enhanced in the irradiated body. The augmentation of the pentose phosphate pathway indicated by the increased glucose-6-phosphate dehydrogenase may be indirectly indicative of stimulated cell proliferation and repair processes after radiation damage.

Gupta et al (234, 235) have also shown that ionizing radiation results in an increase in glucose-6-phosphate dehydrogenase activity. These workers exposed (partial body) rats to a dose of 2 Gy gamma irradiation, and showed an increased activity of the NADPH linked glucose-6-phosphate dehydrogenase in non-germinal

cells of the rat testis. It was proposed (234, 235) that the increased glucose-6-phosphate dehydrogenase activity was due to an increased amount of the enzyme as a result of an increased rate of RNA synthesis.

From the foregoing evidence, it is proposed in this thesis that the augmentation of glucose-6-phosphate dehydrogenase following ionizing radiation is an indicator of the response to injury, and may trigger the repair of lesions at the biochemical level. This augmentation can be envisaged to be part of the homeostatic regulation during the demand for increased metabolism. The results can also support the interpretation that the radiation induced increase of glucose-6-phosphate dehydrogenase is due to enhanced transcription of that genetic information to yield those products required for repair processes.

The effect of ionizing radiation on isocitrate dehydrogenase (ICDH) activity in normoxic conditions also was determined at different times following 10 Gy x-irradiation in CaNT tumours. The activity of the enzyme increased in the tumour, after exposure to this ionizing radiation (215). The detailed results are given in Chapter 4.

As mentioned previously the glucose-6-phosphate dehydrogenase mediated reaction is a source of reducing equivalents. Another source is in fact from the isocitrate dehydrogenase reaction. The increase in normoxic conditions following radiation may be a reflection of the increased biosynthetic metabolism required for repair of radiation-induced damage. It is also interesting that the increased reducing equivalents generated by these enzymes under injury conditions may give protection against further damage due to peroxidative processes (236).

In this thesis, the determination of the levels of tumour glucose-6-phosphate and isocitrate dehydrogenase under normoxic conditions and under hypoxic conditions following irradiation have been described (Chapter 4, Sections 4.2.2.4, 4.2.2.5, 4.4.2.3). In the case of glucose-6-phosphate dehydrogenase, hypoxia for 15 minutes resulted in a significant increase (about 36%) compared with normoxic controls. When tumours were irradiated under hypoxic conditions,

the activity of glucose-6-phosphate dehydrogenase was not increased above the levels seen in hypoxic conditions only. This should be contrasted with the results seen following irradiation in normoxic conditions, where an increase of about 1.5 fold was observed. Tumour isocitrate dehydrogenase activity remained unchanged, compared with the controls, in hypoxic conditions, both with and without x-irradiation. These results are described in Chapter 4, Section 4.4.2.3.

Glucose-6-phosphate dehydrogenase is involved in anaerobic metabolism (237). It has also been clearly demonstrated that when the oxygen supply is inadequate, glucose production increases resulting from accelerated glycogen breakdown. The reason for this is that glycolysis can now compensate to some extent for the decreased energy production in the mitochondria in the citric acid cycle as a result of diminished oxygen. There is also an almost immediate rise in hexose monophosphate production, for example, when the coronary artery in conventional open chest dog preparations was occluded (237). Pyruvate oxidation and mitochondrial respiration undoubtedly occur in the moderately hypoxic state, but this is limited by oxygen availability rather than availability of ADP, phosphate, NADH and NADPH.

In this investigation, the ability of the tumour cell to coordinate the rate of glycolysis in hypoxia, with subsequent metabolic demand in the activity of G-6-PDH, may be an important indicator of cellular biochemical integrity. The increase of flux in the glycolytic anaerobic pathway is related to a homeostatic feed back regulation in the hypoxic cell, to maintain metabolic integrity. Anaerobic glycolysis increments the activity of cytosolic enzymes (238). As discussed above, this is concomitant with the depletion of ATP production in the mitochondria due to deficiency in the oxygen supply in the Krebs cycle. The onset of increased activity of G-6-PDH occurs simultaneously with the onset of high-energy phosphate depletion.

This is demonstrated by the findings reported in this thesis, where hypoxia resulted in a decrease of tumour ATP levels (Chapter 4, Section 4.1.3.1) with a

concomitant increase in glucose-6-phosphate dehydrogenase activity. Total levels of NADP-linked ICDH were shown not to differ significantly, with respect to the controls, in hypoxic conditions. This finding may be due to the fact that part of the total enzyme activity is located in the cytosol and part in the mitochondria (239). Therefore the depletion of ICDH activity in the mitochondria due to deficiency in the oxygen supply, could be compensated for by an increase of the ICDH activity in the cytosol. Zalewska et al (240) have conducted an experiment related to energy utilization and changes in some intermediates of glucose metabolism in hypoxic rat brain. Lactate levels rose over four-fold. Pyruvate, glucose and glucose-6-phosphate concentrations also increased significantly. Metabolic activity in the cortex, expressed as the utilization of high-energy phosphates, decreased by 30% after the hypoxia and remained lowered for 3 hours during recovery. This was accompanied by an elevated glucose consumption and lactate production. These authors suggested that the maintenance of the energy balance during hypoxia was partly due to activation of the glycolytic pathway. During the recovery period, these metabolic abnormalities returned towards control values, but, after 6 hours of recovery the high-energy phosphate utilization increased transitorily above the control values. All these results are in accord with the experimental measurements of glucose-6-phosphate dehydrogenase, isocitrate dehydrogenase and ATP in hypoxic conditions described in this work.

The next biochemical component that will be discussed is glutathione. It exists in virtually all living cells in either a reduced (GSH) or oxidized (GSSH) form. The biosynthesis of GSH has been demonstrated to be catalyzed by two enzymes: gamma-glutamylcysteine synthetase and glutathione synthetase (241). The recent introduction of drugs which specifically deplete (buthione sulfoximine (BSO)) (242) or elevate (2-oxothiazolidine-4-carboxylate (OZT)) (243) cellular glutathione levels has prompted a number of studies reexamining the role of GSH in the cellular response to ionizing radiation. Buthionine sulfoximine (BSO) depletes GSH by inhibition of gamma-glutamylcysteine synthetase (242). On the

other hand, OTZ stimulates GSH synthesis by providing high levels of intracellular cysteine (243). What is not fully appreciated is whether these compounds exert other cellular effects, which might complicate the interpretation of x-ray response data. In marked contrast to other agents, which have been used to deplete GSH such as diamide (244) and diethyl maleate (DEM) (245), no major non-specific cellular effects for GSH depletion by brief exposure to BSO have been reported. The major interest is defining GSH involvement in the response to ionizing radiation, stemmed from the free radical-scavenging hypothesis (246), which proposed that sulfhydryls, such as GSH, particularly at low oxygen tension, would play an important role in the response to ionizing radiation.

Reports describing use of DEM to deplete GSH to low levels have indicated a substantial reduction in the oxygen enhancement ratio (OER). In other words GSH depletion produced dose-modifying radiosensitization of hypoxic cells (247, 248). In contrast, there have been several reports where GSH was depleted by DEM or BSO treatment (249, 250) and sensitization of both aerated and hypoxic cells was observed and no net changes in the OER were seen. All of the above studies have sought to assess the role of sulfhydryls in radiation response by GSH depletion. However, discussion of studies directed toward elevation of GSH levels and subsequent assessment of possible protection should be instructive. OTZ provides an ideal intracellular cysteine delivery system that stimulates GSH synthesis. An effect of OTZ treatment, that of subsequent elevation in GSH levels to 200-300% of control levels, has been reported for aerated cells (251, 252). Jensen et al (252) showed modest radioprotection with OTZ, whereas Russo et al (251) observed no protection.

In this thesis tissue sulphydryl levels were determined in CaNT tumours in CBA mice and Rhabdomyosarcoma R1 tumours in WAG/Rij rats under normoxic conditions following x-irradiation (100 KVp and 8 MV) with a dose of 10 Gy. Determinations were also made after clamping the tumours for 15 minutes with or without x-irradiation. Further tumour sulphydryl levels were determined in CaNT tumours

after the tumour bearing mice were kept in 8% and 12% oxygen at one atmosphere total pressure for 72 hours. No significant changes in tumour sulphydryl levels, compared with the controls, were observed following any of the manipulations.

The results are described in Chapter 4, Sections 4.5.2.1 to 4.5.2.5. It is also important to note that when glutathione was specifically measured in deproteinized tumour tissue samples, there was no difference in levels between controls and in tumours that had been exposed to prior irradiation. This result is similar to that obtained when tissue sulphydryl levels were determined, as opposed to glutathione specifically. It is probable that the tissue sulphydryl levels measured in this work provide a good indication of glutathione levels.

Wolters et al (253) have conducted an investigation related to the radiosensitivity of normal and polyunsatured fatty and supplemented mouse fibroblasts, after depletion of glutathione by DEM. The polyunsaturated fatty acids were introduced into the cells by incubating exponentially growing cells in a medium supplemented with 100 μM eicosatetraenoic acid complexed to 25 μM fatty acid free bovine serum albumin (BSA). The treatment resulted in modification of the phospholipid composition in all subcellular fractions of the fibroblasts, including the nuclear membrane. The content of polyunsaturated fatty acids was significantly increased, but no difference in cell survival after x-irradiation could be observed between the normal and polyunsaturated fatty acids enriched cells. It was concluded that although there are radiosensitive polyunsaturated fatty acids in the membranes, the cells are well protected against radiation damage. The content of GSH was approximately the same in the normal and the modified cells. Reduction of the cellular GSH content by more than 95 per cent using DEM did not alter cellular survival after radiation of either normal or polyunsaturated fatty acid enriched cells under oxic or anoxic conditions. The radiosensitive lipids present in the membranes of the polyunsaturated fatty acid enriched cells proved to be vulnerable to radiation-induced lipid peroxidation when extracted from the cells and

reconstituted into liposomes, indicating that the fatty acids per se are peroxidizable. The authors (252) concluded that the lipids in the membranes of mammalian cells are not the principal target in radiation-induced reproductive death. Also no generalization is possible with respect to glutathione, being the major hydrogen donating species in mammalian cells responsible for the repair of those target molecules concerned with cell survival after radiation. This evidence complements conclusions drawn from the work of this thesis that endogenous GSH levels do not change after x-irradiation under normoxic conditions. However, this finding does not preclude GSH from being involved in cellular repair processes following irradiation.

The next stage of the discussion refers to some of the effects produced by mitoxantrone. As has been demonstrated in this thesis, when tumours and cells in culture are exposed to ionizing radiation in normoxic conditions ATP levels were subsequently increased (Chapter 4, Sections 4.1.4.1, 4.1.4.2, 4.1.4.3). If the increased ATP reflects an increased demand for energy for cellular repair following irradiation, then by blocking this increase in ATP it may be possible to enhance the radiosensitivity of tumour cells (254). Neri et al (148) have shown that mitoxantrone may be a useful agent in this regard. Biochemical evidence suggests that mitoxantrone causes profound changes in chromatin structures including compaction (255). Mitoxantrone intercalates with DNA and shows preferential binding with guanine and cytosine causing a partial unwinding (256). Evidence from x-ray diffraction studies also suggests that there is an additional external binding component.

In an experiment performed by Neri et al (148), it was demonstrated that mitoxantrone produces significant impairment of respiratory control in Wistar rat heart cells (oxygen uptake reduced by 46%) and a marked decrease (86%) of ATP concentration after one hour of exposure to the drug.

This finding is consistent with the results obtained in this work both in vivo and in vitro. In this investigation ATP content in CaNT tumours after treatment with mitoxantrone was reduced by 11% compared with the controls. A more marked

decrease was noted in vitro, where ATP content of B16 cells after exposure to the drug was reduced by 26% (Chapter 4, Sections 4.1.5.1, 4.1.7.2).
The mechanism by which mitoxantrone inhibits oxygen uptake and reduces ATP yield has not been adequately explained. It was suggested that the depletion of oxygen uptake caused by mitoxantrone results in inhibition of oxidative phosphorylation and therefore interferes with generation of ATP (148). Meanwhile there is less outward pumping of protons due to deranged mitochondrial respiration. In the study of the effect of 0.5μg/mℓ mitoxantrone on the radiation dose response of B16 melanoma cells in vitro, a radiosensitization effect was seen. The curves were analysed using the linear quadratic model, and it was of interest to note that the β coefficients for the curves in the presence of mitoxantrone were very small. This implies that the α component is more important, and the dose response curve tends towards an exponential, with loss of the shoulder. As is well known, the shoulder in the curve represents repair of "repairable radiation damage", and can be quite clearly seen in the control survival curve shown in Fig 4.11. Loss of the shoulder can then be construed to represent impaired repair of repairable cellular damage. The mechanism by which mitoxantrone does this is somewhat unclear. One possibility is the suppression of ATP, which can be presumed to be a very important energy source for repair of cellular radiation damage. However, it was not possible to demonstrate that ATP levels were indeed suppressed at the concentration of mitoxantrone used, viz 0.5μg/mℓ. The ATP content in CaNT tumours treated with mitoxantrone following x-irradiation showed an increase 1.37 times compared with controls, i.e. a small augmentation. However, when this result is compared with that obtained where x-irradiation took place in the absence of this cytotoxic drug (3.8 times that of the controls) a significant inhibition of the ATP production occurred. It must be noted that all measurements were made at the same time following irradiation. The results presented here thus have implications for radiation therapy, where combining radiation and mitoxantrone could lead to a therapeutic gain.

It was considered that if the glycolytic pathway could be inhibited, another mechanism would then exist to deplete energy production. It was thought that if there was impaired or low conversion of mannose to glucose-6-phosphate in tumour cells, then by supplying excess mannose, energy production would be inhibited. Measurements of phosphomannose isomerase (which converts mannose-6-phosphate to fructose-6-phosphate) in both the CaNT and Fib/t tumours showed an activity comparable to that found in the liver (Chapter 4, Section 4.3.1). This line of investigation was not pursued futher.

Part of the present investigation involved ultrastructural studies of the CaNT tumour following doses of 10 and 100 Gy x-rays, and using a range of magnifications from 4900 to 23 000. Following irradiation with 10 Gy no morphological changes could be observed in comparison with the non-irradiated control tumours. However, after x-irradiation with 100 Gy distinct morphological alterations occurred in the tumour tissue e.g. clear degeneration of the cristae and matrix of mitochondria (Chaper 4, Section 4.9).

Baldetorp et al (257) have reported the effects of ionizing radiation in an experimental in vitro system using the ciliary cells of the tracheal mucous membrane of rabbits. The specimens were examined in the electron microscope after irradiation. After 10 Gy of x-irradiation no morphological changes were observed compared with the control material. Distinct morphological alterations in the mitochondria occurred following higher radiation doses of 40, 50, 60 and 70 Gy. The same group also studied the effect of irradiation on tracheal ciliary cell activity in rabbits (59). The immediate response of the ciliary activity to 10 Gy of ionizing radiation was presumed to be due to changes of the mitochondrial membrane permeability, resulting in a diffusion of a stored pool of ATP to the extra-mitochondrial space and to an increased enzymatic activity during the ATP hydrolysis in the cilia. This explanation is consistent with the results obtained in this thesis, where ATP content increases in tumour cells after ionizing radiation (Chapter 4, Sections 4.1.4.1, 4.1.4.2, 4.1.4.3).

As explained above (Chapter 4, Section 4.9) many cellular inclusions were observed which are consistent with typical viral particle contamination of murine tumours. Retrovirus type C mouse leukemic virus has an appearance, size and location typical of the observed particles and as has already been noted is also known to bud from the cell membrane. This common contaminant arises from the mouse's blood and is not thought to be more than an incidental finding whose presence does not affect the investigations and results of this thesis.
Until now, the discussion has centred around the effects of ionizing radiation. It is intended now to turn to a dicussion of the effects caused by magnetic fields. Molecular or subcellular structures with anisotropy in magnetic susceptibility will be influenced by a torque depending on the orientation to the applied magnetic field, which is proportional to the strength of field squared. This axis of rotation of this twisting force is aligned with the field and is several orders of magnitude higher on a magnetically anisotropic body than on an isotropic one. These physical effects in turn modify various chemical processes as well as some electrochemical processes resulting in a variety of biological effects. In the present research work, the effects on growth rate have been studied in CaNT murine tumours in CBA mice when exposed to a static magnetic field (0.5 Tesla) using single and multiple exposures. Multiple exposures also took place in static magnetic field (0.5 Tesla) simultaneously with a superimposed varying magnetic gradient field 5×10^{-3} Tesla/m. The tumours exhibited a very significantly delayed tumour volume doubling time and growth rate over 7 days (258). The result is described in Chapter 4 (Sections 4.6.1, 4.6.2). These findings are consistent with several reports (28, 259, 260, 261) in which the biomagnetic effects on growth rates in tumour cells were studied. Mulay et al (262) have reported the effect of a magnetic field (0.04 Tesla) on Sarcoma 37 and ascites tumour cells. The control tumour cells showed normal growth even after 18 hours, whereas most tumour cells exposed to the magnetic field showed complete degeneration at the end of this period.

As has already been considered in Chapter 2, neoplasms are caused by some breakdown in their control mechanism and tumour cells proliferate with little restraint. They migrate to various parts of the body and they generally lack any cohesive organization. One of the first observations characterizing the pleiotropic phenotypes of tumour cells is the general inability of the tumour cells to communicate intercellularly in a proper fashion (80, 263). It has been proposed that extensive interleaving (junctions) of thin cytoplasmic membranes is responsible for growth control. This implies that magneto-stresses on cell membranes may affect their vital functions. Kim (11) suggested that tumour cells, that is, at least some of them, are more susceptible to magnetic fields than normal cells, since they are less organized and less cohesive. This is because their surfaces are more negatively charged than normal cell surfaces, they have larger dielectric constants and they fail to form effective membrane junctions for intracellular communication.

Magnetic fields generate stresses and torques which affect biological processes by distorting membranes and membrane components and the orientation of various intra-cellular structures. These physical and chemical actions may be translated into such biological effects as growth retardation. The effect of magnetism on the biophysical and biochemical properties of cell components is not fully understood. It is possible that cells contain liquid crystal substances and that magnetic fields transform smectic crystals to nematic crystals (264). It is also possible that magnetic torques which distort forces between electric dipoles, may distort chemical bonds.

There is another explanation about the implications of the growth rate of tumour under exposure to magnetic fields which can be given. Electron transfer reactions are common in both chemical and biochemical transformations, e.g. electron transfers during oxidative phosphorylation. Electrons are fed into this sequence by oxidation of compounds derived from dietary fuels. In other words all of the useful energy liberated during the oxidation of fatty acids and amino acids and nearly all of that from the oxidation of carbohydrate is made

available within the mitochondria as reduced equivalents (H or electrons). This is accomplished in the mitochondria via the respiratory chain which is concerned with the transport of reducing equivalents and their final reaction with oxygen to form water, together with the machinery for trapping the liberated free energy as high-energy phosphate. These reactions involve the formation of transient free radicals. For example, the ubiquinones may be reduced one electron at a time through the semiquinone free radical, or may be reduced directly to the dihydroquinone by two electrons. This free radical, initially in the singlet state, will develop into the triplet state. External perturbations of the transient free radical may permit some control over the course of the electron transfer reaction during oxidative phosphorylation and perhaps may perturb the synthesis of high energy phosphate. The transient free radical lives about 20 ns without any external perturbation, but the lifetime of free radicals increase with increasing magnetic field from 0 to 0.04 Tesla by approximately 25% (31). It is possible that this perturbation can be used to control the lifetime of the initially formed transient free radical in the oxidative phosphorylation. The external perturbation mediated magnetic field may alter the oxidative phosphorylation, which interferes with ATP synthesis since energy in the form of ATP is required for growth, with the net result being a growth delay in tumours.

The first of these mechanisms of interaction (depending on magnetic anisotropy) involves a well established physical law which has been known for many decades. The second effect, concerned with properties of transient free radicals, was first described recently (265) and its fundamental mechanism is less well understood. Yet the resulting biophysical manifestation is clear. Explanations given are not mutually exclusive, and both can be involved in part or totally to explain to biomagnetic properties of tumours described in this thesis.

CONCLUSIONS

Adenosine-5'-triphosphate (ATP) most probably has a major role in repair to intracellular damage after ionizing radiation in the tumours studied. The increased levels of ATP following irradiation described in this thesis are probably related to physiological demands which follow radiation injury (199, 200, 201). An energy provision is necessary for repairing appropriate damage in rodent tumours. This can be expressed as a transient increased cellular demand for glucose, which in turn may be due to an increased amount of ATP needed for cellular repair processes (266). This energy may be supplied by anaerobic glycolysis in the cytosol and total oxidation in the mitochondria. It is necessary therefore to activate demands for prompt energy by mobilizing glucose rapidly from glycogen. This increase in metabolic rate is expressed in terms of non-equilibrium reactions which increase glycolysis, by accelerating enzymatic activation and free energy (ATP) yield and could be related to negentropic repair mechanisms and higher entropy in the entire injured cell. The major supply of ATP to repair this damage could be from the mitochondria of adequately oxygenated cells. Consequently in tumour ATP content, there is greater concentration per unit mass, or per cell, in the aerobic fraction than in the hypoxic fraction of the tumour tissue.

It can be suggested that the enhanced tumour glucose-6-phosphate dehydrogenase activity which has been measured in this work, may also be a consequence of cellular requirements for increased metabolism to maintain homeostasis during repair of radiation damage (233, 235). This enzyme is the first enzyme in the pentose phosphate pathway and its increased activity can be associated with an enhanced rate of nucleic acid synthesis, for which glycogen is a reserve substrate (234).

Isocitrate dehydrogenase and glucose-6-phosphate dehydrogenase mediated reactions are sources of reducing equivalents. The augmentation in the specific

activities and increased reducing equivalents associated with these enzymes may give protection against radiation damage. The explanation of the above metabolic responses to irradiation is complex and cannot be explained only in terms of direct radiation effects.

Modification of the cellular energy supply by using cytotoxic compounds, might provide a way to modulate cellular repair processes (23, 187, 254).

Mitoxantrone has been shown to decrease ATP production in rat heart slices in vitro (148), and in this present work it was shown for the first time that this drug also decreases ATP production in tumours as well as in cells in culture. Irrespective of the mechanism involved in the phenomena of repair, the present data show that if ATP production falls by interference from mitoxantrone, repair processes may be markedly inhibited. Hence, for there to be effective repair processes, a higher ATP production must be superimposed upon the requirement for the normal maintenance activities of the tumour cells.

With regard to the effects caused by magnetic fields, the significant conclusions are that this quality of radiation which can generate stress and torques within the rodent tumours, does affect their growth rate, possibly by distorting membranes, membrane components and disturbing the orientation of various intracellular structures, so affecting energy production, energy demand and other metabolic processes (31). The magnetic fields of 0.5 Tesla, used in this work, have sufficient energy density to modify the life time of transient free radicals in the normal biochemical processes. The fields were observed to cause a delay in the growth of the experimental tumours (11). This approach provides insight into the interactions between this type of non-ionizing radiation and tumour cell metabolism.

It is hoped that the work presented here gives increased understanding of basic radiobiological mechanisms in tumour cells subjected to ionizing and non-ionizing radiations, together with indications that can lead to improved radiotherapeutic strategies.

APPENDIX A

THERMODYNAMIC RELATIONS

Thermodynamic concepts used in this thesis, such as entropy and Gibbs free energy, will be defined in this appendix and some important thermodynamic relations which involve them will be briefly described.

A.1. Entropy

The second law of thermodynamics is a statistical law which can only be applied to a system consisting of a large number of particles, as, for example, an assemblage of molecules. The probability that all the molecules in a macroscopic amount of gas will be equally spaced and move in an ordered manner relative to each other is vanishingly small. This is because as a result of impacts the distances of separation and velocities of the molecules will vary continuously. The establishment of a condition of chaotic movement and of random distribution, which occurs quite spontaneously, is far more probable than an ordered state. All spontaneous processes are accompanied by an increase of entropy. It is possible, therefore to regard entropy as a measure of the "randomness" or "disorder" in a given system, and to suppose that all natural processes lead to an increase in disorder. Since a disordered state is usually more probable than one of complete order, entropy and probability are evidently related. L. Boltzmann defined the thermodynamic probability of a system as the ratio of the probability of an actual state (microstate) to one, having the same total energy and volume, in which the molecules are completely ordered. If S is the entropy and W the thermodynamic probability of a system then it is possible to write $S=f(W)$.

W is also known as the number of microstates. To ascertain the nature of the function, consider two systems having entropies S_1 and S_2 and

probabilities W_1 and W_2. The entropy S of the combined system is $S_1 + S_2$ whereas its probability W is the product $(W_1 \times W_2)$

so that

$$S = S_1 + S_2 = f(W_1 W_2) \qquad \text{(Equation A.1)}$$

but since $S_1 = f(W_1)$ and $S_2 = f(W_2)$,

it follows that $f(W_1 W_2) = f(W_1) + f(W_2)$

To satisfy this condition it is obvious that the function must be logarithmic and hence it is possible to write (Equation A.2)

$$S = K \ln W + \text{constant} \qquad \text{(Equation A.2)}$$

The constant K was shown by Boltzmann to be equal to the gas constant per single molecule, i.e. R/N, where R is the molar gas constant and N is the Avogadro number. If it is assumed that the entropy depends only on the thermodynamic probability of the system (Equation A.3) then

$$S = K \ln W \qquad \text{(Equation A.3)}$$

This means that in a completely ordered arrangement i.e. W = 1, which might exist in the solid state at absolute zero, the entropy is zero.

A.2 Gibbs Free Energy

The entropy change that must be considered if the direction of chemical reaction is to be deduced is that of the "universe of the reaction". This entropy change is the sum of that occurring in the system and that occurring in the thermal surroundings.

Consider a chemical reaction system in which the reaction occurs at constant temperature and constant pressure. The entropy change in the thermal reservoir is $-q/T$ or $-\Delta H/T$ (where H is the enthalpy which the sum of internal energy and external work done). Both this thermal-energy-reservoir term $-\Delta H/T$ and ΔS, the entropy change in the system as a result of the reaction, can be deduced from data for the reactants and products. Thus from properties of the system we can evaluate ΔS_{univ} (the entropy change of the "universe of the reaction")

$$\Delta S_{univ} = \Delta S + \Delta S_{therm\ res} = \Delta S - \frac{\Delta H}{T} \qquad \text{(Equation A.4)}$$

(ΔS is the entropy change of the system as a result of the reaction and $\Delta S_{therm\ res}$ is the entropy change in the thermal reservoir).

To convert the expression in Equation A.4 to one with the more familiar units of energy, we multiply it by T, the constant absolute temperature of the reaction, to give

$$T\,\Delta S - \Delta H$$

then we introduce a symbol ΔG where

$$-\Delta G = T\Delta S - \Delta H \text{ or } \Delta G = \Delta H - T\Delta S \ (T = \text{constant}) \qquad \text{(Equation A.5)}$$

This function, G, whose change is ΔG in the above example, is called the Gibbs free energy.

The free-energy function, from which the relation of Equation A.5 stems, is defined by

$$G = H - TS \qquad \text{(Equation A.6)}$$

The defining equation $H = E + PV$, is substituted in Equation A.6 to give

$$G = E + PV - TS \qquad \text{(Equation A.7)}$$

For an infinitesimal change in G one now has

$$dG = dE + PdV + VdP - TdS - SdT \qquad \text{(Equation A.8)}$$

For constant temperature and constant pressure processes as in living organism (where $dP = dT = 0$), the Gibbs free energy is therefore defined as

$$dG = dE + PdV - TdS \qquad \text{(Equation A.9)}$$

Change in free energy (ΔG) is that portion of the total energy change in a system which is available for doing work. In other words Gibbs free energy is a thermodynamic function (or function of state) which describes a system's maximum potential for doing work.

The second law of thermodynamics can therefore also be stated in these terms, spontaneous reactions are those which, when carried out under suitable conditons, can be made to perform work. Since ΔG is a thermodynamic function, it is possible to obtain a value for an over-all ΔG

of a complete reaction, say in a metabolic process, by adding the values of ΔG for each component part of the total reaction.

Although thermodynamic theory was first derived for simple mechanical systems (e.g. a perfect gas) its principles are universal and have been applied to complex biological systems.

APPENDIX B

METHODS OF CALCULATION

The most important formulae required for calculations concerning spectrophotometry and statistical analysis are given in this Appendix, together with some remarks about their interdependence, their components and their units.

B.1 Absorption spectrum and extinction coefficient

When light or other radiation passes through matter, some is absorbed and some transmitted. This situation is described by the Lambert-Beer law which states that:

$$E = \varepsilon \times c \times d \qquad \text{(Equation B.1)}$$

where E is extinction; c is concentration; d is light path length and E is the molar extinction coefficient. E is defined by $E = \log (I_0/I)$ where I_0 and I are intensities of incident and transmitted radiation respectively. The law states that the extinction is proportional both to the light path d and the concentration c of the absorbing substance. The proportionality constant ε is the extinction of the substance in question at a concentration of unity with a light path of 1cm.

If, as is usual in some countries, the quantity of substance in moles is associated with a volume in cm^3 (i.e. mol/mℓ), the dimensions found for ε are (cm^2/mol) as is shown by the following relation.

$$\varepsilon = \frac{\log (I_0/I)}{c \times d} \qquad \left\{ \frac{1}{(\text{mol}/\text{cm}^3) \times \text{cm}} = \text{cm}^2/\text{mol} \right\}$$

(Equation B.2)

However for greater convenience the concentration (c) is also expressed in (mol/litre or M). Hence the molar extinction coefficient then has dimensions ($M^{-1}.cm^{-1}$).

The following symbols and numerical values are also used in this thesis.

ε molar extinction coefficient for NADP = 6.22×10^3 ($M^{-1}.cm^{-1}$) or 6.22 ($cm^2/\mu mol$)

ΔE extinction change

V assay volume (mℓ)

v = volume of sample used in assay (mℓ)

d = light path length (cm)

c = concentration (mol/litre) or (nmol/mg)

t = time (min)

Δt = interval between measurements (min)

B.2 Adenosine-5'-triphosphate concentration

When a biochemical reaction takes place it follows from Equation B.1 that

$$c_1 - c_2 = \frac{E_1 - E_2}{\varepsilon \times d}\ ; \qquad \Delta c = \frac{\Delta E}{\varepsilon \times d} \quad \{nmol/m\ell\} \qquad \text{(Equation B.3)}$$

If there is complete conversion ($c_2 = 0$) then c can be written for Δc.

For the determination of the concentration of the sample the ratio of assay volume: sample volume (V:v) is to be considered:

$$c = \frac{\Delta E \times V}{\varepsilon \times d \times v} \quad \{nmol/ml\} \quad \text{(in the sample)} \qquad \text{(Equation B.4)}$$

From the concentration ($c_{(measured)}$) of the sample of volume v (e.g. tumour tissue extract) the ATP content of the tissue under investigation (whole tumour) can be calculated by relating to its concentration in the sample:

$$\text{ATP Content} = \frac{c_{(measured)}\ \{nmol/m\ell\}}{c_{(weighed\ out)}\ \{mg/m\ell\}} \quad \{nmol/mg\} \qquad \text{(Equation B.5)}$$

B.3 Enzyme activities

The enzymes studied in this thesis were:

1. Glucose-6-phosphate dehydrogenase (G6P-DH)
2. Isocitrate dehydrogenase (ICDH)

3. Phosphomannose isomerase (PMI)

For measuring the rate of substrate conversion or product accumulation, change in concentration per unit time (min) was used

$$\text{Volume activity} = \frac{V}{\varepsilon \times d \times v} \times \Delta E/\Delta t \ (\mu mol/min/m\ell)$$

(Equation B.6)

$$\text{Specific activity} = \frac{V}{\varepsilon \times d \times v \times c_{protein}} \Delta E/\Delta t \ (\mu mol/min/mg)$$

(Equation B.7)

The specific activity is defined as µmol of substrate converted per min per mg of enzyme.

$$\text{Turnover number} = \frac{(\text{substrate converted})}{(\text{amount of enzyme} \times \text{time})}$$

$$\text{Units are} \quad \frac{(\mu mol/min/m\ell)}{(mg\ protein/m\ell)} = \mu mol\ converted/min/mg\ protein$$

(Equation B.8)

B.4 Statistical Methods (267)

I. The mean ($\bar{x}$) is given by

$$(\bar{x}) = \frac{\Sigma x}{n}$$

(Equation B.9)

Where Σx = sum of all observations in the sample population
n = number of observations

II. The standard deviation (s) is given by

$$s = ((\Sigma x^2 - (\Sigma x)^2/n)/(n-1))^{\frac{1}{2}}$$

(Equation B.10)

Where Σx^2 = the sum of the squares of all observations in the sample population

III. The standard error of the mean (S.E.M.) is given by

$$S.E.M. = s/(n)^{\frac{1}{2}}$$

(Equation B.11)

IV. The significance of difference between two mean values was ascertained by using Student's two-tailed t test, with $(n_1 + n_2 - 2)$ degrees of freedom

$$t = (\bar{x}_1 - \bar{x}_2)/(s_1^2/n_1 + s_2^2/n_2)^{\frac{1}{2}}$$

(Equation B.12)

where $\bar{x}_1$ and $\bar{x}_2$ are the mean values of observations, s_1 and s_2 are the

standard deviations and n_1 and n_2 are the numbers of observations. (Suffices 1 and 2 denote first and second sample populations respectively). The value of P was ascertained from appropriate tables.

V. The coefficients of regression (a and b) in the regression line whose equation is $y = a + bx$ and the coefficient of determination (r^2) are given by

$$b = (\Sigma xy - (\Sigma x)(\Sigma y)/n)/(\Sigma x^2 - (\Sigma x)^2/n) \qquad \text{(Equation B.13)}$$

$$a = (\Sigma y)/n - b(\Sigma x)/n \qquad \text{(Equation B.14)}$$

$$r^2 = \frac{(\Sigma xy - (\Sigma x)(\Sigma y)/n)^2}{(\Sigma x^2 - (\Sigma x)^2/n)(\Sigma y^2 - (\Sigma y)^2/n)} \qquad \text{(Equation B.15)}$$

The formulae given in this Appendix are applied in Chapters 3 and 4 of this thesis.

REFERENCES

1. Cairns, J. (1985): The treatment of diseases and the war against cancer. Sci. Amer. 253: 31-39.

2. Sealy, G.R.H. (1984): Cancer. Cont. Med. Educ. 2: 5.

3. Mould, R.F. (1983): Cancer statistics, Adam Hilger, Bristol.

4. Blekkenhorst, G.H. (1984): The actions and clinical effects of radiation. Cont. Med. Educ. 2: 7-12.

5. Dattatreyudu, N., Kim, J.H., Hilaris, B.S. and Chu, F. (1984): Radiosensitizers and protectors. Cancer Invest. 2: 321-330.

6. Peters, G., Lee, A.E. and Dickson, C. (1986): Concerted activation of two potential proto-oncogenes in carcinomas induced by mouse mammary tumour virus. Nature 320: 628-631.

7. Land, H., Parada, L.F. and Weinberg, R.A. (1983): Tumorigenic conversion of primary embryo fibroblast requires at least two cooperating oncogenes. Nature 304: 596-602.

8. Levitzki, A., Rudick, J., Pastan, I., Vass, W.C. and Lowy, D.R. (1986): Adenylate cyclase activity of NIH 3T3 cells morphologically transformed by ras genes. FEBS 197: 134-137.

9. Astrin, S.M. and Rothberg, P.G. (1983): Ongogenes and cancer. Cancer Invest. 1: 355-364.

10. Trosko, J.E., Chang, C.C. and Medcalf, A. (1983): Mechanism of tumour promotion: Potential role of intracellular communication. Cancer Invest. 1: 511-526.

11. Kim, Y.S. (1976): Some possible effects of static magnetic fields on cancer. J. Life Sci. 6: 11-28.

12. Kairento, A.L., Brownell, G.L., Elmaleh D.R. and Swartz, M.R. (1985): Comparative measurement of regional blood flow, oxygen and glucose utilization in soft tissue tumour of rabbit with positron imaging. Brit. J. Radiol. 58: 637-643.

13. Pohlit, W. and Juling, L. (1984): Split-dose recovery explained quantitatively by repair of potentially lethal lesions. J. Cancer 49: 213-216.

14. Symington, T. (1980): In Cancer Assessment and Monitoring Eds. T. Symington, A.E. Williams and J.G. McVie p.3-24, Churchill Livingstone, London.

15. Mathis, G. and Althaus, F.R. (1986): Periodic changes of chromatin organization associated with rearrangement of repair patches accompany DNA excision repair of mammalian cells. J. Biol. Chem. 261: 5758-5765.

16. Masker, W.E. (1976): The ATP dependence of the incision and resynthesis steps of excision repair. Biochem. Biophys. Acta 442: 162-173.

17. Sato, C., Kojima, K. and Nishizawa, H. (1975): Recovery from radiation-induced decrease in cell membrane charge by added adenosine triphosphate and its modification by colchicine or cytochalasin B. Biochem. Biophys. Res. Comm. 67: 22-27.

18. Edwards, J.C., Chapman, D., Cramp, W.A. and Yatvin, M.B., (1984): The effects of ionizing radiation on biomembrane structure and function. Prog. Biophys. Molec. Biol. 43: 71-93.

19. Vranska, T.G., Pantev, T.P., Ryzhov, N.I. and Fedorenko, B.S. (1985): Electrophoretic mobility of erythrocytes exposed to accelerated helium nuclei or to γ-rays, as modified by adeturone. Int. J. Radiat. Biol. 47: 285-290.

20. Matsudaira, H., Furuno, I. and Otsuka, H., (1970): Possible requirement of adenosine triphosphate for the rejoining of x-ray-induced breaks in the DNA of Ehrlich ascites-tumour cells. Int. J. Radiat. Biol. 17: 339-347.

21. Little, J.B., (1969): Repair of sub-lethal and potentially lethal radiation damage in plateau phase cultures of human cells. Nature 224: 804-806.

22. Hetzel, F.W., (1976): Repair of potentially lethal damage in x-irradiated V79 cells. Radiat. Res. 68: 308-319.

23. Nishizawa, K., Sato, C. and Morita, T. (1979): Alterations in the survival of x-irradiated cells by 2,4 dinitrophenol depending on ATP deprivation. Int. J. Radiat. Biol. 35: 15-22.

24. Anderson, R.F., Patel, K.B. and Evans, M.D. (1985): Changes in the survival curve shape of E. coli cells following irradiation in the presence of uncouplers of oxidative phosphorylation. Int. J. Radiat. Biol. 48: 495-504.

25. Hess, D. and Prasad, K.N. (1981): Modification of radiosensitivity of mammalian cells by cyclic nucleotides. Life Sci. 29: 1-4.

26. Borst, P. (1972): Mitochondrial nucleic acids. Ann. Rev. Biochem. 49: 333-376.

27. Savitski, I., Musiko, V.A. and Erigova, S.G. (1985): Changes in fructosediphosphate aldolase and glucose-6-phosphate dehydrogenase activity after irradiation of animals with an absolute lethal dose of gamma rays. Radiobiologiia 25: 245-249.

28. Weber, T. and Cerrilli, G.J. (1971): Inhibition of tumour growth by the use of non-homogeneous magnetic fields. Cancer 28: 340-343.

29. Budinger, T.F. (1981): Nuclear magnetic resonance (NMR) in vivo studies: Known thresholds for health effects. J. Comput. Assist. Tomogr. 5: 800-811.

30. Renshaw, P.F., Owen, C.S., McLaughlin, A.C., Frey, T. and Leigh, J. (1986): Ferromagnetic contrast agents: A new approach. Mag. Res. Med. 3: 217-225.

31. Wasielewski, M.R., Bock, C.H., Bowman, M.K. and Norris, J.R. (1983): Controlling the duration of photosynthetic charge separation with microwave radiation. Nature 309: 520-522.

32. Adey, W.R. (1981): Tissue interactions with nonionizing electromagnetic fields. Physiol. Rev. 61: 435-514.

33. Kimball, G.C. (1938): The growth of yeast in a magnetic field. J. Bacteriol. 35: 109-121.

34. Schulten, K. and Weller, A. (1978): Exploring fast electron transfer processes by magnetic field. Biophys. J. 24: 295-305.

35. Wynchank, S. (1982): NMR Imaging. Med. Dig. 8: 17-29.

36. Bellosi, A., Belossi, G. and Certaines, J. (1981): The effect of a constant and uniform magnetic field on mouse brain: A study by magnetic nuclear resonance. Aviat. Sp. Environ. Med. 53: 537-539.

37. Lea, D.E. (1955): "Actions of radiations on living cells". 2nd Ed. Cambridge University Press, New York.

38. Mossman, K.L. (1984): Ionizing radiation and cancer. Cancer Invest. 2: 301-310.

39. Zimmer, K.G. (1961): "Studies on quantitative radiation biology". Oliver and Boyd, Edinburgh.

40. Alper, T. (1979): In: Cellular Radiobiology, Cambridge University Press, 50-86 and 227-249, Cambridge.

41. Pohlit, W. and Heyder, I.R. (1981): The shape of dose survival curves for mammalian cells and repair of potentially lethal damage measured by hyperthermia treatment. Radiat. Res. 87: 613-619.

42. Iliakis, G. and Pohlit, W. (1979): Quantitative aspects of repair of potentially lethal damage in mammalian cells. Int. J. Radiat. Biol. 36: 649-655.

43. Billen, D. (1981): Yield of DNA strand breaks and their relationship to DNA polymerase I-dependent repair synthesis and ligation following x-ray exposure of toluene-treated Escherichia coli. Radiat. Res. 85: 202-206.

44. Chadwick, K.H. and Leenhouts, H.P. (1981): In: The molecular theory of Radiation Biology, 143-181, Springer-Verlag, New York.

45. Semm, P., Schneider, T. and Vollrath, L. (1980): Effects of an earth-strength magnetic field on electrical activity of pineal cells. Nature 288: 607-608.

46. Kimball, G.C. (1937): The growth of yeast in a magnetic field. J. Bacteriol. 35: 109-121.

47. Levengood, W.C. (1966): Cytogenetic variations induced with a magnetic probe. Nature 209: 1009-1013.

48. Barnothy, M. (1963): Biological effects of magnetic fields on small mammals. Biomed. Sc. Instrum. 1: 127-131.

49. Feinendegen, L.E. and Mühlensiepen, M. (1985): Magnetic field affects thymidine kinase in vivo. Int. J. Radiat. Biol. 47: 723-730.

50. Hanneman, G.D. (1967): Changes produced in urinary sodium, potassium, and calcium excretion in mice exposed to homogeneous electromagnetic fields. Aerosp. Med. 38: 275-279.

51. Rajeswari, K.R., Satyanarayana, M., Sanker, P.V. and Subrahmanyam, S. (1985): Effect of extremely low frequency magnetic fields on serum cholinesterase in humans and animals. Ind. J. Exp. Biol. 23: 194-197.

52. Liburdy, R.P., Tenforde, T.S. and Magin, R.L. (1986): Magnetic field-induced drug permeability in liposome vesicles. Radiat. Res. 108: 102-111.

53. Hoff, A.J., Rademaker, H, Grondelle, R. and Duysens, L.N.M. (1977): On the magnetic field dependence of the yield of the triplet state in reaction centers of photosynthetic bacteria. Biochem. Biophys. Acta 460: 547-554.

54. Geacintov, C.T., Nostrand, F., Beckel, J.F. and Tinkel, J.B. (1972): Magnetic field induced orientation of photosynthetic systems. Biochem. Biophys. Acta 276: 65-79.

55. Okada, S. (1970): In: Radiation Biochemistry. Eds K.I. Altman, G.B. Gerber and S. Okada. Vol 1: 77-147, Academic Press, New York.

56. Klochko, E.V., Kovalchuk, L.V., Kruglyakova, K.E., Seits, I.F., Luganova, I.S., Blinov, M.N., Emanuel, N.M. (1970): Free radicals and energy metabolism of the leukocytes during leukemia. Transl. of Dokl. Akad. Nauk, SSSR. 190: 476-479.

57. Révész, L. and Edgren, J. (1984): Glutathione-dependent yield and repair of single-strand DNA breaks in irradiated cells. Br. J. Cancer 49: 55-60.

58. Szeinfeld, D. and Rubbo, A. (1977): Bacterial irradiation induced in vitro. Revta. Fac. Farm. Univ. Venez. 38: 38-44.

59. Baldetorp, B. and Baldetorp, L. (1985): Effect of repeat irradiation on the tracheal ciliary cell activity. Acta Radiol. Oncol. 24: 369-373.

60. Brown, J.M., Twentyman, P.R., Zamvil, S.S. (1979): The response of the RIF-1 tumor in vitro and in C_3H/Km mice to x-radiation (cell survival, regrowth delay, and tumor control), chemotherapeutic agents, and activated macrophages. J. Nat. Cancer Inst. 64: 605-611.

61. Westergaard, O. (1970): Separation of two DNA polymerase fractions from tetrahymena cells after excision - repairable damage to DNA. Biochem. Biophys. Acta 213: 36-44.

62. Reynolds, C. and Wills, E.D. (1974): The effect of irradiation on lysosomal activation in HeLa cells. Int. J. Radiat. Biol. 25: 113-120.

63. Jain, V.K., Pohlit, W., Purohit, S.C. (1975): Influence of energy metabolism on the repair of x-ray damage in living cells. Rad. Environm. Biophys. 12: 315-320.

64. Alper, T. (1956): The modification of damage caused by primary ionization of biological targets. Radiat. Res. 5: 537-586.

65. Traut, H. (1963): Repair from genetic radiation damage. Ed. F.H. Sobels, London.

66. Johansen, I. and Howard-Flanders, P. (1965): Macromolecular repair and free radical scavenging in the protection of bacteria against x-rays. Radiat. Res. 24: 184-200.

67. Petkau, A., and Chelack, W.S. (1976): Radioprotective effect of superoxide dismutase on model phospholipid membranes. Biochem. Biophys. Acta 433: 445-456.

68. Liboff, A.R., Williams, T., Strong, D.M. and Wistar, R. (1984): Time-varying magnetic fields: Effect on DNA synthesis. Science 223: 818-820.

69. Hong, F.T., Mauzerall, D., Mauro, A. (1971): Magnetic anisotropy and the orientation of retinal in a homogeneous magnetic field. Proc. Nat. Acad. Sci. USA. 68: 1283-1285.

70. Murayama, M. (1965): Orientation of sickled erythrocytes in a magnetic field. Nature 206: 420-422.

71. Aarholt, E., Flinn, E.A. and Smith, C.W. (1981): Effects of low-frequency magnetic fields on bacterial growth rate. Phys. Med. Biol. 26: 613-621.

72. Malinin, G.I., Gregory, W.D., Morelli, L., Sharma, V.K. and Houck, J.C. (1976): Evidence of morphological and physiological transformation of mammalian cells by strong magnetic fields. Science 194: 844-846.

73. Olcese, J., Reuss, S. and Vollrath, L. (1985): Evidence for the involvement of the visual system in mediating magnetic field effects on pineal melatonin synthesis in the rat. Brain Res. 333: 382-384.

74. Farndale, R.W. and Murray, J.C. (1985): Pulsed electromagnetic fields promote collagen production in bone marrow fibroblasts via athermical mechanisms. Calcif. Tissue Int. 37: 178-182.

75. Cohen, D., Palti, Y., Cuffin, B.N. and Schmid, S.J. (1980): Magnetic fields produced by steady currents in the body. Proc. Nat. Acad. Sci. USA 77: 1447-1451.

76. Ueno, S., Lövsund, P. and Oberg, P.A. (1986): Effects of alternating magnetic fields and low-frequency electric currents on human skin blood flow. Med. Biol. Eng. Comput. 24: 57-61.

77. Monnat, R.J. and Loeb, L.A. (1983): Mechanisms of neoplastic transformation. Cancer Invest. 1: 175-183.

78. Farber, E. and Cameron, R. (1980): The sequential analysis of cancer development. Adv. Cancer Res. 31: 125-226.

79. Diamond, L., O'Brien, T.G. and Baird, W.M. (1980): Tumour promoters and the mechanism of tumour promotion. Adv. Cancer Res. 32: 1-74.

80. Borek, C. and Sachs, L. (1966): The difference in contact inhibition of cell replication between normal cells and cells transformed by different carcinogens. Proc. Nat. Acad. Sci. USA 56: 1705-1711.

81. Borek, C., Higashino, S. and Loewenstein, W.R. (1969): Intracellular communication and tissue growth. J. Memb. Biol. 1: 274-293.

82. Nowell, P.C. (1976): The clonal evolution of tumour cell populations. Science 194: 23-28.

83. Rubenstein, E. (1980): Diseases caused by impaired communication among cells. Sci. Amer. 242: 102-121.

84. Enomoto, T., Sasaki, Y., Kanno, Y. and Yamasaki, H. (1981): Tumour promoters cause a rapid and reversible inhibition of the formation and maintenance of electrical cell coupling in culture. Proc. Nat. Acad. Sci. USA 78: 5628-5632.

85. Kaplan, P.L. and Ozanne, B. (1983): Cellular responsiveness to growth factors correlates with a cell's ability to express the transformed phenotype. Cell 33: 931-938.

86. Heldin, C.H. and Westermark, B. (1984): Growth factors: Mechanism of action and relation to oncogenes. Cell 37: 9-20.

87. Suit, H.D. and Maeda, M. (1966): Oxygen effect factor and tumour volume in the C_3H mouse mammary carcinoma. Am. J. Roentg. 96: 177-182.

88. Hume, D.A., Radik, J.L. and Feber, E. (1978): Aerobic glycolysis and lymphocytic transformation. J. Biochem. 174: 703-709.

89. Weinhouse, S. (1956): On respiratory impairment in cancer cells. Science 124: 267-268.

90. Marx, J.L. (1984): What do oncogenes do? Science 223: 673-676.

91. Slamon, D.J., Kernian, J.B. and Verma, I.M. (1984): Expression of cellular oncogenes in human malignancies. Science 224: 256-262.

92. Rous, P. (1911): A sarcoma of the fowl transmissible by an agent separable from the tumour cells. J. Exp. Med. 13: 397-411.

93. Cairns, J. (1981): The origin of human cancers. Nature 289: 353-357.

94. Blair, D.G., Oskarsson, M., Wood, T.G., McClements, W.L., Fischinger, P.J. and Woude, G.F. (1981): Activation of the transforming potential of a normal cell sequence. A molecular model for oncogenesis. Science 212: 941-943.

95. Hardy, W.D. (1983): Naturally occuring retroviruses (RNA tumour viruses). I: Cancer Invest. 1: 67-83.

96. Barret, J.C., Thomassen, D.G. and Hesterberg, T.W. (1983): Role of gene and chromosomal mutations in cell transformation. Ann. N.Y. Acad. Sci. 407: 291-300.

97. Seif, R. (1980): Factors which disorganize microtubules on microfilaments increase the frequency of cell transformation by polynoma virus. J. Virol. 36: 421-428.

98. Loewenstein, W.R. (1981): The cell-to-cell membrane channel. Physiol. Rev. 61: 829-913.

99. Edelman, G.M. (1976): Surface modulations in cell recognition and cell growth. Science 192: 218-226.

100. Potter, V.R. (1978): Phenotype diversity in experimental hepatomas: The concept of partially blocked ontogeny. Br. J. Cancer 38: 1-23.

101. Cheung, W.Y. (1980): Calmodulin plays a pivotal role in cellular regulation. Science 207: 19-27.

102. Azarnia, R., Dahl, G. and Loewenstein, W.R. (1981): Cell junction and cyclic AMP: III. Promotion of junctional membrane permeability and junctional particles in a function-deficient cell type. J. Memb. Biol. 63: 133-146.

103. Rasmussen, H. (1970): Cell communication, calcium ions and cyclic adenosine monophosphate. Science 170: 404-412.

104. Flagg-Newton, J.L., Dahl, G. and Loewenstein W R (1981): Cell junction and cyclic AMP: II. Modulations of junctional membrane permeability, depend on serum and cell density. J. Memb. Biol. 63: 105-121.

105. Warburg, O. (1956a): The origin of cancer cells. Science 123: 309-314.

106. Warburg, O. (1956b): Untitled. Science 124: 269-270.

107. Cater, D.B. and Silver, I.A. (1960): Quantitative measurements of oxygen tension in normal tissue and in the tumours of patients before and after radiotherapy. Acta Radiol. 53: 233-256.

108. Ardawi, M.S.M. and Newsholme, E.A. (1982). Maximum activities of some enzymes of glycolysis, the tricarboxylic acid cycle and ketone-body and

glutamine utilization pathways in lymphocytes of the rat. Biochem. J. 208: 743-748.

109. Hume, D.A. and Weidemann, H. (1979): Role and regulation of glucose metabolism in proliferating cells. J. Nat. Cancer Inst. 62: 3-8.

110. Sachs, L. (1980): Constitutive uncoupling of pathways of gene expression that control growth and differentation in myeloid leukemia: A model for the origin and progression of malignancy. Proc. Nat. Acad. Sci. USA 77: 6152-6156.

111. Homsher, E. and Kean, C.J. (1978): Skeletal muscle energetics and metabolism. Am. Rev. Physiol. 40: 93-131.

112. Krebs, H.A. (1954a): Some aspects of the metabolism of adenosine phosphates. Bull. Johns Hopkins Hosp. 95: 34-44.

113. Krebs, H.A. (1954b): Considerations concerning the pathways of synthesis in living matter. Bull. Johns Hopkins Hosp. 95: 19-51.

114. Skov, S., Tribukait, B. and Sundius, G. (1982): Energy metabolism and ATP turnover time during the cell cycle of Ehrlich ascites tumour cells. Exp. Cell Res. 141: 23-29.

115. Sheetz, M.P., Chasan, R. and Spudich, J.A. (1984): ATP-dependent movement of myosin in vitro: Characterization of a quantitative assay. J. Cell. Biol. 99: 1867-1871.

116. Huxley, H.E. (1969): The mechanism of muscular contraction. Science 164: 1356-1366.

117. Defuria, R.R. and Dygert, M.K. (1983): Techniques to study metabolic changes at the cellular and organ level. Int. Rev. Cyt. 83: 27-61.

118. Burton, K. and Krebs, H.A. (1953): The free energy changes associated with the individual step of the tricarboxylic acid cycle, glycolysis and alcoholic fermentation and with the hydrolysis of the pyrophosphate groups of adenosine triphosphate. Biochem. J. 54: 94-107.

119. Vary, T.C., Reibel, D.K. and Neely, J.R. (1981): Control of energy metabolism of heart muscle. Ann. Rev. Physiol. 43: 419-430.

120. Jacobus, W.E., Moreadith, R.W. and Vandegaer, K.M. (1982): Mitochondrial respiratory control. J. Biol. Chem. 257: 2397-2402.

121. Williamson, D.H., Lund, P. and Krebs, H.A. (1967): The redox state of free nicotinamide-adenine dinucleotide in the cytoplasm and mitochondria of rat liver. Biochem. J. 103: 514-527.

122. Grootegoed, J.A., Jansen, R. and Molen, J. (1984): The role of glucose, pyruvate and lactate in ATP production by rat spermatocytes and spermatids. Biochem. Biophys. Acta 267: 248-256.

123. Hughes, W. (1979): "Aspects of Biophysics" J. Wiley, New York.

124. Lipmann, F. (1941): Metabolic generation and utilization of phosphate bond energy. Adv. Enzymol. 1: 99-160.

125. Pratt, M.M. (1984): ATPases in mitotic spindles. Int. Rev. Cyt. 87: 83-105.

126. Morel, J.E. (1984): A theoretical and semi-empirical approach of muscle mechanics and energetics, independent of the mechanical role of the crossbridges. Part I: Mechanics of a single fibre. Part II: Energetics of a whole muscle. Prog. Biophys. Molec. Biol. 44: 73-96.

127. Waldstein, E.A., Sharon, R. and Ben-Ishai, R. (1974): Role of ATP in excision repair of ultraviolet radiation damage in Escherichia coli. Proc. Natl. Acad. Sci. USA. 71: 2557-2654.

128. Seeberg, E. and Strike, P. (1976): Excision repair of ultraviolet-irradiated deoxyribonucleic acid in plasmolyzed cells of Escherichia coli.J. Bacteriol. 125: 787-795.

129. Ciarrocchi, G. and Linn, S. (1978): A cell-free assay measuring repair DNA synthesis in human fibroblasts. Proc. Natl. Acad. Sci. USA. 75: 1887-1891.

130. Curtin, N.A. and Woledge, R.C. (1978): Energy changes and muscular contraction. Physiol. Rev. 48: 690-761.

131. Letko, G., Kuster, U., Bohnensack, R., Böhme, G., Pohl, K. and Kunz, W. (1982): Interrelationship between oxidative energy transformation and energy consumption at mitochondrial and cellular levels. Acta Biol. Med. Germ. 41: 735-750.

132. Kirkman, H.N., Gaetani, G.F. and Clemons, E.V. (1986): NADP-binding proteins causing reduced availability and sigmoid release of $NADP^+$ in human erythrocytes. J. Biol. Chem. 261: 4039-4045.

133. Roy, D. and Singh, R.. (1983): Age-related changes in glucose-6-phosphate dehydrogenase and 6-phosphogluconate dehydrogenase in the subcellular fractions from the rat brain and the effect of dimethylaminoethanol. Biochem. Int. 7: 43-53.

134. Kirkman, H.N. and Gaetani, G.F. (1986): Regulation of glucose-6-phosphate dehydrogenase in human erythrocytes. J. Biol. Chem. 261: 4033-4038.

135. Ammon, H.P., Amm, U., Eujen, R., Hoppe, E., Trier, G. and Versphol, E.J. (1984): The role of old age in the effects of glucose on insulin secretion, pentosephosphate shunt activity, pyridine nucleotides and glutathione of rat pancreatic islets. Life Sci. 34: 247-257.

136. Bitensky, L., Chayen, J. and Husain, O.A.N. (1984): Cytochemical detection of cancer: a review. J. Roy. Soc. Med. 77: 677-681.

137. Henderson, N.S. (1965): Isoenzymes of isocitrate dehydrogenase: subunit structure and intracellular location. J. Exp. Zool. 158: 263-267.

138. Hildebrand, R. (1984): Quantitative and qualitative histochemical investigation on $NADP^+$-dependent dehydrogenases in the limiting plate and the residual parenchyma surrounding terminal hepatic venules. Histochemistry 80: 91-95.

139. Rieder, H., Teutsch, H.F. and Sasse, D. (1978): NADP-dependent dehydrogenases in rat liver parenchyma I. Methodological studies on the qualitative histochemistry of G6PDH, 6PGDH, malic enzyme and ICDH. Histochemistry 56: 283-298.

140. Hubbard, S.C. and Ivatt, R.J. (1981): Synthesis and processing of asparagine-linked oligosaccharides. Ann. Rev. Biochem. 50: 555-583.

141. Ronnett, G.V. and Lane, M.D. (1981): Post-translational glycosylation induced activation of aglycoinsulin receptor accumulated during tunicamycin treatment. J. Biol. Chem. 256: 4704-4707.

142. Gracy, R.W. and Noltmann, E.A. (1968): Studies of phosphomannose isomerase: Isolation, homogeneity measurements, and determinations of some physical properties. J. Biol. Chem. 243: 3161-3168.

143. Bruns, F.H. and Noltmann, E. (1958): Phosphomannoisomerase, an SH-dependent metal-enzyme complex. Nature 181: 1467-1468.

144. Guha, S.K. and Rose, Z.B. (1985): The synthesis of mannose-1-phosphate in brain. Arch. Biochem. Biophys. 243: 168-173.

145. Arias, A., Gardiol, A. and Martinez-Drets, G. (1982): Transport and catabolism of D-mannose in Rhizobium meliloti. J. Bacteriol. 151: 1069-1072.

146. Miles, J.S. and Guest, J.R. (1984): Nucleotide sequence and transcriptional start point of the phosphomannose isomerase gene (manA) of Escherichia coli. Gene 32: 41-48.

147. Anjaneyulu, R., Anjaneyulu, K., Carpinelli, A.R., Sener, A. and Malaisse, W.J. (1981): The stimulus-secretion coupling of glucose-induced insulin release: Enzymes of mannose metabolism in pancreatic islets. Arch. Biochem. Biophys. 212: 54-62.

148. Neri, B., Cini-Neri, G. and D'Alterio, M. (1984): Effect of anthracyclines and mitoxantrone on oxygen uptake and ATP intracellular concentration in rat heart slices. Biochem. Biophys. Res. Comm. 125: 954-960.

149. De Jager, R., Cappelaere, P., Armand, J.P., Keiling, R., Fargeot, P., Bastit, P., Renaud, J., Earl, H. and Rubens, R. (1984): An EORTC phase II study of mitoxantrone in solid tumors and lymphomas. Eur. J. Cancer Clin. Oncol. 20: 1369-1375.

150. Arlin, Z.A., Dukart, G., Schoch, J., Reisman, A., Moore, J., Silver, R.A., Cassileth, P., Bertinon, J. and Gams, R. (1985): Phase I-II trial of mitoxantrone in acute leukemia: an interim report. Invest. New Drugs 3: 213-217.

151. Cornbleet, M.A., Stuart-Harris, R.C., Smith, I.E., Coleman, R.E., Rubens, R.D., McDonald, M., Mouridsen, H.T., Rainer, H., Oosterom, A.T. and Smyth,

J.F. (1984): Mitoxantrone for the treatment of advanced breast cancer: single-agent therapy in previously untreated patients. Eur. J. Cancer Clin. Oncol. 20: 1141-1146.

152. Oosterom, A.T., Fossa, S.D., Mulder, J.H., Calciati, A., Pauw, M. and Sylvester, R. (1985): Mitoxantrone in advanced bladder carcinoma. A Phase II study of the EORTC genito-urinary tract cancer cooperative group. Eur. J. Cancer Clin. Oncol. 21: 1013-1014.

153. Stuart-Harris, R.C., Bozek, T., Parlidis, N.A. and Smith, I.E. (1984): Mitoxantrone: an active new agent in the treatment of advanced breast cancer. Cancer Chemother Pharmacol. 12: 1-4.

154. Di Marco, A. (1975): Adriamycin (NSC 123127): mode and mechanism of action. Cancer Chemother Rep. 6: 91-96.

155. Double, J. and Brown, J.R. (1976): Evaluation of the binding of some substituted anthraquinones and naphtacenequinones to DNA. J. Pharm. Pharmacol. 28: 166-169.

156. Wynert, W.R., Harvey, H.A., Lipton, A., Schweitzer, J. and White, D. (1982): Phase I study of a 5-day schedule of mitoxantrone (dihydroxyanthracenedione). Cancer Treat. Rep. 66: 1303-1306.

157. Durr, F.E., Wallace, R.E. and Citarella, R.V. (1983): Molecular and biochemical pharmacology of mitoxantrone. Cancer Treat Rev. 10 Suppl. B: 3-11.

158. Cohen, L.F., Glaubiger, D.L., Kann, H.E. and Kohn, K.W. (1980): Protein associated DNA single strand breaks and cytotoxicity of dihydroxyanthracenedione (DHAD) NSC-301739, in mouse L1210 leukemia cells. Assoc. Cancer Res. 21: 277-279.

159. Roboz, J., Richardson, C.L. and Holland, J.F. (1982): Comparison of the interaction of antineoplastic aminoanthraquinone analogs with DNA using competitive fluorescence polarization. Life Sciences 31: 25-30.

160. Foye, W.O., Vajragupta, O.P.A. and Sengupta, S.K. (1982): DNA-binding specificity and RNA polymerase inhibitory activity of bis (aminoalkyl)

anthraquinones and bis (methylthio) vinylquinone iodides. J. Pharm. Sci. 71: 253-257.

161. Karpuscinski, J., Darzynkiewicz, Z., Traganos, F. and Melamed, M.R. (1981): Interactions of a new antitumor agent, 1,4-dihydroxy-5,8-bis((2-((2-hydroxyethyl)amino)-ethyl)amino)-9,10-anthracenedione with nucleic acids. Biochem. Pharm. 30: 231-240.

162. Traganos, F., Evenson, D.P., Starano, L., Darzynkiewicz, Z. and Melamed, M.R. (1980): Action of dihydroxyanthraquinone on cell cycle progression and survival of a variety of cultured mammalian cells. Cancer Res. 40: 671-681.

163. Meyers, C.E., McGuire, W.P., Liss, R.A., Infrim, I. and Gnotzinger, K. (1977): Adriamycin: the role of lipid peroxidation in cardiac toxicity and tumour response. Science 197: 165-167.

164. Kharasch, E.D. and Novak, R.F. (1982): Inhibition of adriamycin-stimulated microsomal lipid peroxidation by mitoxantrone and ametantrone, two new anthracenedione antineoplastic agents. Biochem. Biophys. Res. Comm. 108: 1346-1352.

165. Puck, T.T. and Marcus, P.I. (1956): Action of x-rays on mammalian cells. J. Exp. Med. 103: 653-666.

166. Jennings, W.A. and Harrinson, R.M. (1983): X-rays: Half-value layer range 0.01-8.0mm Al (approx. 6-150kV peak potential difference). Br. J. Radiol. Suppl. 17: 1-22.

167. Bottomley, P.A. (1984): NMR in medicine. Computerized Radiol. 8: 57-77.

168. Lohr, G.W. and Waller, H.D. (1974): In: Methods of Enzymatic Analysis. Ed. H.U. Bergmeyer Vol 2: 636-642, Academic Press, New York.

169. Bernt, E. and Bergmeyer, H.U. (1974): In: Methods of Enzymatic Analysis. Ed. H.U. Bergmeyer Vol. 2: 624-627, Academic Press, New York.

170. Albert, W., Opher, B.S., John, W., Leonard, J. and Miller, J.M. (1969): Isoenzymes of isocitrate dehydrogenase in cytoplasm of human cells. Exp. Med. Surg. 27: 256-266.

171. Islan, M., Bell, J.L. and Baron, D.N. (1972): Purification and comparative properties of isoenzymes of nicotinamide-adenine dinucleotide phosphate-isocitrate dehydrogenase from rat heart and liver. Biochem. J. 129: 1003-1011.

172. Gottschalk, A. (1947): The effect of temperature on the fermentation of d-mannose by yeast. Biochem. J. 41: 276-281.

173. Slein, M.W. (1955): In: Methods in enzymology, Ed. S.P. Colowick and N.O. Kaplan. Vol 1: 299-306. Academic Press, New York.

174. Gawhn, K. (1974): In: Methods of Enzymatic Analysis, Ed. H.U. Bergmeyer, Vol 1: 505 and Vol 3: 1263-1267. Academic Press, New York.

175. Lamprecht, W. and Trautschold, I. (1974): In: Methods of Enzymatic Analysis, Ed. H.U. Bergmeyer, Vol 4 : 2101-2110, Academic Press, New York.

176. Strehler, B.L. (1974): In: Methods of Enzymatic Analysis Ed. H.U. Bergmeyer, Vol 4: 2112-2121, Academic Press, New York.

177. Snoke, J.E. and Bloch, K. (1955): Studies on the mechanism of action of glutathione synthetase. J. Biol. Chem. 213: 825-835.

178. Deakin, H, Ord, M.G. and Stocken, L.A. (1963): Glucose 6-phosphate-dehydrogenase activity and thiol content of thymus nuclei from control and x-irradiated rats. Biochem. J. 89: 296-304.

179. Tietze, F. (1969): Enzymic method for quantitative determination of nanogram amounts of total and oxidized glutathione. Analytic Biochem. 27: 502-522.

180. Lowry, O.H., Rosebrough, N.J., Farr, A.L. and Randall, R.J. (1951): Protein measurement with the folin phenol reagent. J. Biol. Chem. 193: 265-275.

181. Foster, M.A. (1984): In: Magnetic Resonance in Medicine and Biology. Ed. R. Amtey. 1-27 Pergamon Press, New York.

182. Hall, E.J. (1978): Radiobiology for the Radiologist, 31-62, Harper and Row, London.

183. Gray, L.H., Conger, A.D. and Elbert, M. (1953): The concentration of oxygen dissolved in tissues at the time of irradiation as a factor in radiotherapy. Br. J. Radiol. 26: 638-648.

184. Sivak, A. and Van Duuren, B.L. (1967): Phenotypic expressions of transformation: Induction in cell culture by a phorbol ester. Science 157: 1443-1447.

185. Otten, J., Johnson, G.S. and Partan, I. (1971): Cyclic AMP levels in fibroblasts: Relationship to growth rate and contact inhibition of growth. Biochem. Biophys. Res. Commun. 44: 1192-1198.

186. Weinstein, I.B., Horowitz, A.D. and Fisher, P. (1982): In: Tumour cell heterogeneity. Origins and Implications. Eds. Owens, A.H., Coffrey, D.S., Baylin, S.B. Academic Press, New York.

187. Nagle, W.A., Moss, A.J., Roberts, H.G. and Baker, M.L. (1980): Effects of 5-thio-D-glucose on cellular adenosine triphosphate levels and deoxyribonucleic acid rejoining in hypoxic and aerobic Chinese hamster cells. Radiology 137: 203-211.

188. Benova, D.K. and Baev, I.A. (1974): Simultaneous ATP-AET-serotonin protection of spermatogonia from mutations induced by 300 R x-rays in the mouse. Int. J. Radiat. Biol. 26: 47-50.

189. Benova, D. and Baev, I. (1978): Protection of the mouse from genetic radiation damage by an optimal-dose-ratio combination of ATP, AET, and serotonin. Experientia 34: 876-877.

190. Kaufmann, W.K., Kaufman, D.G., Stenstrom, M. and Grisham, J.W. (1982): Requirements for adenosine triphosphate in DNA repair in isolated hepatic nuclei. Biochem. Biophys. Res. Comm. 108: 1040-1047.

191. Gärtner, C., Waldstein, E.A. and Hagen, U. (1980): Mechanism of the ATP effect in the DNA repair synthesis of gamma-irradiated Escherichia coli cells. Biochem. Biophys. Acta 607: 247-255.

192. Soderhäll, S. (1976): DNA ligases during rat liver generation. Nature 260: 640-642.

193. Castellazzi, M. (1976): Deoxyribonucleic acid degradation in vivo and in permeabilized Escherichia coli repair-deficient (recAzablexA) derivates. J. Bacteriol. 127: 1150-1156.

194. Dresler, S.L., Roberts, J.D. and Lieberman, M.W. (1982): Characterization of deoxyribonucleic acid repair synthesis in permeable human fibroblasts. Biochemistry 21: 2557-2564.

195. Soderhall, S. and Lindahl, T. (1976): DNA ligases of eukaryotes. FEBS Letters 67: 1-8.

196. Tikhomirova, M.V., Iashkin, P.N., Fedorenko, B.S. and Chertkov, K.S. (1984): Radiation-protective effectiveness of ATP and adenosine against high-energy protons. Kosm. Biol. Aviakosm. Med. 18: 75-77.

197. Nikolov, I., Rogozkin, V.D., Pantev, T, Chertkov, K.S., Dikovenko, E.A. and Davidova, S.A. (1986): Protection of monkeys against prolonged gamma-irradiation. Strahlenther Onkol. 162: 200-204.

198. Barbe, J., Villaverde, A. and Guerrero, R. (1983): Evolution of cellular ATP concentration after UV-mediated induction of SOS system in Escherichia coli. Biochem. Biophys. Res. Commun. 117: 556-561.

199. Passarella, S., Casamassima, E., Molinari, S., Pastore, D., Quagliariello, E., Catalano, I.M. and Cingolani, A. (1984): Increase of proton electrochemical potential and ATP synthesis in rat liver mitochondria irradiated in vitro by helium-neon laser. FEBS Lett. 175: 95-99.

200. Sijens, P.E., Bovee, W.M.M.J., Sijkens, D., Los, G. and Rutgens, D.H. (1986): In vivo ^{31}P-nuclear magnetic resonance study of the response of a murine mammary tumor to different doses of gamma-radiation. Cancer Res. 46: 1427-1432.

201. Szeinfeld, D. and Blekkenhorst, (1987): Effect of x-irradiation on adenosine triphosphate and glucose-6-phosphate dehydrogenase in the CaNT mouse tumour. Radiat. Res. 110: 305-307.

202. Vikhanskaia, F.L., Efimova, E.V. and Zhestianikov, V.D. (1985): Isoproterenol stimulation of the repair of single-stranded DNA breaks in

Chinese hamster cells induced by gamma irradiation. Tsitologiia 27: 233-236.

203. Lehnert, S. (1975): Intracellular cyclic AMP levels and radiosensitivity in synchronized V-79 cells. Radiat. Res. 64: 394-398.

204. Lehnert, S. (1975): Modification of postirradiation survival of mammalian cells by intracellular cyclic AMP. Radiat. Res. 62: 107-116.

205. Ojeda, F, Aravena, G. and Felch, H. (1980): Modification of radiation response by agents that elevate the intracellular c-AMP level. Experientia 36: 957-958.

206. Langendorff, H., and Langendorff, M. (1971): Chemical radiation protection and the c-AMP mechanism. Int. J. Radiat. Biol. 19: 493-495.

207. Raev, B.A., Chirkov, Y.Y. and Parhomenko, I.M. (1983): The effect of low dose of x-ray irradiation on c-AMP level in Chinese hamster fibroblasts. Experientia 39: 1310-1311.

208. Sarkar, S.R., Singh, L.R., Uniyal, B.P. and Chandhuri, B.N. (1985): Tissue adenyl cyclase and phosphodiesterase enzymes in whole body gamma irradiated rats. Radiobiol. Radiother. 5: 613-617.

209. Carafoli, E. and Penniston, J.T. (1985): The calcium signal. Sci. Amer. 285: 50-58.

210. Bessman, S.P. and Geiger, P.J. (1981): Transport of energy in muscle: The phosphorylcreatine shuttle. Science 211: 448-452.

211. Matthews, P.M., Bland, J.L., Gadian, D.G. and Radda, G.K. (1981): The steady-state rate of ATP synthesis in the perfused rat heart measured by ^{31}P NMR saturation transfer. Biochem. Biophys. Res. Commun. 103: 1052-1059.

212. Dzeja, P., Kalvenas, A., Toleikis, A. and Praskevicius, A. (1985): The effect of adenylate kinase activity on the rate and efficiency of energy transport from mitochondria to hexokinase. Biochem. Int. 10: 259-265.

213. Blekkenhorst, G. and Sealy, G.R.H. (1984): Changes in the redox state in mouse neck tumour after x-irradiation. Br. J. Cancer 49 Supplement VI: 306.

214. Collier, J. (1986): Entropy in evolution. Biol Philosph. 1: 5-24.

215. Szeinfeld, D., Blekkenhorst, G. and Wynchank, S. Changes in ATP and isocitrate dehydrogenase in the CaNT tumour following x-irradiation. In: "10th National Congress of Radiation Therapists" (Abstract), Johannesburg, (1986).

216. Rockwell, S., Moulder, J.E. and Martin, D.F. (1986): Effectiveness and biological effects of techniques used to induce hypoxia in solid tumours. Radiotherap. Oncol. 5: 311-319.

217. Kintner, D., Fitzpatrick, J.H., Lovie, J.A. and Gilboe, D.D. (1984): Cerebral oxygen and energy metabolism during and after 30 minutes of moderate hypoxia. Am. J. Physiol. 247: 475-482.

218. Pass, L.J., Schloerb, P.R., Chow, F.T., Graham, M., Pearce, F.J., Franklin, M.W. and Drucker, W.R. (1982): Liver adenosine triphosphate (ATP) in hypoxia and hemorrhagic shock. J. Trauma 22: 730.735.

219. Jones, D.P. and Kennedy, F.G. (1982): Intracellular oxygen supply during hypoxia. Am. J. Physiol. 243: 247-253.

220. Kane, A.B., Petrovich, D.R., Stern, R.O. and Farber, J.L. (1985): ATP depletion and loss of cell integrity in anoxic hepatocytes and silica-treated P388D_1 macrophages. Am. J. Physiol. 249: 256-266.

221. Ukikusa, M., Takeshi, I., Kazue, D. and Takayoshi, T. (1979): The influence of hypoxia and hemorrhage upon adenylate energy change and bile flow. Surg. Gyn. Obst. 149: 346-352.

222. Wilson, D.F., Ericinska, M., Drown, C. and Silver, I.A. (1977): Effect of oxygen tension on cellular energetics. Am. J. Physiol. 233: 135-140.

223. Hoerter, J. (1978): Effect of hypoxia on glycolysis in isolated fetal rat heart. C.R. Acad. Sc. 286: 411-414.

224. Drewes, L.R. and Gilboe, D.D. (1973): Cerebral metabolite and adenylate energy charge recovery following 10 min of anoxia. Biochem. Biophys. Acta 320: 701-707.

225. Bachelard, H.S., Lewis, L.D., Ponten, U and Siesjo, B.K. (1974): Mechanisms activating glycolysis in the brain in arterial hypoxia. J. Neurochem. 22: 395-401.

226. Bonventre, J.V. and Cheung, J. (1985): Effects of metabolic acidosis on viability of cells exposed to anoxia. Am. J. Physiol. 249: 149-159.

227. Matsudaira, H., Furuno, I. and Otsuka, H. (1970): Possible requirement of adenosine triphosphate for the rejoining of x-ray-induced breaks in the DNA of Ehrlich ascites-tumour cells. Int. J. Radiat. Biol. 17: 339-347.

228. Freudenberger, H. and Mager, J. (1971): Studies on the mechanism of the inhibition of protein synthesis induced by intracellular ATP depletion. Biochem. Biophys. Acta 232: 537-555.

229. Matsudaira, H., Nakagawa, C. and Bannai, S. (1969): Rejoining of x-ray-induced breaks in the DNA of Ehrlich ascites-tumour cells in vitro. Int. J. Radiat. Biol. 15: 575-581.

230. Moss, A.J., Dalrymple, G.V. and Sanders, J. (1971): Dinitrophenol inhibits the rejoining of radiation-induced DNA breaks by L-cells. Biophys. 11: 158-174.

231. Soderhäll, S. and Lindahl, T. (1976): DNA ligases of eukaryotes. FEBS Lett. 67: 1-8.

232. Song, C.W., Clement, J.J. and Levitt, S.H. (1977): Cytotoxic and radiosensitizing effects of 5-thio-D-glucose on hypoxic cells. Radiology 123: 201-205.

233. Engstrom, H, Magnusson, B.C. and Turesson, I. (1983): Effect of 50kV irradiation on enzyme activities of growing rat bone. Acta Radiol. Oncol. 22: 65-70.

234. Gupta, G.S. and Bawa, S.R. (1975): Radiation effects on rat testes. IX Studies on oxidative enzymes after partial body gamma irradiation. Strahlentherapie 150: 158-161.

235. Gupta, G.S. and Bawa, S.R. (1978): Studies of glucose 6-phosphate dehydrogenase following partial-body gamma irradiation. Radiat. Res. 73: 490-501.

236. Hayes, J.A., Snider, G.L. and Palmer, K.C. (1976): The evolution of biochemical damage in the rat lung after acute cadmium exposure. Am. Rev. Respir. Dis. 113: 121-130.

237. Opie, L.H. (1976): Effects of regional ischemia on metabolism of glucose and fatty acids. Cir. Res. 38: 52-68.

238. Piper, H.M., Hütter, J.F. and Spiecherman, P.G. (1984): Relation between enzyme release and metabolic changes in reversible anoxic injury of myocardial cells. Life Sci. 35: 127-134.

239. MacFarlane, N., Mathews, B. and Dalziel, K. (1976): The purification and properties of NADP-dependent isocitrate dehydrogenase from ox-heart mitochondria. Eur. J. Biochem. 74: 553-559.

240. Zalewska, T. and Janik, D.K. (1979): Energy utilization and changes in some intermediates of glucose metabolism in normal and hypoxic rat brain after decapitation. Resuscitation 7: 199-205.

241. Kondo, T., Taniguchi, N. and Kawakami, Y. (1984): Significance of glutathione S-conjugate for glutathione metabolism in human erythrocytes. Eur. J. Biochem. 145: 131-136.

242. Griffith, O.W. and Miester, A. (1979): Potent and specific inhibition of glutathione synthesis by buthiomine sulfoximine (S-n-butyl homocysteine sulfoximine). J. Biol. Chem. 254: 7558-7560.

243. Williamson, M., Boettcher, B. and Meister, A. (1982): Intracellular cysteine delivery system that protects against toxicity by promoting glutathione synthesis. Proc. Natl. Acad. Sci. USA 79: 6246-6249.

244. Biaglow, J.E. and Nygaard, O.F. (1973): The use of the oxidant "diamide" for studying the non-mitochondrial reducing capacity of Ehrlich ascites tumour cells. Biochem. Biophys. Res. Commun. 54: 874-881.

245. Webb, J.L. (1966): In: Enzyme and metabolic inhibitors. Ed. J.L. Webb, Vol 1: 285-335. Academic Press, New York.

246. Howard-Flanders, P.H., Levin J. and Theriot, L. (1963): Reactions of deoxyribonucleic acid radicals with sulphydryl compounds in x-irradiated bacteriophage systems. Radiat. Res. 18: 593-606.

247. Bump, E.A., Yu, Y.Y. and Brown, J.M. (1982): Radiosensitization of hypoxic tumour cells by depletion of intracellular glutathione. Science 217: 544-545.

248. Evans, J.W., Taylor, Y.C. and Brown, J.M. (1984): The role of glutathione and DNA strand break repair in determining the shoulder of the radiation survival curve. Br. J. Cancer 49: 49-53.

249. Mitchell, J.B., Russo, A., Biaglow, J.E. and McPherson, S. (1983): Cellular glutathione depletion by diethyl maleate or buthionine sulfoximine: No effect of glutathione depletion on the oxygen enhancement ratio. Radiat. Res. 96: 422-428.

250. Biaglow, J.E., Clark, E.P., Epp, E.R., Guadio, M.M., Varnes, M.E. and Mitchell, J.B. (1983): Nonprotein thiols and the radiation response of A549 human lung carcinoma cells. Int. J. Radiat. Biol. 44: 489-495.

251. Russo, A. and Mitchell, J.B. (1984): Radiation response of Chinese hamster cells after elevation of intracellular glutathione levels. Int. J. Radiat. Oncol. Biol. Phys. 10: 1243-1247.

252. Jensen, G.L. and Meister, A. (1983): Radioprotection of human lymphoid cells by exogenously supplied glutathione is mediated by gamma-glutamyl transpeptidase. Proc. Natl. Acad. Sci. USA 80: 4714-4717.

253. Wolters, H. and Konings, W.T. (1984): Radiosensitivity of normal and polyunsaturated fatty acid supplemented fibroblasts after depletion of glutathione. Int. J. Radiat. Biol. 46: 161-168.

254. Jain, V.K., Gupta, I. and Lata, K. (1982): Energetics of cellular repair processes in a respiratory-deficient mutant of yeast. Radiat. Res. 92: 463-473.

255. Citarella, R.V., Wallace, R.E., Murdock, K.C., Angier, R., Durr, B. and Forbes, M. (1982): Activity of a novel anthracenyl bishydrazone, 9,10-anthracenedicarboxaldehyde bis{(4,5-dihydro-1H-imidazol-z-yl)hydrazone}. Cancer Res. 42: 440-444.

256. Lown, J.W., Morgan, A.R., Yen, S.F., Wang, Y.H. and Wilson, W.D. (1985): Characteristics of the binding of the anticancer agents mitoxantrone and

2 MAY 1988

ametantrone and related structures to deoxyribonucleic acids. Biochemistry 24: 4028-4035.

257. Baldetorp, L., Mecklenburg, C. and Hakansson, C.H. (1977): Ultrastructural alterations in ciliary cells exposed to ionizing radiation. A scanning and transmission electron microscopic study. Cell Tiss. Res. 180: 421-431.

258. Szeinfeld, D., Blekkenhorst, G. and Wynchank, S. (1986): Biological effect on CaNT mouse tumours after exposure in static and varying fields of a nuclear magnetic resonance imager. Proceedings IV World Congress of Nuclear Medicine and Biology (in press), Buenos Aires.

259. Butler, B.C. and Dean, W.W. (1964): The inhibitory effect of a magnetostatic field upon the tissue culture of KB cells. Am. J. Med. Electronics. 3: 123-129.

260. Mulay, I.L. and Mulay, L.N. (1964): In: Biological effects of magnetic fields Vol. 1. Ed. M.F. Barnothy, Plenum Press, New York.

261. Barnothy, J.M. (1964): In: Biological effects of magnetic fields. Vol. 1. Ed. M.F. Barnothy, Plenum Press, New York.

262. Mulay, I.L. and Mulay, L.N. (1961): Effect of a magnetic field on sarcoma 37 ascites tumour cells. Nature 190: 1019.

263. Lowestein, W.R. and Kanno, Y. (1966): Intercellular communication and the control of tissue growth: Lack of communication between cancer cells. Nature 209: 1248-1251.

264. Hessler, J.D. (1970): In: Liquid Crystals and Oriented Fluids. Ed. A. Johnson and J. Panter, Plenum Press, New York.

265. Schenck, C.C., Blankenship, R.E. and Parson, W.W. (1982): Radical-pair decay kinetics, triplet yields and delayed fluorescence from bacterial reaction centers. Biochem. Biophys. Acta 680: 44-59.

266. Vegt, G.B., Wassenaar, A.M., Kawilarang, M., Schutte, P.P., Linden, M., Ruijter, M. and Boon, A. (1985): Radiation-induced changes in the cell membrane of cultured human endothelial cells. Radiat. Res. 104: 317-328.

267. Snedecor, G.W. and Cochrane, W.G. (1967): Statistical Methods 6th Ed., Iowa State University Press, Ames.

8 FEB 1988